TAMPEREEN TEKNILLINEN YLIOPISTO
TAMPERE UNIVERSITY OF TECHNOLOGY

KIRSIKKA STENLUND

FABRICATION AND PROPERTIES OF WOVEN STRUCTURES FOR BIOMEDICAL APPLICATIONS

Master of Science Thesis

Examiners: Professor Minna Kellomäki, Professor Pertti Nousiainen, Dr Tech Ville Ellä
Examiners and topic approved in the Faculty Council of Materials Engineering on 9th of January 2013

TIIVISTELMÄ

TAMPEREEN TEKNILLINEN YLIOPISTO
Materiaalitekniikan koulutusohjelma
STENLUND, KIRSIKKA: Fabrication and properties of woven structures for biomedical applications
Diplomityö, 86 sivua, 5 liitesivua
Lokakuu 2013
Pääaine: Kuitutekniikka
Tarkastaja: professori Minna Kellomäki, professori Pertti Nousiainen, Dr Tech Ville Ellä
Avainsanat: kutominen, biolääketiede, AMD, RPE solut, polyetyleenitereftalaatti, huokoisuus

Monen eri tyyppisiä tekstiiliteknisin menetelmin valmistettuja rakenteita on jo jonkin aikaa käytetty biolääketieteen sovelluksissa, kuten implantteina ja kudosteknologiassa. Tyypillisiä rakenteita ovat esimerkiksi tyrien korjaamiseen käytettävät verkkorakenteet ja verisuoni-implantteina käytetyt punotut tai kudotut rakenteet. Nimenomaan kudosteknologisissa sovelluksissa, joissa rakenne on tarkoitettu solujen kasvamisalustaksi, ongelmana on kudottujen, neulottujen ja punottujen rakenteiden kanssa ollut liian suuri huokoskoko. Kuitukankaissa huokoskoko on huomattavasti sopivampi, mutta näiden ongelma usein on, että ne eivät ole mekaanisesti tarpeeksi kestäviä.

Työn tarkoituksena oli valmistaa biolääketieteen tutkimuskäyttöön tiivis pienihuokoinen alusta kutomalla hienoa multifilamenttilankaa nauhakutomakoneella. Työssä pyrittiin saamaan kudotun rakenteen loimi- ja kudetiheydet mahdollisimman suuriksi, mikä saisi langat mahdollisimman lähelle toisiaan ja pienentäisi siten rakenteen huokoskokoa. Rakenteita kudottiin käyttämällä yhdeksää erilaista sidosta eri loimitiheyksillä ja mahdollisimman suurella kudetiheydellä. Näytteiden huokoskokoa ja tasaisuutta vertailtiin käyttäen apuna mikroskooppia. Lisäksi näytteiden neliömassat, paksuudet ja vetolujuudet olivat vertailtavina. Kaksi parhainta näytettä näistä yhdeksästä, palttina sekä palttinajohdos, kudottiin myös käyttäen apuna parafiiniöljyä voiteluaineena, jotta loimitiheyksiä saatiin vielä suuremmiksi. Parafiiniöljyä käytettiin kudonnan aikana vähentämään loimilankojen välistä kitkaa ja siten estämään niiden katkeamista. Myös kontaktikulmat mitattiin näistä kahdesta parhaasta näytteestä, mikä kertoi enemmän niiden läpäisevyydestä ja huokoisuudesta. Mittauksissa käytettiin de-ionisoitua vettä ja DMEM-soluviljelymediumia.

Parhaimmat sidokset olivat nimenomaan ne, joissa sidospisteitä oli tiheässä ja ne olivat tasaisesti jakautuneet kankaan pinnalle. Voiteluainetta apuna käyttämällä saatiin parhaat tulokset; läpimeneviä huokosia oli hyvin vähän, ne olivat jakaantuneet satunnaisten sidospisteiden ympäristöön ja ne olivat kooltaan vain muutamia mikrometrejä.

Tulosten valossa rakenteilla olisi mahdollisesti potentiaalia tulla käytetyksi soluviljelyalustoina, erityisesti isommilla soluilla. Pienemmille soluille huokoskokoa voitaisiin pienentää ja kolmiulotteisuutta vähentää esimerkiksi lämpö-painekäsittelyllä. Tulevaisuutta ajatellen olisi tärkeää valmistaa samanlaisia näytteitä käyttäen materiaalia, joka mahdollistaisi rakenteen implantoimisen, esimerkiksi samanvahvuista PLA-lankaa. Näytteiden permeabiliteetin testaaminen olisi tärkeää, koska se kertoisi enemmän näytteiden huokoisuudesta ja paljastaisi läpimeneviä huokosia, jotka eivät näy valomikroskoopilla.

ABSTRACT

TAMPERE UNIVERSITY OF TECHNOLOGY
Master's Degree Programme in Material Engineering
STENLUND, KIRSIKKA: Fabrication and properties of woven structures for biomedical engineering
Master of Science Thesis, 86 pages, 5 Appendix pages
October 2013
Major: Fibre Technology
Examiner: Professor Minna Kellomäki, Professor Pertti Nousiainen, Dr Tech Ville Ellä
Keywords: weaving, biomedicine, AMD, RPE cells, polyethylene terephthalate, porosity

Many structures manufactured by different textile techniques have already been used in biomedical applications, such as for implants and in tissue engineering. Typical structures are for instance mesh-like structures in hernia repair and woven and braided structures used as artificial blood vessels. Especially in tissue engineering applications, where the structure is intended to be surface for culturing the cells, the main problem with woven structures and knits is too large pore size. In the case of nonwovens the pore sizes are smaller but the problem related to them is their inadequate mechanical strength.

The purpose of this work was to manufacture a dense structure with small pores for biomedical studies. The structures are made of fine multifilament yarn by weaving with narrow weaving machine. The aim was to get the warp and weft densities as high as possible, which would get the yarns as close together as possible, and thus decrease the pore size of the structure. Nine different samples were woven by using different weave patterns using different warp densities and as high weft density as possible.

Pore sizes and evenness of the structures were compared by microscope imaging. In addition mass per unit area, thickness and tensile strength of the samples were compared. Two of the best structures of the nine, plain weave and plain weave derivative, were also woven with the help of paraffin oil as a lubricant to get even higher warp densities. Paraffin oil was used during the weaving process to reduce the friction between the warp yarns, and thus preventing them from breaking. Contact angles of two of the best samples were measured to get a better view of the permeability and porosity of the samples. De-ionized water and DMEM culture medium were used in the measurements.

The best weave patterns were those that had several interlacing points, which were evenly distributed on the fabric surface. Best results were achieved by using the paraffin oil; there were only few through-going openings and they were only a few micrometres in size and they were distributed randomly around interlacing points.

Considering the results, the structures could have potential to be used in cell cultures, especially for bigger cells. For smaller cells the pore structure and three-dimensionality can be reduced by for example heat-pressure treatment. In the future would be important to fabricate similar structures out of a material, which would enable the implanting of the structure, e.g. by using PLA yarn of the same fineness. Investigating the water permeability of the samples would be important, since it would tell more about the porosity and reveal the through-going pores, which are not visible with light microscope.

PREFACE

This work is a part of the Human Spare Parts project in Tampere University of Technology and funded by TEKES. I want to thank all my examiners, Professor Minna Kellomäki, Dr Tech Ville Ellä and Professor Pertti Nousiainen for their advice and guidance throughout the work. I owe my gratitude to the Textile and Fibre Materials research group for letting me use the Saurer narrow weaving machine and premises. Special thanks for the Department of Automation Science and Engineering Micro- and Nanosystems research group, especially Mathias von Essen, for the help of microscope imaging and patience. I also want to thank Esa Leppänen and Raimo Peurakoski for helping me with the machinery problems.

I want to thank my loving husband, Pekka, and my daughter, Karla, and other family for the patience and understanding during my work. You all have been an incredible support throughout this time! Special thanks to my mother, Anne, who had time to read through my work and give feedback.

17.10.2013

Kirsikka Stenlund

Contents

LIST OF SYMBOLS AND ABREVIATIONS

AMD	age-related macular degeneration
BRB	blood-retinal barrier
CF	cover factor
DI-water	de-ionized water
DMEM	Dulbecco's Modified Eagle Medium
OC	optical cover factor
PET	polyethylene terephthalate
PCL	poly-ε-caprolactone
PDLA	poly-D-lactic acid, poly-D-lactide
PDO	polydioxanone
PGA	polyglycolic acid, polyglycolide
PLA	polylactic acid, polylactide
PLLA	poly-L-lactic acid, poly-L-lactide
RPE	retinal pigment epithelium
ROP	ring opening polymerization
SPCL	starch blended with ε-polycaprolactone
SPLA	starch blended with polylactic acid
T_g	glass transition temperature

INTRODUCTION

Retinal pigment epithelial (RPE) cells are located at the bottom of retina as a monolayer of cells. Their main functions are light absorption, epithelial transport to nourish photoreceptor cells, taking part to the visual cycle, phagocytosis, regulation of homeostasis of the ionic environment, and growth factor secretion. This epithelial tissue also acts as a barrier between the retina and blood vessels (blood-retinal barrier, BRB). (Juuti-Uusitalo et al. 2012; Onnela et al. 2012; Treharne et al. 2012) Bruch's membrane is a thin yet dense layer constructed of fibres. It is situated between the retina and vascular choroid. It is semipermeable and its main function is to pass nutrients through to the retina. The RPE cells are located directly on the Bruch's membrane. (Lu et al. 2012; Shadforth et al. 2012)

There is a great need to create solutions to replace damaged RPE tissue due to for instance age related macular degeneration, which can lead to loss of vision (Kearns et al. 2012; Onnela et al. 2012; Shadforth et al. 2012). RPE cell transplanting is a potential therapy in avoiding blinding (Kearns et al. 2012; Shadforth et al. 2012; Treharne et al. 2012). However, implanting plain RPE cells has not been successful because their adherence to the natural Bruch's membrane is poor. The replacement for native Bruch's membrane must have similar permeability and support the RPE cells' growth. Several polymers, both biostable and biodegradable, have been investigated. (Lu et al. 2012) The existing solutions in cell culturing are mostly different types of membranes, either porous or semipermeable. The problem with the non-degradable membranes is that they are barrier materials even though there are pores in the structure. That is the reason why textile option is studied: textiles have naturally different type of porous structure and especially woven structures can be manufactured very densely.

The purpose of this study was to create a dense woven structure that would have similar permeability compared to the native Bruch's membrane and that it would support the adherence and growth of the human retinal pigment epithelial cells. The woven surface should have a desired porosity to enable the flow of the nutrients yet stop the passage of the cells on to the other side of the surface. A cam-controlled Saurer narrow weaving machine and multifilament PET yarn were used to model different weave patterns. Microscope imaging, tensile testing, thickness and yarn count measurements were carried out to characterize the differences between weave patterns and evaluate the usability of the structures for cell culturing purposes. Two of the best weave patterns were chosen and woven with extremely high warp densities using paraffin oil as a lubricant. Contact angle measurements were done to these specimens to get a better view of the permeability and porosity.

THEORETICAL PART

1 OCULAR ANATOMY

The eye is a complex system, which has its special internal vascular system, various specialized fluid transportation systems and complex musculature. The most outermost parts of the eye are cornea and sclera. They are made up of tough connective tissue that protects and takes part to maintaining the shape of the eye (*Figure 1*). The cornea is optically transparent, and it is located in front of the eye. It enables the light entering the eye, since non-transparent sclera surrounds the rest of the eye. (Ethier and Simmons, 2007)

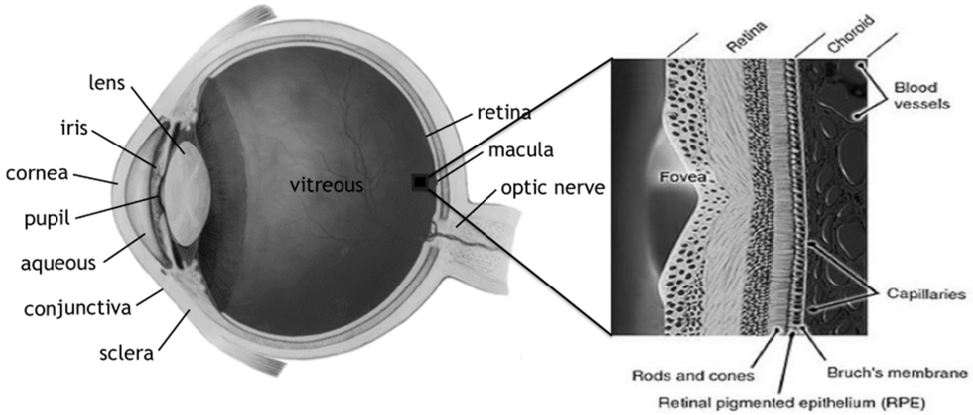

Figure 1 *Location of RPE cells and Bruch's membrane (modified from http://www.blundelloptometry.com/images/eye_diagram.gif and Normal Macula on American Health Assistance Foundation, 2000 – 2012).*

When light enters the eye, it passes through the cornea, aqueous fluid in the anterior chamber, pupil, lens and the vitreous humor. The vitreous humor fills the content of the eye and partly maintains the shape of the eye. Iris controls the pupil size and thus regulates the amount of light entering the eye. Specialized muscles take care of the contraction and dilation of the pupils. The iris is coloured and it defines the eye colour. Conjunctiva is located inside the eyelids and covers the sclera. It helps to lubricate the eye by secreting tears and mucus. Finally the light reaches the retina and the photoreceptor cells on it. The photoreceptors convert the light further into electrochemical signals. Macula is the part of retina, which has the sharpest vision. The optic nerve leaves the eye from the back of the eye through the scleral canal to the visual cortex of the brain. (Ethier and Simmons, 2007)

1.1 Retinal pigment epithelial cells

Retinal pigment epithelial (RPE) cells are located at the bottom of retina as a monolayer of cells, seen in *Figure 1*. Their main functions are light absorption, epithelial transport to nourish photoreceptor cells, taking part to the visual cycle, phagocytosis, regulation

of homeostasis of the ionic environment, and growth factor secretion. It also acts as a barrier between the retina and the vascular choroid (blood-retinal barrier BRB). Mature retinal pigment epithelial tissue has a compact and polarized structure. (Juuti-Uusitalo et al. 2012; Onnela et al. 2012; Treharne et al. 2012) Bruch's membrane is a thin (2 – 4 μm), dense layer constructed of fibres, between the retina and vascular choroid. It is semipermeable and its main function is to pass through nutrients to the retina. The RPE cells are located directly on the Bruch's membrane. (Lu et al. 2012; Shadforth et al. 2012)

There is a need to create solutions to replace damaged RPE tissue, due to several different eye diseases, such as the dry and wet forms of age related macular degeneration (AMD). The RPE tissue is important to replace because the lack of it causes the loss of photoreceptor cells. This induces blind spots to the field of sight and can eventually lead to complete loss of vision. (Kearns et al. 2012; Onnela et al. 2012; Shadforth et al. 2012) Transplantation of RPE cells is a potential therapy to avoid blinding (Kearns et al. 2012; Shadforth et al. 2012; Treharne et al. 2012). However, implanting only RPE cells has not been successful because their adherence to the natural Bruch's membrane is very poor. Thus, feasible replacements for the Bruch's membrane are studied. The replacement must be biocompatible, have similar permeability and support the RPE cells' growth. Several clinically used polymers, both biostable and biodegradable, have been investigated. (Lu et al. 2012)

1.2 Age-related macular degeneration

Age-related macular degeneration causes blurred vision and eventually vision loss, since the macula, the central area of the retina, is the area of sharp vision. There are two different forms of AMD: dry and wet forms of which the dry form is the most common (85 – 90 %). In the dry form the RPE cells start to die and the metabolic waste of the photoreceptor cells starts to accumulate, and forms deposits called *drusen*. In the wet form some abnormal blood vessels start to form under the macula. The vessels leak blood and fluids that accumulate and lift the macula thus damaging it. This further distorts the vision. (Macular Degeneration Research. Macular Degeneration: The Essential Facts. American Health Assistance Foundation, 2000 – 2012)

The vision loss cannot be stopped and the blind spots do not disappear but especially in the case of wet AMD the progress can be slowed down by using injectable angiogenesis inhibitors to the eye. The inhibitors prevent the growth of the abnormal blood vessels by blocking the vascular endothelial growth factor, VEGF. There are three regularly used angiogenesis inhibitors: EYLEA™ (approved by FDA in 2012), Lucentis® (approved in 2006) and Macugen® (approved in 2004). There is also a fourth drug, Avastin®, that is originally a blood vessel growth inhibitor intended for use in cancer therapies. It is occasionally used for treating age-related macular degeneration. (Macular Degeneration Research. Macular Degeneration: The Essential Facts. American Health Assistance Foundation, 2000 – 2012)

2 MATERIALS AND PROCESSING

Both polyethylene terephthalate (PET) and polylactide (PLA) are thermoplastic, hydrophobic and biocompatible polymers. They can be used for different biomedical applications due to their excellent mechanical durability and processability.

2.1 Polyethylene terephthalate

Polyethylene terephthalate (PET) is a thermoplastic, hydrophobic, biostable polymer, which is polymerized from terephthalic acid and ethylene glycol. The chemical structure and polymerization of PET is presented in *Figure 2*. Terephthalic acid is produced from *p*-xylene with bromide-controlled oxidation. Terephthalic acid is esterificated to dimethyl terephthalate with the help of methyl alcohol. Dimethyl terephthalate can be achieved also by oxidation and esterification process. Diethylene glycol terephthalate is generated from dimethyl terephthalate and ethylene glycol. Diethylene glycol terephthalate is further generated into polyethylene terephthalate. (Hedge et al. 2004)

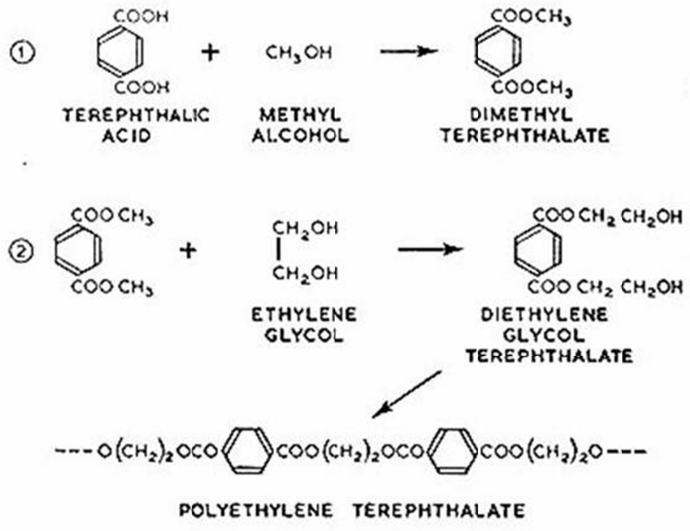

Figure 2 *The chemical structure and polymerization of PET (Hedge et al. 2004).*

It has excellent mechanical properties, chemical resistance and stability to degradation, also in human body environment. The molecular weight is generally high, 15 000 – 20 000 g/mol. (Tsunashima et al. 1999, p. 320-352; Hedge et al. 2004) PET has high tear strength, modulus, elasticity and elastic recovery, good abrasion resistance (Wulfhorst et al. 2006, p. 13-73), and also low shrinkage compared to natural fibres such as cotton (Hedge et al. 2004). These are the main reasons why it is much used in

technical textiles (Wulfhorst et al. 2006, p. 13-73). It is also highly resistant to micro-organisms (Hatch 2006, p. 212-224), and it is a fairly low-cost material, optically transparent, electrical insulator, and thermally stable. Because of its thermoplastic properties and high melting point, PET can be easily processed by different techniques from melt extrusion to film blowing. (Tsunashima et al. 1999, p. 320-352) High processing temperatures are caused by the PET chain structure, since it contains a stiff benzene ring that prevents effectively the deformation of amorphous regions, and makes crystallization more demanding. The processing temperatures vary depending on the molecular weight of the polymer. The molecular weight of PET intended for fibre spinning can vary from 12 000 to 15 000 g/mol, and thus the processing temperatures range from 265 to 300 °C. (Hedge et al. 2004) In textile applications PET fibre is usually made round, even and smooth in profile. The fibre diameter varies from 12 to 25 μm, and the fibres are about 35 % crystalline and highly oriented. When yarns are made of for textile applications, PET fibres are usually mixed with other fibre materials, e.g. with acrylic fibres in knitting or with cotton in weaving. (Hatch 2006, p. 212-224) The use of PET as film and their properties are described later in Chapter 7.1.

2.2 Polylactide

Polylactide (PLA) is a member of a group called poly-*α*-hydroxyl acids, and they are clinically widely used in biomedical applications (Nair and Laurencin, 2007). PLA is hydrophobic and thermoplastic polymer, although compared to PET it is more hydrophilic (Hutmacher and Hürzeler, 1996). Lactic acid can form two stereoisomers, L-lactic acid and D-lactic acid, and the properties of polylactides are dependent on their stereoisomeric composition (Södergård and Stolt, 2002; Hatch 2006; Mochizuki 2009 p. 257-275). PLLA is polylactide composed entirely of L-form of lactic acid. Due to the regular structure of PLLA, where the polymer backbone does not contain large side groups, the polymer is highly crystalline and has high mechanical properties. The properties of PDLA (polylactide composed of 100 % D-lactic acid) are, however, identical to PLLA because they are mirror images of each other. (Bigg 2005; Hatch 2006) Of the two different forms of lactide, the L-form is the one that is familiar to human body, since the lactic aced generated by the body is L-form. (Nair and Laurencin, 2007)

PLA can be polymerized by ring opening polymerization (ROP) or direct condensation. ROP is more often used due to its low-cost and possibility of continuous process to produce high molecular weight PLA. The process starts by condensation of aqueous lactic acid and preparing low molecular weight prepolymer. The prepolymer is depolymerized to cyclic lactide with the help of a tin catalyst. The mixture is molten and purified and lactide is polymerized to high molecular weight PLA by opening the ring structure using a tin catalyst. (Mochizuki 2009, p. 257-275) The forming of the prepolymer and ROP is presented in *Figure 3*.

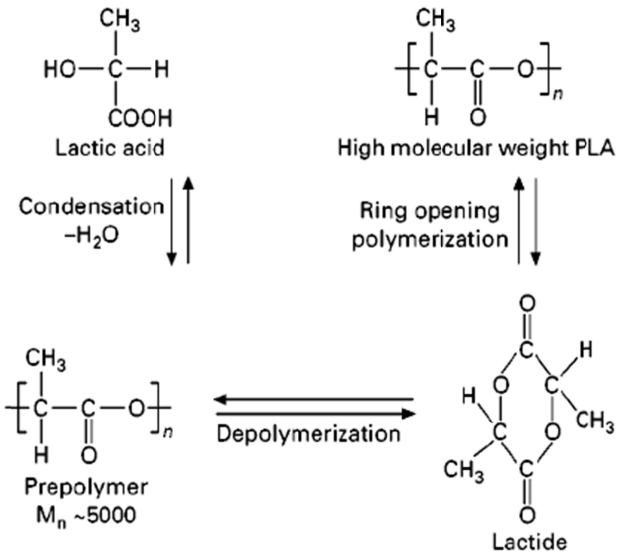

Figure 3 *Condensation of low molecular weight prepolymer from lactic acid, forming of cyclic lactide and ring opening polymerization of PLA (Mochizuki 2009, p. 257-275).*

L- and D-lactide can be copolymerized in different ratios, to achieve different properties, because adding D-lactide to the backbone of L-lactide causes irregularities to the polymer chain. This causes the polymer to be less crystalline. (Bigg 2005) When the content of D-lactide exceeds 15 – 20 % the polymer becomes totally amorphous (Södergård and Stolt, 2002). The irregularities affect also the polymer's biodegradation time, because amorphous polymer degrades faster due to the faster water uptake (Li 1999). The copolymerization has also an effect on other thermal properties of PLA. The addition of D-lactide to L-lactide backbone decreases both glass transition temperature and melting point (Bigg 2005). Melting point of PLA increases as the content of D-lactide is decreased. It can vary between 130 and 180 °C. (Mochizuki 2009, p. 257-275) PLLA and PDLA can also be blended together. The result is a polymer with totally different properties compared to copolymers. When PLLA and PDLA are mixed, these different molecules pack tightly together forming so called stereocomplexes. The blends degrade much more slowly than PLLA, PDLA or their copolymers. The glass transition temperatures of the blends are higher than of PLLA and they can even have two melting points (one on the typical range of PLA's 130 – 180 °C where "normal" polylactide crystals melt and the other on ca. 250 °C, where the stereocomplexes melt. (Tsuji 2007; Eichhorn et al. 2009, p. 206-231; Mochizuki 2009, p. 257-275)

PLA is mainly degraded via hydrolytic cleavage of the ester bonds in the polymer backbone. The typical mechanism to PLA to degrade is bulk erosion, because the hydrolytic cleavage of ester bonds is slower than the water absorption into the material. The metabolic degradation products exit through the natural body metabolic routes, since lactic acid as degradation product is familiar to the body. (Nair and Laurencin, 2010) The crystalline parts are more densely packed than the amorphous sections; that is why their hydrolysis is slower. Mechanical properties of the polymer decrease as the molecular weight decreases. (Li 1999)

Because PLA is a thermoplastic polymer it can be processed by common melt processing techniques such as melt extrusion, injection molding, compression molding, fibre drawing and film blowing. (Södergård and Stolt, 2002) PLA can easily be drawn into a fibre, usually by solvent- or melt spinning process. However, because the polymer is biodegradable the effect of the high temperature to the rate of polymer's degradation must be considered carefully. Therefore, in the processing temperatures must be carefully adjusted to prevent the polymer from degrading due to over heating. Solvent-spun fibres have high mechanical properties (Södergård and Stolt, 2002) but since the technique uses solvents, there is a possibility of toxic residues in the material, which is not a problem when melt spinning is used. (Lim and Auras et al. 2008) To produce nano or micron scale fibres, methods such as electrospinning can be used (Sell et al. 2007). However, also electrospinning demands the use of solvents.

2.3 Properties of polylactide and polyethylene terephthalate fibres and textiles

Polylactide and polyethylene terephthalate are both aliphatic polyesters, and thus their properties as yarns and fibres are relatively similar. *Table 1* summarizes some important properties of both, PLA and PET. They both are hydrophobic in nature although PLA is more hydrophilic than PET. Furthermore, PLA is biodegradable unlike PET. PLA has lower specific gravity and lower melting point than PET. Although the melting point of PLA is lower than PET's, the variation range is wider due to the wide range of possibilities in copolymerizing and blending the L- and D-forms. (Hatch 2006; Mochizuki 2009, p. 257-275) Due to the lower melting point, glass transition temperature and crystallization temperature also the processing temperatures of PLA are lower than of PET's (Hedge et al. 2004; Hatch 2006; Wulfhorst et al. 2006, p. 13-73; Mochizuki 2009 p. 257-275). PLA's crystallinity, crystal structure, morphology and orientation of the polymer chains have great effect on the mechanical properties, as well as thermal and degradation properties. Tensile modulus of PLA is very comparable with for example oriented PET, 3500 – 4000 MPa. In general, tenacity, toughness, bending and shear modulus, dimensional stability and heat resistance of PLA are very good, although a little lower than PET's. (Mochizuki 2009, p. 257-275)

Table 1 *Comparison of PLA and PET textile properties (1: Wulfhorst et al. 2006, p. 13-73; 2: Hatch 2006; 3: Mochizuki 2009, p. 257-275; 4: Hedge et al. 2004; 5: East 2009, p. 206-231).*

	PLA	**PET**
Specific gravity	1.25 a) (3)	1.34 d) (3)
Glass transition temperature T_g (°C)	60 – 65 f), 55 – 60 g) (5)	75 e) (4)
Melting point T_m (°C)	173 – 178 f) (5), 210 – 230 c) (3)	254-250 b) (1)
Crystallization temperature T_c (°C)	110 a) (3)	130 e) (4)
Stability (degradation / months *in vivo*)	>24 f), 12-16 g) (5)	Non-degradable (2)
Modulus (GPa)	2.7 f), 1.9 g) (5)	2.0 – 2.7 h) (5)
Bending modulus (gf cm^2/cm)	0.068 a) (3)	0.122 d) (3)
Shear modulus (gf/cm deg)	0.64 a) (3)	1.53 d) (3)
cos θ (water droplet contact angle)	0.254 a) (3)	0.135 d) (3)
Water absorption (w-%)	0.5 a) (3)	0.3 d) (3)
Dry tenacity (g/den)	2.5 – 5.0 (2)	4.5 (2), 0.8 N/tex h) (5)
Wet tenacity (% of dry value)	-	95 – 100 b) (1)
Dry elongation (%)	-	24 – 40 b) (1)
Wet elongation (% of dry value)	-	100 – 105 b) (1)
Modulus of elasticity (cN/tex at E=5 %)	-	N: 9 – 16, T: 35 – 45 b) (1)

a) Commercially available PLA, PLA fibres/nonwoven products, which are available under the trademark Terramac® of Unitika Ltd.

b) Polyethylene terephthalate, no further material information available.

c) 1:1 racemic mix of PLLA and PDLA.

d) Conventional poly(ethylene terephthalate), no further material information available.

e) PET filament yarn for knitted and woven fabrics. No further material information.

f) Poly-L-lactide, PLLA.

g) Poly-DL-lactide, PDLA, amorphous.

h) Additional information of PET in Allied Technical Bulletin P-1, p. 1300-1392.

3 FIBRE AND YARN FABRICATION

There are several methods to produce man-made fibres depending on the raw material and fibre or fabric's intended properties. The most common methods to spin fibres out of polymers are melt spinning, dry spinning, wet spinning and electrospinning. There are also several different possibilities to manufacture continuous fibres into filament yarns. These processes are described in this chapter.

3.1 Melt spinning and drawing of thermoplastic fibres

Melt spinning (*Figure 4*) is a common method of manufacturing fine fibres of thermoplastic polymers. The polymer material is dried thoroughly before the actual spinning process to remove the moisture from the polymer pellets. The moisture will evaporate during the heating and make irregularities to the fibre and thus lower the mechanical properties. In case of certain sensitive polymers, such as PLA, the polymer backbone is delicate to degradation in the touch of oxygen and air moisture. The polymer is contained in the hopper in inert gas. In the screw extruder it is heated above its crystallization temperature, where the screw mixes and transfers the polymer melt further from screw to the spinneret. (East 2009, p. 206-231) There can be a rough filter between the extruder and the melt block to purify the polymer melt from larger impurities. In the melt block there can be several spinning packs (usually 2 – 8) depending on the extruder and technique, and every one of them has their own pump, auxiliary filter and spinneret. The positive displacement gear pump drives the polymer melt forward, through a finer filter to the spinneret. The filter can be manufactured of fine particles of silica or aluminium oxide, or a fine metallic mesh. The openings of the spinneret are usually 0.180 – 0.400 mm in diameter but they can be as small as 0.05 mm. In the spinneret there can be several hundred spinneret holes (Wulfhorst et al. 2006, p. 13-73), and the polymer is pressed through them in high temperature to form the filaments. The shape of the spinneret hole can vary and the most common shapes are presented in *Figure 5*.

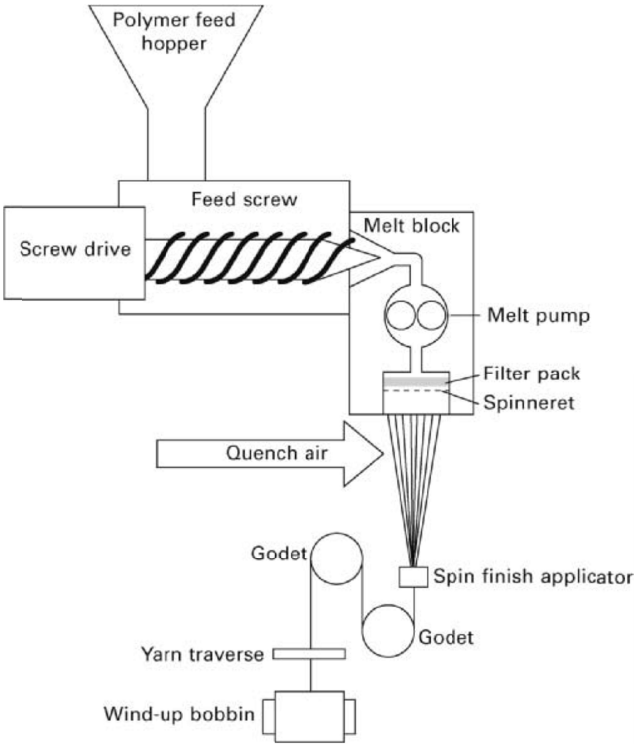

Figure 4 *Melt spinning equipment and the winding of the fibres (East 2009, p. 206-231).*

The polymer mass solidifies rapidly after the spinneret, and non-turbulent air jets help the cooling process. Some crystals are forming already at this stage. Next the fibres are led around the take-off godet and further to the wind-up bobbin or straight to other processing steps such as fibre drawing. The velocity of the first godet is always higher than the speed of the emerging fibres, which causes drawing and orientation of the fibre structure. The ratio of these velocities is called the draw-down factor. This pre-drawn fibre is called as-spun fibre. To achieve higher tensile properties further drawing must be done. (East 2009, p. 206-231)

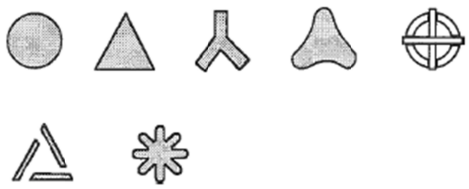

Figure 5 *Examples of shapes of the spinneret holes (Adanur 2000, p. 9-17).*

The fibre drawing is usually done right after the spinning process as a continuous process since the fibres are usually only partially drawn during the actual spinning process. The purpose of the drawing is to reduce the size of the amorphous regions and orientate the crystalline parts. The fibre consists of amorphous and crystalline regions. Heating the polymer again above its glass transition temperature (T_g) softens the amorphous regions and further enables the fibre drawing. The drawing causes the polymer chains to orientate in the fibre direction, and thus the modulus of elasticity rises. As the fibre is drawn its diameter decreases significantly. In general, the degree of

crystallinity, orientation (*Figure* 6) and size of crystalline/amorphous parts affect the fibre strength. (Wulfhorst et al. 2006, p. 13-73)

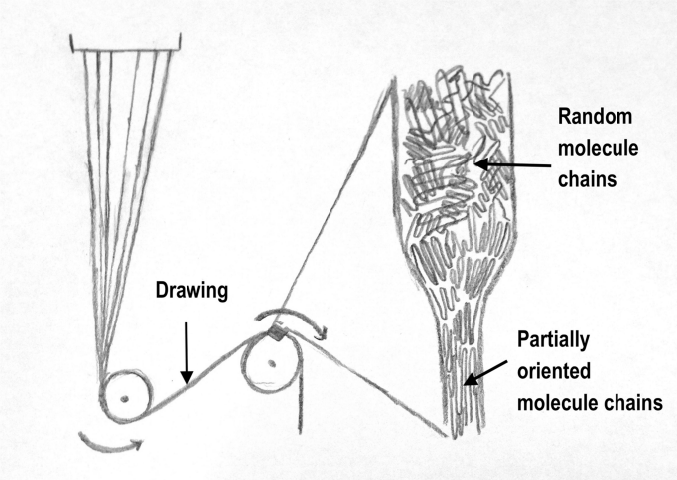

Figure 6 *The orientation of polymer chains in fibre drawing (modified from Wulfhorst et al. 2006, p. 13-73, see [44])*

How much the fibre is drawn, is determined by adjusting the speed ratios of the heated godets. The drawing causes also inner tensions to the fibre as increasing the crystallinity, which further causes instability of the fibre. That is why the fibre needs to be handled with heat, i.e. thermoset, after the drawing process. In thermosetting the material is once again heated to open chemical bonds between the polymer chains and cooled down to achieve new permanent bonds and to prevent deformation of the fibre. (Wulfhorst et al. 2006, p. 13-73)

3.2 Other means of fibre spinning

The two other main methods of fibre spinning in addition to melt spinning are dry spinning and wet spinning. In **dry spinning** (*Figure 7a*) the polymer is dissolved in an appropriate solvent, extruded through a spinneret to an evaporating cabinet. The solvent is evaporated in the warm air and fibres are formed. (Adanur 2000, p. 9-17; Wulfhorst et al. 2006, p. 13-73) The dry spinning method can be used, e.g. for polyvinyl chloride (Wulfhorst et al. 2006, p. 13-73). Also in **wet spinning** (*Figure 7b*) the polymer is dissolved in a solvent, but it is extruded into a coagulation bath where the solvent is neutralized and extracted from the fibre surface and the fibres are coagulated. (Adanur 2000, p. 9-17; Wulfhorst et al. 2006, p. 13-73) E.g. polyacrylnitrile, viscose and cupro (*Cuprammonium rayon*) fibres are spun according to this principle (Wulfhorst et al. 2006, p. 13-73).

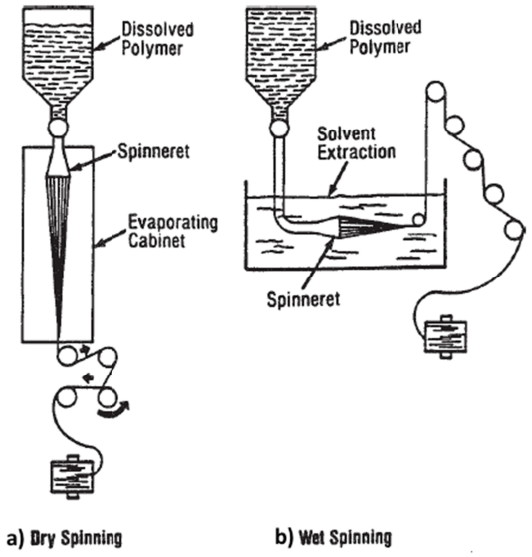

Figure 7 *Schematic pictures of a) dry spinning and b) wet spinning techniques (courtesy of Hoechst Celanese according to Adanur 2000, p. 9-17).*

A process called **electrospinning** is also one way of producing very fine filaments, but since the fibre itself cannot be used alone, the whole process of making nonwovens via electrospinning is described in more detail in chapter 4.3.3.

Sometimes fibres can be produced also by other more unusual methods, especially when ultrathin fibres are wanted. They all have their disadvantages, and thus they are used very seldom. (van der Schueren and de Clerck, 2011) **Meltblowing** produces nano-scale fibres by pressing molten polymer through an orifice die by using high pressure. Drawing the fibres with hot air jets results in relatively strong fibres. However, these fibres are not nearly as strong as via meltspinning. On the other hand, meltblowing technique is not time consuming. (Ellison et al., 2007 according to van der Schueren and de Clerck, 2011)

Template synthesis system generates nano-scale fibres by using a nanoporous membrane. The fibre is formed by inside the pores of the membrane. Mechanically strong fibres cannot be synthesized due to the manufacturing method, because the fibres are not drawn. In addition, continuous fibres cannot be produced via this method and it is a slow process. (Martin, 1996; Li et al., 2005b; Ikegame et al., 2003; Feng et al., 2006 according to van der Schueren and de Clerck, 2011).

3.3 Production of filament yarn

Formation of spun yarns from staple fibres and filament yarns differ from each other, but considering this work the filament yarns are more important. A filament is a continuous fibre and usually manmade. Yarn formed of just one fibre is called monofilament yarn and multifilament yarn consists of several fibres (Hatch 2006, p. 276-285; Adolf 1999, p. 33-54). In multifilament yarns the number of filaments can vary greatly from a few to ten filaments or even hundreds. Generally multifilament

yarns are preferred because of their better mechanical properties. They are stronger and less stiff than monofilament yarns of same size. In multifilament yarn the damage of one fibre filament is not crucial for the mechanical strength, unlike with monofilaments. (Hatch 2006, p. 276-285)

So-called producer's yarns can be done by spinning the fibres and collecting them together. These yarns have only the minimum twist required to keep the yarn together and they are rarely used, since they are hard to handle. (Adanur 2000, p. 9-17) Multifilament yarns can be classified further into different categories, which are discussed next.

3.3.1 Flat filament yarn

Flat filament yarns (*Figure 8a*) are straight aligned with the yarn axis, i.e. they are not twisted more than required. With round-shaped fibres the yarn that is formed is also smooth and even. Because the fibres are parallel to each other also the yarns are tightly packed. This type of yarn can be woven very densely and the fabric that is formed has low water vapour permeability. (Hatch 2006, p. 276-285)

This type of yarn is commonly used in applications such as seat belt fabrics. The flat filament yarn is usually formed straight after fibre spinning process when all the filaments are drawn and oriented together by the use of heated godets. The oriented filament can be twisted on a draw-twist bobbin, or packed to a draw-wind package, where no twist is given to the yarn. The amount of twist is kept small in draw-twist bobbin, for example one turn per every five centimetres of yarn. (Hatch 2006, p. 276-285)

3.3.2 Bulk filament yarn

Bulk multifilament yarns, on the other hand, are formed by twisting or texturing the fibres. The fibres are not as tightly packed than in flat filament yarns, and thus, they have greater covering power and they stretch more (*Figure 8b*). (Adanur 2000, p. 9-17; Hatch 2006, p. 276-285) However, due to the greater distance of the fibres from each other the fabric is also not as dense. In general fabrics made of bulk filament yarns are more vulnerable for pilling and snagging because of the irregularities of the yarns. Their abrasion resistance is also weaker. (Hatch 2006, p. 276-285)

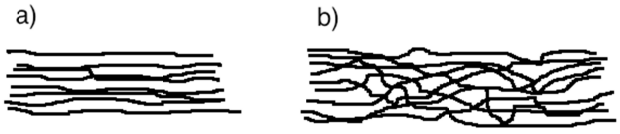

Figure 8 *a) Flat filament yarn, b) textured filament yarn.*

The fully drawn fibres can be textured into "curls" or loops. Fibres with low elasticity are curled or looped to attain elastic behaviour. These textures are formed by heat setting: the yarn is twisted or curled as wanted, heated to break chemical bonds,

and after cooling new bonds are formed between polymer chains and the new form of yarn becomes permanent (Adolf 1999, p. 33-54; Hatch 2006, p. 276-285; Wulfhorst et al. 2006, p. 13-73). Yarns can be also false-twist textured. The false twisting means that the filaments are tightly twisted, heat set and untwisted again. That gives the yarn a twisted appearance without any actual twist in the structure. The actual twisting process can be done by spindle or a friction device, or by air-jet texturing, in which an air-jet makes random loops to the yarn. Stretch yarns are made of elastic fibres by arranging them as linearly as possible. Stretch yarns have elasticity of 300 – 500 % with rapid and complete recovery. Bulky yarns are made of partly or fully hollow fibres. (Hatch 2006, p. 276-285) *Figure 8* represents the main differences between the structure of a flat filament yarn, which was described in the previous chapter, and one type of a textured filament yarn.

4 FABRICATION OF TEXTILE STRUCTURES

There are different textile technical methods to produce textile structures. As the methods are different, also the manufactured structures differ a lot in their properties. The different ways to manufacture textiles are weaving, knitting, braiding, and various nonwoven techniques. The methods are described in the following chapters in more detail.

4.1 Weaving

4.1.1 Principles

The principle of weaving is to make a planar, dense structure by using at least two yarn systems, weft and warp yarns, which are at 90 degrees angle to each other. Different types of weaves are created by altering the order of yarns, since the warp yarns and weft yarns can interlace with each other in different orders. The interlacing points of yarns can differ in number and position. There are three basic types of weave: plain weave, twill and satin weave (*Figure 9*). (Kipp 1989, p. 145-157; Adolf 1999, p. 33-54; Adanur 2000, p. 19-34; Hatch 2006, p. 317-370; Wulfhorst et al. 2006, p. 124-151)

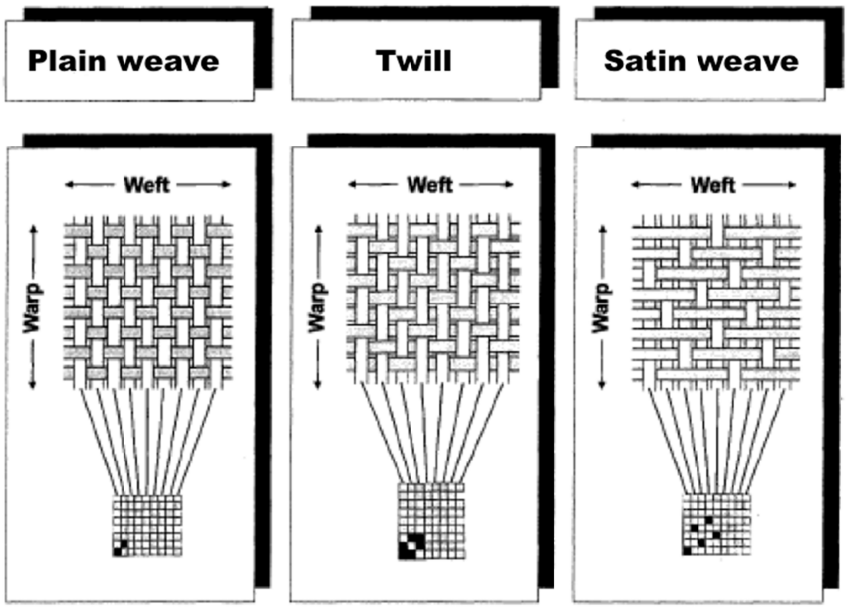

Figure 9 *Structure of plain weave, twill weave and satin weave (modified from: Adolf 1999, p. 33-54).*

Plain weave is the simplest weave pattern. It has the highest number of interlacing points and it is similar on both sides of the fabric. In *twill weave* the interlacing points are located so that they form diagonal lines that cover the fabric surface on both sides. *Satin* has the least interlacing points and thus it has long yarn floatings. This makes the fabric surface very smooth due to the yarn floatings that cover the interlacing points. Satin can be either warp-faced or weft-faced (so called sateen). The difference between satin and twill is that in satin the progression of the interlacing points is greater than one, which means that the interlacing points are not in touch with each other unlike they are in twill. (Kipp 1989, p. 145-157; Adolf 1999, p. 33-54; Adanur 2000, p. 19-34; Hatch 2006, p. 317-370; Wulfhorst et al. 2006, p. 124-151) The weaving process is described in more detail in the Chapter 4.1.3. "*Weaving with cam loom*".

4.1.2 Warp beam and weft preparation

Before the start of weaving the warp yarns must be positioned to the warp beam and prepared for the stresses in the weaving process, such as constant drawing and friction. *Figure 10* summarizes all the processes, which must be done before the actual weaving.

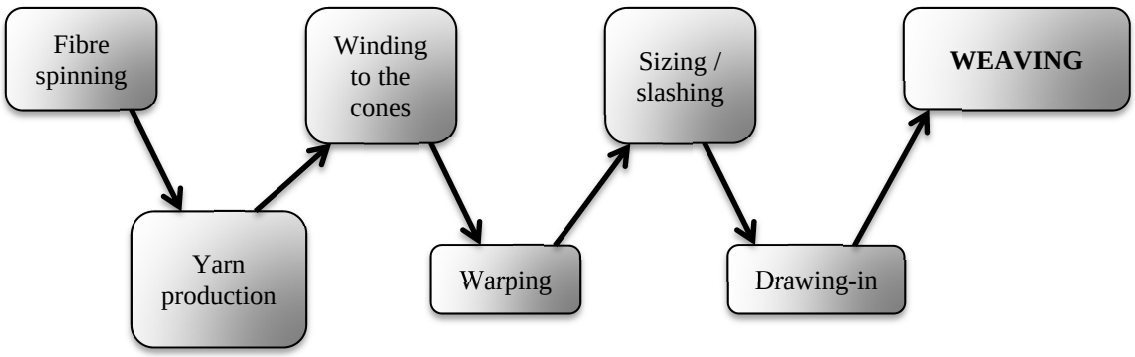

Figure 10 *Processes done before weaving (according to Kipp 1989, p. 9-16).*

The yarns are taken out of the initial packages, mounted on a frame as cones and carefully wound to the first warp beam/section beams through guide rollers and an expanded reed (Kipp 1989, p. 9-16). The expanded reed is wider than a regular reed (*Figure 11*), which is used in weaving machines. It helps to separate the warp yarns during the process, since all the yarns must be on the beam without any entanglements (Hatch 2006, p. 317-370). On these initial beams, which have the same width than the final beam, the warp density is lower. Yarns of several initial warp beams are transferred to the final beam to create much higher warp density. (Kipp 1989, p. 9-16)

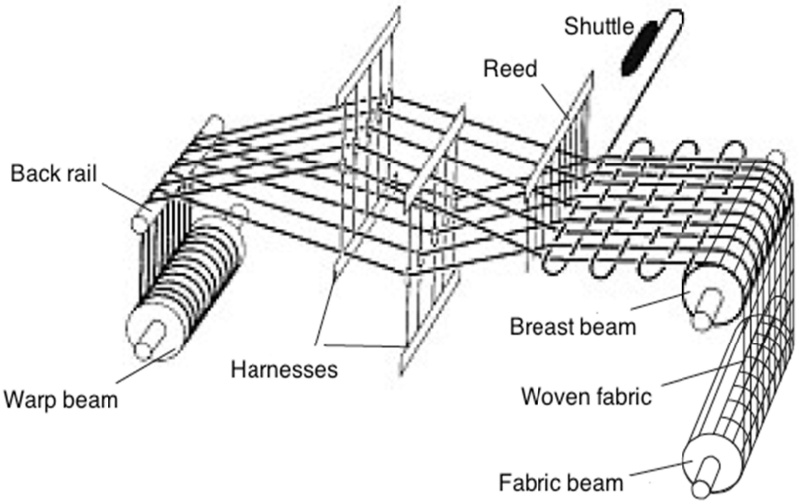

Figure 11 *A weaving machine and its essential parts (modified from Wulfhorst et al. 2006, p. 124-151, see [4]).*

To make the yarns stronger to withstand the weaving and to reduce static electricity they are handled with water-soluble starch, resins or gums. This is called the *sizing* or *slashing process* (*Figure 12*), during which the warp yarns are run through a sizing bath and then carefully rewound to the final warp beam. The sizing makes the yarns more resistant to abrasion and pulling forces. It also reduces the hairiness yarn and makes it smoother. The yarns flow (from right to left) from the (section) beam/beams to the sizing bath, to the drying cylinders, which make the solvent evaporate and dry the yarns, and finally back to the beam. The sizing can be done to the final warp beam or also to the section beams. (Kipp 1989, p. 9-16)

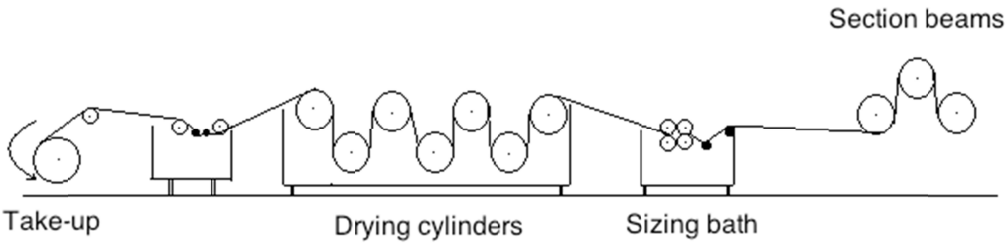

Figure 12 *A schematic picture of sizing/slashing process (Kipp 1989, p. 9-16).*

When the warp beam is ready and mounted on the weaving machine, all the yarns must be drawn in. Every single yarn goes through its own eye of a heddle and a reed dent. (Kipp 1989, p. 9-16; Hatch 2006, p. 317-370) Sizing is usually not done in narrow fabric weaving and when using monofilament yarns. The weft preparation is done by transferring the weft yarn from the cone to the bobbin by an automated winding machine (Kipp 1989, p. 9-16).

4.1.3 Weaving with a narrow weaving loom

In general a weaving machine consists of a warp yarn system, warp beam, warp letting-off system, fabric beam, heddles in at least two harnesses, a reed and a shuttle containing a bobbin for the weft yarn. The principle of a weaving machine is presented in *Figure 11.* Some of this concerns the Saurer narrow weaving loom (Aktiengesellschaft Adolph Saurer, Arbon, Switzerland, model number or name not available), which was used in this work.

The warp yarns are released to the weaving process from a warp beam or section beams, and from there they flow to the front of the weaving machine through harnesses and the reed. Each of the warp yarns goes through one eye of a heddle, and one or more yarns go through one reed dent. The fabric beam is located in the front and the ready-made fabric is collected on it. The shuttle moves the weft across the loom, which is created of two planes of warp yarns that are alternating in up and down positions. (Kipp 1989, p. 20-134; Adanur 2000, p. 109–128; Hatch 2006, p. 317-370; Wulfhorst et al. 2006, p. 124-151) In the shuttle there is a side spring that controls the weft tension when the weft yarn is released from the shuttle during the shedding (Kipp 1989, p. 20-134). This applies to the Saurer loom, but there are also other ways of weft insertion, such as water or air jets or mechanical gripper.

The motion, where certain warp yarns are moved up and certain yarns down, is called shedding. The weft is inserted in the formed opening. An open shed is presented in *Figure 13.* The shut shed is formed when all the warp yarns are in the middle position, i.e. in one plane. The warp yarns are arranged again before every weft yarn is inserted and after every weft insertion the reed beats up the yarn to form the fabric. The order of lifting the warp yarns is decided depending on the wanted weave pattern and guided by the cams. (Adanur 2000, p. 109–128; Hatch 2006, p. 317-370)

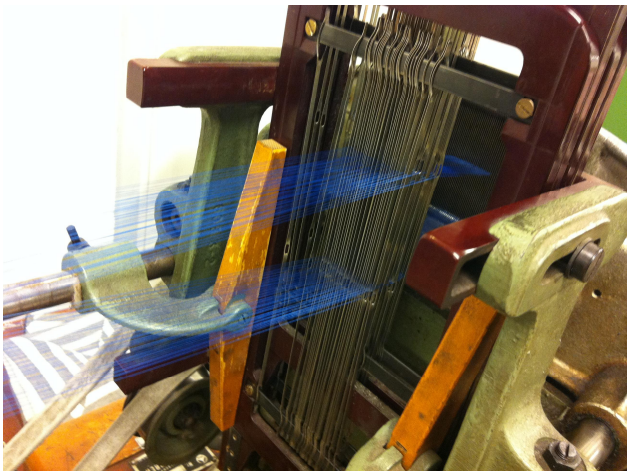

Figure 12 *Open shed in a Saurer narrow weaving machine.*

The warp let-off in Saurer narrow weaving loom is controlled by mechanical let off weights that act as a break to the warp yarns and controls their tension so that the yarns will not be loose. In the case of using several section beams there are as many identical

let-off weights as there are beams. The constant tension of the warp yarns is a very important factor when weaving a uniform fabric (Kipp 1989, p. 20-134; Adanur 2000, p. 109–128; Hatch 2006, p. 317-370; Wulfhorst et al. 2006, p. 124-151). The take-up motion removes the woven fabric from the weaving area by collecting the forming fabric around the fabric beam. The fabric take-up controls the weft density and it can be adjusted: the greater the take-up speed the smaller the weft density and vice versa. It also has great effect on the warp tension. That is why the take-up speed cannot be too small, because it will cause the warp yarns to be loose, which causes uneven fabric or yarn breakage. (Adanur 2000, p. 109-128; Hatch 2006, p. 317-370) The weft density can be made greater by adding the let-off weights as the fabric take-up speed is decreased, thus preventing the loosening of the warp yarns. The let-off weights of the section beams in the Saurer loom are presented in *Figure 14.*

Figure 13 *Warp let-off weights in Saurer narrow weaving machine.*

When weaving with a cam-controlled machine the weave pattern is decided first. A cam is a disc with a centre of rotation in the middle and unsymmetrical track going around it. A cogwheel turns the cams and a cam follower connects the cam to the harness causing them to be lifted or lowered. The weave pattern determines how many harnesses the warp yarns are drawn in. The simplest plain weave requires two harnesses, simplest twill three harnesses, and satin at least five harnesses. The harnesses have to be lifted and lowered in certain order and in relation to each other. One harness is moving all the warp yarns that are supposed to be lifted and lowered in the same way. This order is called the lifting order. Thus, there are as many cams as there are harnesses. (Kipp 1989, p. 20-157; Adanur 2000, p. 109–128; Hatch 2006, p. 317-370)

The shedding must be timed depending on the movements of the shuttle and the beating up of the reed. The shuttle goes through the shed every time it is open, and it must stay open until the shuttle passes through. When the weft is placed it must be beaten up by the reed to push it to its intended position. Without the beating-up the dense fabric will not be formed. The reed’s motion must be carefully timed, since the beating-up can be done only when the shuttle is not any more in the shed and the

shedding can be done again only when the reed is in the back-position again. The reed also controls the warp density, since different number of warp yarns can go through one reed dent. Usually the beat up is done on a closed shed with staple yarns and on an open shed with filament yarns. (Kipp 1989, p. 20-134; Adanur 2000, p. 109–128)

4.2 Knitting and braiding

There are two types of knitted structures, weft and warp knit. In **weft knitting** (*Figure 15a*) the same yarn goes through the loops of the previous layer and forms a 2D-structure. The yarn travels parallel to courses, and each weft yarn lies at right angle to the fabric forming direction. In the simplest knit only one yarn can be used, but with different number of yarns and stitches different three-dimensional structures can be created. In **warp knitting** (*Figure 15b*) there are as many yarns as there are wales, and the yarns travel parallel to the wales and fabric forming direction. In general knitted structures are more flexible and not as dense as woven fabrics. (Adolf 1999, p. 33-54; Hatch 2006, p. 317-370; Wulfhorst et al. 2006, p. 152-166)

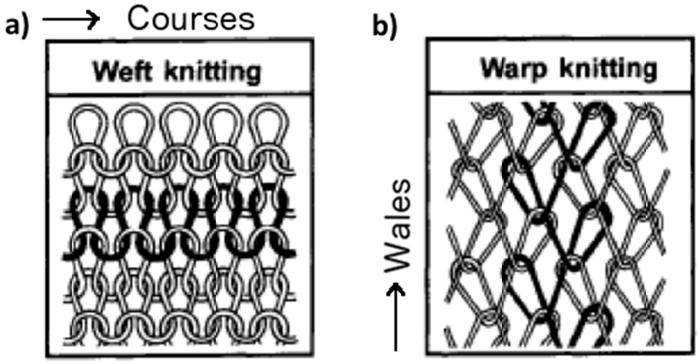

Figure 15 *Difference between weft and warp knitting (modified from: Adolf 1999, p. 33-54).*

Braiding is a technique to manufacture a longitudinal two- or three-dimensional structure that can be planar but often also tubular. Fibres or yarns are intertwined with each other and they cross each other in diagonal direction. The simplest braid is made of three yarns and it is called a plait. The braided structures are generally very strong in longitudinal direction. (Hatch 2006, p. 317-370; Wulfhorst et al. 2006, p. 188-204) The principle of one type of machine-made tubular braid is presented in *Figure 16.*

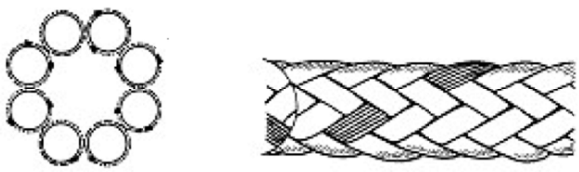

Figure 16 *Principle of machine-made braiding (Wulfhorst et al. 2006, p. 188-204).*

With special braiding machines very complex structures can be created and the complexity depends on the number of the threads and the way to intertwine them. (Hatch 2006, p. 317-370; Wulfhorst et al. 2006, p. 188-204)

4.3 Nonwoven techniques

In nonwoven structures separate fibres, either staple fibres or filaments, are bound together mechanically, thermally or with an adhesive to form a planar structure. Producing nonwoven fabrics can be divided into two processes: batt production and bonding of the fibres. In the direct methods both of the processes are happening simultaneously. (Smith, 2000) The mechanical properties vary a lot depending on the used fibre, bonding technique and density (Hatch 2006, p. 317-370).

4.3.1 Batt production

The fibre batt can be produced in **drylaying**, via *carding* or *airlaying*. Both of the techniques organize the fibres to form a uniform batt, carding mechanically and airlaying by airjets. **Wet-laid** nonwovens can be made by a technique very similar to paper making, in which the fibres are in water dispersion and filtered to form a batt. There are several **direct laying** methods. *Spunbonding* **(**or spunlaying) uses melt spinning: the filament fibres are collected as a batt directly after the fibre spinning and the still half-melt fibres are bonded spontaneously. *Melt blowing* is very similar, but in that process the spun fibres are stretched and cut into staple fibres by hot air stream. In *flash spinning* the polymer is dissolved into a solvent and extruded into a film. The solvent is evaporated very rapidly, which causes bubble formation and with mechanical stretching the structure breaks into fibrils. (Smith, 2000) *Electrospinning* is also a direct method, and it is described in more detail in Chapter 4.3.3.

4.3.2 Bonding methods

Bonding of the fibre batt can be done mechanically, thermally or chemically. **Mechanically** the fibres can be intertwined by *needle punching* or by small water jets (*hydroentaglement*), which induces entangled fibres. Another way to bond the fibres mechanically is to use another yarn system, and bond them by *separate stitches*. In that technique a knit is created on or through the nonwoven mesh. (Smith, 2000; Hatch 2006, p. 317-370) The fibres can be bonded together by heating the fibre surface to attach them to each other from connective points. This is called **thermal bonding** and it can be done by heated rollers, hot air or ultrasound. **Chemical bonding** uses a chemical bonding agent, which is usually water-based. The bonding agent makes the fibres stick to each other and it can be applied by laminating, spraying or printing or by impregnating the batt. (Smith, 2000)

4.3.3 Electrospinning

Nowadays one studied method to manufacture nonwovens is electrospinning (*Figure 17*). The machinery consists of a syringe-type reservoir with a nozzle, electric field, a high voltage power supply and a movable, grounded collection target. (Boland et al. 2005; Sell et al. 2007; van der Schueren and de Clerck, 2011)

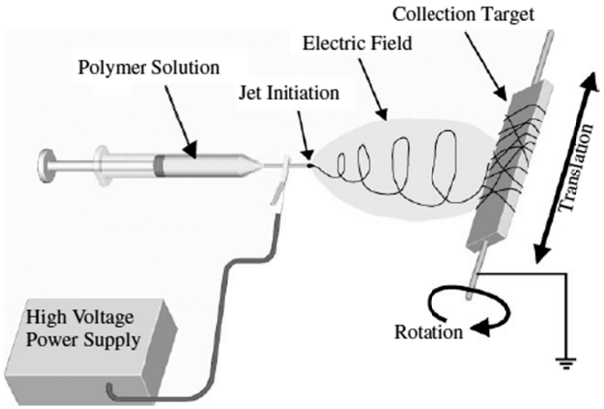

Figure 17 *The principle of electrospinning (Sell et al. 2007).*

The polymer is dissolved into a solvent before the spinning process. In liquid state the polymer is pressed through the nozzle. As the electric potential exceeds the surface tension of the polymer drop, the polymer starts to stretch towards the collection target. The solution evaporates and the fine polymer strand forms a fibre. The fibre that is formed can be from 50 nm to 10 μm in diameter. This process can be used for several different raw materials, such as collagen, elastin, fibrinogen, polyglycolide (PGA), PLA and poly-ε-caprolactone (PCL). (Sell et al. 2007; van der Schueren and de Clerck, 2011)

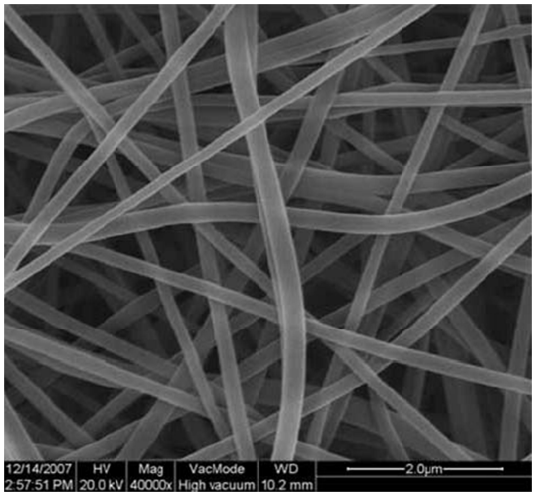

Figure 18 *A typical structure of randomly oriented electrospun nonwoven (van der Schueren and de Clerck, 2011).*

In general the structures manufactured via electrospinning are highly porous and have large surface area (*Figure 18*) (Boland et al. 2005; Hunley and Long, 2008). The

challenge of electrospinning is the difficulty to get a 3D-structure instead of a planar structure. It is also difficult to control the size, shape and interconnectivity of the pores. (Ma, 2004) The mechanical properties are not comparable with most of the connective or load-bearing tissues (Boland et al. 2005). In addition, the process is very complex compared to many textile fabrication methods. Many times the nonwoven structures for biomedical applications are electrospun and they are especially randomly oriented to create a suitable texture for the cells. (Sell et al. 2007)

5 YARN AND WOVEN FABRIC PROPERTIES

There are several measurable and calculable textile properties that affect the mechanical behaviour of the fabric. Those are for example yarn count calculation, cover factor calculations and calculations involving yarn crimp. In addition there are numerous mechanical and permeability properties that affect the usage of the fabrics. Examples for those are tensile strength, elongation at break, elastic recovery and water vapour permeability.

5.1 Yarn and fabric properties

There are several important yarn and fabric properties that have an effect on the fabric. Those are for instance fineness of the yarn, yarn twist and yarn count numbers, mass per unit area and thickness of the fabric, which describe the compactness of the fabric. **The fineness** or linear density of the yarn can be expressed in different ways: *denier* is a measure of how many grams 9000 meters of yarn weigh. On the other hand, *tex* system describes how many grams 1000 meters of yarn weigh. (Kipp 1989, p. 371-400; Adanur 2000, p. 9-17) The fineness of the yarn can be count according to the following equation (1) (Adanur 2000, p. 9-17). Another basic property of the yarns, **yarn twist**, the degree of twist is turns per a unit length (inch, meter, centimetre). Yarn twist is an important property when especially weaving dense structures is considered due to the fact that yarns with low twist are denser and more easily handled during the weaving process. (Hatch 2006, p. 287-299)

$$n = (s \cdot w) / L \tag{1}$$

where *n = yarn linear density (tex or den)*
L = yarn length (m)
m = yarn weight (g)
s = standard length (1000 m for tex and 9000 m for denier)

Yarn count means the counting of the warp and weft yarns per a measure of length. Yarn count can be expressed, e.g. 80 x 80 and it is count according to equation (2). The finer the fabric, the higher yarn count. The yarn count tells about the fabric construction and yarn density. (Hatch 2006, p. 317-370)

number of warp yarns x number of weft yarns (2)

The mass per area of the fabric is affected by several factors such as fibre density, yarns size, fabric construction, weave pattern and tension during weaving. It can be expressed as g/m^2. Thickness of the fabric is often measured, because it has an effect on the permeability and insulation characteristic. The thickness is measured according to standard SFS-EN ISO 5084:1996 Tekstiilit. Tekstiilien ja tekstiilituotteiden paksuuden määrittäminen. Textiles. Determination of thickness of textiles and textile products. or ASTM D1777, using a thickness gauge and specified pressure. (Adanur 2000, p. 361-373)

5.2 Fabric coverage and filling

There are two types of cover factors for woven fabrics, optical and geometrical cover factor. The optical cover function (OF) is related to the reflection and scattering of light on the fabric surface. Geometrical cover factor (CF) is more relevant considering this work. It is defined as the ratio of fabric surface area that is covered by yarns to the total fabric surface area. (Adanur 2000, p. 361-373; Mäkinen 1998) CF can be calculated by following equation (3) (Behera et al. 2012; Mäkinen 1998):

$$CF(\%) = C_w + C_f - C_w \cdot C_f \tag{3}$$

where C_w is the warp cover factor and C_f weft cover factor. In addition:

$$C_w = \frac{d_w \sqrt{T_w}}{280 \cdot K} \tag{4}$$

$$C_f = \frac{d_f \sqrt{T_f}}{280 \cdot K} \tag{5}$$

where d_w = *warp count (yarns/cm)*
d_f = *weft count (yarns/cm)*
T_w = *linear density of warp yarn (tex)*
T_f = *linear density of weft yarn (tex)*
K = *square root of fibre density*

The maximum value for cover factor is one, which describes that the yarns are as close together as they can be. The factor is the greater the denser the fabric is. The cover factor affects the liquid and gas permeability, since the denser the yarns are together, the less permeable the fabric is. (Adanur 2000, p. 361-373) The theory assumes that the yarns have round cross-sections and that they are nor compressed in the weaving, which results usually in a higher cover factor than the fabric actually has (Järvinen 2005).

Factor telling about the three-dimensional construction of the fabric, is called a filling factor. Filling factor takes also into account the used weave pattern and it is always larger than the cover factor. The filling factor describes the ratio of the fabric, which is filled by yarns and fibres. The smaller the factor the more free space there is between the yarns. The results can be over hundred percent because the yarns are flattened as they are woven. To count the filling factor a factor *c* must be calculated. The factor *c* depends on the weave pattern and whether the warp and weft yarns have the same linear density or not. (Mäkinen 1998) If the weave patterns and linear density for warp and weft are the same, factor *c* can be count with equation (6).

$$c = \frac{w}{w+i} \tag{6}$$

If the weave patterns differ from each other but the linear density of warp and weft yarns is the same, *c* is count according to equations (7) and (8):

$$c_w = \frac{w_w}{w_w + i_w} \tag{7}$$

$$c_f = \frac{w_f}{w_f + i_f} \tag{8}$$

where *w = number of grids in the weave pattern*
i = number of interlacing points in the weave pattern
X_w *=warp*
X_f *=weft*

The final filling factor comes from the cover factors and the factor *c*. Thus, the filling factors for warp and filling are:

$$T_w = \frac{C_w}{c_w} \tag{9}$$

$$T_f = \frac{C_f}{c_f} \tag{10}$$

The complete filling factor is:

$$T = \frac{T_w + T_f}{2} \tag{11}$$

It should be noted that both of these factors are theoretical and they are count by using certain presumptions about the yarns and weave patterns, such as that a yarn has a circular cross-section, which it does not have in woven form. (Mäkinen 1998)

5.3 Permeability and pore size

The air permeability of a fabric is affected by the open area, the pores in the fabric. It is measured as airflow through the fabric at the standard pressure drop, in cubic meter of air per square meter of fabric. For example higher level of yarn twist increases the open area, and thus increases the air permeability (Adanur 2000, p. 361-373; Hatch 2006, p. 287-299). The weave pattern affects the density of fabric and thus the permeability. The air permeability is smaller with patterns with few interlacing points. (Hatch 2006, p. 317-370) Void volume is the volume of empty space inside the fabric. The fabric thickness and the weave pattern have an effect on the void volume. (Adanur 2000, p. 361-373) It can be calculated from the following equation (12):

$$V_{total} = \frac{Vol_{total} - \frac{m}{\rho}}{Vol_{total}} \tag{12}$$

where Vol_{total} = *total volume of the sample*
m = *mass of the sample*
ρ = *density of the material*

Water vapour permeability is the ability of water vapour to pass through (diffuse) the fabric via yarns and between the fibres. The yarn twist affects the water absorbance. Higher twist decreases the yarn's surface area, and thus decreases the water absorbance. The more the yarn is twisted the higher is the water vapour permeability. (Hatch 2006, p. 287-299) Hydrophobic and hydrophilic fibres act differently due to the water repelling nature of hydrophobic fibres. Water repellency causes water to form droplets on the fabric surface rather than absorbing the water into the fabric. Different types of fabrics and materials act differently and the water repellency can be estimated by the contact angle between the water droplet and the fabric surface. The surface energy of the fabric inflicts the water drop behaviour. If the surface energy of the fabric is lower than of the water, water forms drops on the surface. If the fabric's surface energy is higher than of the water, water spreads and wets the fabric. (Hatch 2006, p. 14-43)

There are several theories to calculate the pore sizes of woven fabrics. The most accurate method to know the pore sizes is to use a microscope, but that is very time-consuming. Thus, different mathematical models have been developed. The pores of a fabric are rarely the same size or shape or distributed evenly on the fabric surface. This complicates the calculation of porosity or permeability of the fabric. Darcy's equation (13) can be used to determine the effective pore size of a multifilament woven fabric, if the measured permeability, porosity and pressure drop data are known. Unfortunately

this equation does not compare the measured and the calculated effective pore sizes. (Järvinen, 2005)

$$d_{p,eff} = \sqrt{\frac{32K}{\varphi}} = \sqrt{\frac{32cL\mu}{\varphi \Delta p}} \tag{13}$$

where K = *Kozeny constant (dimensionless)*
φ = *porosity (dimensionless)*
L = *thickness of the fabric (m)*
c = *effective concentration of solids in the feed, % w/w or kg/m^3*
μ = *fluid viscosity (Pa s)*
Δp = *pressure difference (Pa)*

According to Järvinen Brasquet and Cloirec determined effective pore sizes using equation (14).

$$d_{p,eff} = 2 \cdot \sqrt[4]{\frac{4LA\mu}{\pi N N_0}} \tag{14}$$

where L = *thickness of the fabric (m)*
A = *cross sectional area of the fabric (m^2)*
μ = *fluid viscosity (Pa s)*
N = *viscous energy loss coefficient, dimensionless*
N_0 = *number of opening per unit area*

The bubble point measurement can be used to determine the pore size of a woven fabric. The fabric is wetted, in the case of very tightly woven multifilament fabric by using vacuum impregnation to eliminate any possible air pockets. Then the airflow is increased and the pore diameter (assumed as cylindrical) can be calculated from the first air bubbles going through the fabric (liquid film break-through pressure, *p*), which depends on the contact angle between the liquid and the pore (zero for totally wetted fabrics) and the surface tension of the liquid. (Järvinen, 2005) The equation (15) is used to calculate the pore diameter:

$$d = \frac{4\sigma}{p} \tag{15}$$

where σ = *surface tension of fluid*
p = *liquid film break-through pressure*

However, these equations are not the best way to determine the pore diameters and sizes, since all the pores are not in same shape or size. The fact that many of the equations assume the pores being cylindrical and straight, distorts the results, since the pore are seldom cylindrical in woven fabrics. In addition, there are always two types of pores: pores between the yarns, i.e. macroporosity, and pores between the fibres, i.e. intra-yarn microporosity. Also the compression of yarns as woven affects the pore dimensions, which results in errors in the calculated values. (Järvinen, 2005)

5.4 Crimp and fabric yield

Crimp is caused by the interlacing of warp and weft. The warp yarn cannot flow completely straight when it is interlacing with the weft yarn. As a result of the crimp the length of the forming fabric is not as long as the initial warp on that length. The same applies for the weft yarns. The crimp is the higher the more there are interlacing points, i.e. plain weave has the highest crimp of weave patterns, and in the contrast satin has much lower crimp due to the long yarn floatings of the weave pattern, during which the yarn has no crimp. The crimp can be controlled to a certain extent by changing the yarn tension in weaving or for example by heat setting in case of thermoplastic polymers. Increasing the tension of the yarn the crimp can be reduced, but this will result in an increase of tension in the other yarn system. The increase of crimp in one direction affects also the modulus and elongation of the fabric by decreasing the modulus and increasing the elongation on that direction. The crimp affects further the weight, thickness, cover and flexibility of the fabric. The fabric with more crimp stretches more and has higher mass per unit area and greater thickness. (Adanur 2000, p. 361-373) In *Figure 19a* the warp is crimped and the filling can stay straight, and in *Figure 19b* the warp yarn is pulled straight making the filling yarn crimp. *Figure 20* gives the parameters to the crimp calculation.

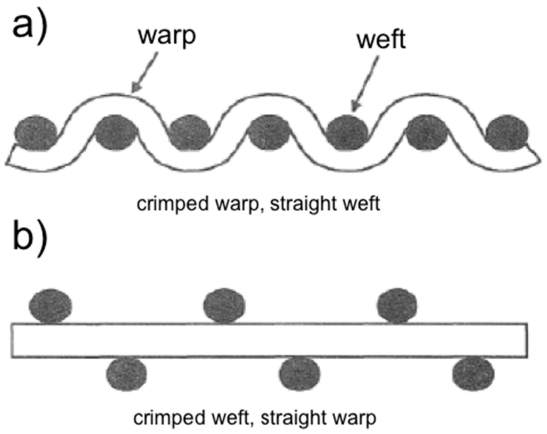

Figure 19 *Variation of crimp, a) warp is crimped and weft straight, b) weft is crimped and warp straight (modified from: Adanur 2000, p. 361-373).*

The crimp factor, i.e. percent crimp can be calculated by following equation (16):

$$Crimp - \% = \frac{L - X}{X} \times 100\% \tag{16}$$

where L = *length of the yarn*
X = *length of the woven fabric*

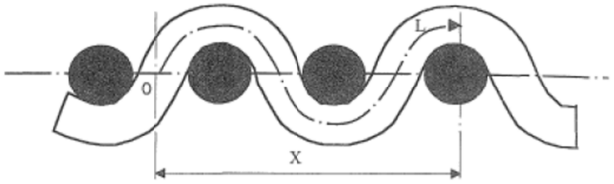

Figure 20 *Parameters to yarn crimp calculations (Adanur 2000, p. 361-373).*

Another very similar term is yield, which can be defined as the ratio of length of woven fabric to the warp length. Yield is a very practical term since it tells how much warp yarn is needed to weave a certain length of fabric and it affects the fabric modulus, thickness, air permeability, width, filling density and overall appearance. That is why the yield must be kept uniform during the weaving. (Adanur 2000, p. 361-373)

5.5 Mechanical properties

For woven fabrics, there are several important mechanical factors that can be measured. It is important to measure durability of the fabric because they are not supposed to tear, break, rupture or develop holes too easily in use (Hatch 2006, p. 14-43). Modulus, tensile strength and elongation at break are important values when investigating the quality of the fabric. **Tensile strength** describes the ability of the fabric to resist longitudinal pulling force. Thus, the tensile strength is the greatest force the fabric can withstand without breaking. (Adanur 2000, p. 361-373; Hatch 2006, p.14-43) Fabrics with few interlacing points in the weave pattern have usually higher strength than plain weave, but when the yarn packing becomes too high also the strength is decreased. For instance, twill weaves have higher strength than plain weaves. (Hatch 2006, p. 317-370). **Elongation** describes the fabric's ability to give in to the applied force without breaking or tearing (Hatch 2006, p.14-43). **Elongation at break** is the value of elongation just before the fabric breaking. In addition, **elastic recovery** is the amount that the fabric can still recover when it is no longer under stress. (Adanur 2000, p. 361-373; Hatch 2006, p.14-43)

Tear strength describes the ability of the fabric to resist a pulling force applied in lateral direction, and when the tear strength exceeds the fabric's maximum durability it tears progressively along one line (Hatch 2006, p. 14-43). The weave pattern affects greatly the magnitude of tear strength. In the case of low yarn density the yarns are able

to move and form groups of yarns to resist the tear more than a single yarn. For example 2 x 2 basket weave resists tear better than simple plain weave because there are always two yarns to resist the tear instead of one. (Adanur 2000, p. 361-373) **Bursting strength** describes the ability to resist a perpendicular force applied, i.e. force pushing through the fabric surface. The bursting strength can be measured in two ways: the diaphragm test (ASTM D3786 Mullen burst test) and the ball burst test (ASTM D3787). (Adanur 2000, p. 361-373; Hatch 2006, p. 14-43)

Abrasion resistance is the ability of the fabric to resist friction applied onto its surface. It is an important value to measure because abrasion can cause movement of yarns and for instance “hairy” surface and other changes to appearance of the fabric. (Hatch 2006, p. 14-43) Abrasion resistance can be tested in several manners by changing the abrasion force, time, direction, etc. The fibre material and the construction of the fabric affect the abrasion resistance. Considering synthetic materials, some are just naturally better to resist abrasion than others. The yarn’s twist level, crimp and the weave pattern have also an effect. In general, the more surface area of the fabric is in contact with the abrading surface, the better the fabric resists abrasion. Low twist level of the yarn can make the surface area larger, and thus it can increase the abrasion resistance (Adanur 2000, p. 361-373; Hatch 2006, p. 287-299). However, too low level of twist can leave loose fibres, and thus lower the resistance whereas high twist reduces the resistance (Adanur 2000, p. 361-373).

6 TEXTILES FOR BIOMEDICAL APPLICATIONS

Textiles and fibres can be used in biomedical applications for instance as sutures and if needed, also as implants. Textiles are in use as clean room textiles and as protective garments in hospitals. There is a possibility to use textiles as implants if it is not possible or reasonable to replace the damaged tissue with a transplant, e.g. vascular implants. Both implants and sutures can be stable or biodegradable. Textile structures for biomedical applications can be manufactures by several techniques such as weaving, knitting, braiding and nonwoven techniques.

6.1 Tissue engineering

6.1.1 Scaffolds and tissue engineering

Scaffold is a supporting structure that is used as growing surface for cells and the basis for the implant and new forming tissue. The surface is supposed to be favorable to cells to adhere onto it, proliferate and spread. Probably the most important factor is the biocompatibility of the material, the material or its degradation products cannot be toxic to cells. In addition, material that is in contact with blood cannot be thrombogenic. (Liu, Xia and Czernuszka, 2007) It acts as the extracellular matrix of the damaged tissue and it should help the tissue to maintain its shape, guide the tissue growth and release free space for the new forming tissue. If wanted, the scaffold can release for example growth factors or medicaments to the tissue as it degrades. The structure of a scaffold must be highly porous and the pores must be suitable size for the target cells to grow into them. The pores must be interconnected for the cells to be able to grow into the structure, get nutrients and form vascularization and eventually functional tissue. Due to the porosity also the surface area is large compared to the volume. (Liu, Xia and Czernuszka, 2007; van der Schueren L. and de Clerck K., 2011) The mechanical properties of the scaffold should mimic the mechanical properties of the target tissue, since it is supposed to act as supporting matrix until the tissue has healed enough. The stability of the material or biodegradation profile is a very important factor. The structure is supposed to degrade in intended speed to release space for the growing tissue, but still support it. (Liu, Xia and Czernuszka, 2007)

Tissue engineering uses scaffolds and in ideal case autologous cells to restore the function of the damaged tissue. (Liu, Xia and Czernuszka, 2007) The scaffolds can be manufactured by various techniques, also by textile techniques. (van der Schueren and de Clerck, 2011) In more detail, wanted cells are harvested from the patient and in some cases differentiated from stem cells. The cells are cultivated *in vitro* to increase their

number and seeded onto the scaffold. The scaffold and cells can be cultured in a bioreactor, with chemical, biological, mechanical or electrical stimulus to form new functioning tissue. After sufficient time it is implanted. (Rabkin and Schoen 2002, according to Liu, Xia and Czernuszka 2007) In some cases the scaffold alone can be implanted to a highly vascularized site in body, and the tissue is naturally growing inside the scaffold forming its own vascular system. This technique is called *in situ* tissue engineering. After sufficient tissue growth the implant can be moved to the intended position in the patient. (Liu, Xia and Czernuszka, 2007)

6.1.2 Biodegradation

When implanted the scaffold material starts to degrade and tissue starts to regenerate. New blood vessels grow into the scaffold pores and simultaneously new tissue forms as the scaffold slowly degrades. (Liu, Xia and Czernuszka 2007) There are two separate factors affecting the rate of the loss of mechanical strength: water diffusion into the material and hydrolysis, which constantly scissions the polymer chains. There are two different mechanisms via a material can degrade and it is dependent on the polymer type. In surface eroding polymers hydrolysis chops the polymer chains faster on the material's surface than the water can diffuse inside the material. This is normally the more desirable option for the drug releasing applications. (von Burkersroda F., Schedl L. and Göpferich A. according to East 2009, p. 206-231)

On the other hand, if the water up-take is faster than the hydrolysis on the surface, the material is bulk eroding. In bulk eroding materials the amorphous parts are affected first by the hydrolysis because the molecular structure allows the water to penetrate these parts more easily. The yet unaffected crystalline parts hold the bulk material together and it does not lose all its mechanical strength even though the molecular weight is constantly decreasing. When the degradation progresses the mechanical strength is lost and the material falls apart. The remaining oligomers and monomers are slowly broken down and metabolized. (von Burkersroda F., Schedl L. and Göpferich A. according to East 2009, p. 206-231)

6.2 Textile structures for biomedical applications

Textiles used in biomedical applications can be manufactured in different ways, described earlier, and the properties of the resulting textiles differ very much depending on the manufacturing method. For instance scaffolds can be manufactured via electrospinning, weaving, braiding and knitting (both warp and weft knitting). (Adanur 1995, p. 334-344) *Table 2* summarizes the most usual applications, fibre types and manufacturing methods.

Table 2 *Sutures and implantable textile structure categorized by fibre raw material and manufacturing method (modified from Rigby and Anand 2000. p. 407-424).*

Product application	Fibre type	Manufacture system
Soft-tissue implants		
Artificial tendon	PTFE, PET, polyamide, silk, polyethylene	Woven, braided
Artificial ligament	PET, carbon	Braided
Artificial cartilage	Low density polyethylene	Nonwoven
Artificial skin	Chitin	
Eye contact lenses/artificial cornea	Polymethyl methacrylate, silicone, collagen	
Orthopedic implants		
Artificial joints/bones	Silicone, polyacetal, polyethylene	
Cardiovascular implants		
Vascular grafts	PET, PTFE	Knitted, woven
Heart valves	PET	Woven, knitted

There are several advantages in textile structures for biomedical applications. They are usually flexible, elastic and naturally highly porous. The properties can be altered easily by changing fibre and yarn properties in addition to manufacturing techniques and parameters. When considering especially cell cultivation the fibrillar structure is important for the cell attachment, proliferation and differentiation. (Doser and Planck, 2011)

6.2.1 Textiles for soft-tissue applications

Textiles are usually strong and flexible, and those features make them suitable for soft tissue replacements. The chosen fabrication technique depends on the mechanical properties of the target tissue.

Textiles can be used in *wound care applications* due to their porousness. Many large damages of skin are treated with autografts, which have a problem of creating a new damaged site in the skin. Allo- and xenografts are always temporary and they are later replaced with autografts. (Sell et al. 2007) In some cases in deeper skin damages, when there are no more cells available for proper wound healing process, there is a need for new wound care products. The material should prevent excessive evaporation of moisture, and act as a substrate for regenerating tissue, and possibly deliver active agents during the healing process. (van der Schueren and de Clerck, 2011)

Nonwovens are considered useful in wound care for their high porosity, interconnected pores and large surface area. They absorb and prevent dehydration, promote cell adhesion and cell spreading. Especially biodegradable polymers, both synthetic and natural, are favoured in nanofibrous wound care products. Natural polymers, such as collagen or fibrinogen, have better interactions than synthetic polymers, such as PLA, PGA and PCL. Since natural polymers often have lower mechanical properties, combining synthetic polymers with natural polymers enables both, good mechanical properties and natural interactions. The biodegradability is an advantage since the repetitive removal of regular bandages is usually a setback for the healing process. (van der Schueren and de Clerck, 2011)

There is a need for designing a suitable textile scaffold for skin damage repair. Chen et al. have noted that **warp knitted** scaffold alone had too large openings for the cell attachment, and their PLGA-scaffolds worked better when the openings were made smaller with a spongy collagen structure (Chen et al. 2008). Sell et al. have studied the use of **electrospun nonwoven** scaffolds of several different materials for skin applications. In general the structure was better for cell seeding since the small pores did not allow the cells to go through the structure like they did in knitted structure. (Sell et al. 2007)

Textiles are used frequently as *supportive structures* such as hernia repair in the form of meshes. One type of typical **warp knitted** hernia repair mesh is shown in *Figure 21*. The first warp knitted meshes were made of PET multifilaments or polypropylene monofilaments. Also expanded polytetrafluoroethylene and polyvinylidene fluoride were used, because they naturally inhibit adhesion, but they are not as elastic as PET. There are also biodegradable or partly biodegradable meshes on the market, made of PGA (DEXON mesh®, Covidien), PLA or 50 % PGA and 50 % PP (Vypro II, Ethicon). In addition to more conventional meshes, there are self-fixating meshes, e.g. Parietex™ ProGrip mesh (SOFRADIM, France) knitted of PP and incorporated with PLA micro hooks. (Doser and Planck, 2011)

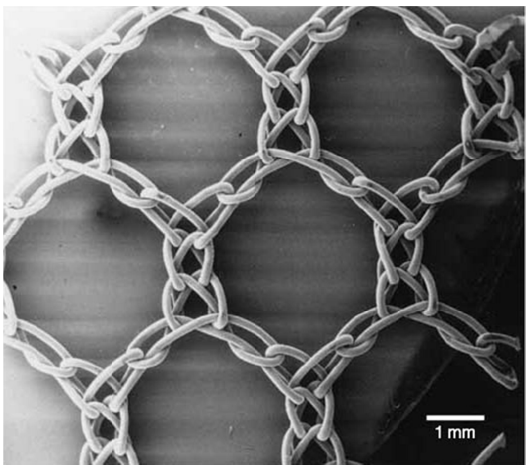

Figure 21 *A typical warp knitted hernia repair mesh (Doser and Planck, 2011).*

Isotalo et al. manufactured two types of **braided** biodegradable urethral stents of PLLA (*Figure 22a*). They were compared with stainless steel braided stents. With the metallic stents there were chronic inflammatory changes and fibrosis seen even after 12 months of implantation, unlike there was not with the biodegradable stents. With all the stents there was increasing epithelial hyperplasia as time was passing, which indicated that the braided biodegradable structure did not prevent it. No obstructing pieces were found in the urethra when the material was degrading. It was noticed that due to the thinner fibers and smaller mass the braided stents had a shorter degradation time than more traditionally used spiral stents (*Figure 22b*) made of PLLA. (Isotalo et al. 2005)

Also Kotsar, Isotalo et al. fabricated a biodegradable **braided** urethral stent to treat acute urinary retention caused by benign prostatic enlargement. The stent was manufactured of poly(lactic-co-glycolic) acid (PLGA). When the stents were in place, there were no migration or release of large particles as there were with the former spiral biodegradable stents. They were degraded in 2 – 3 months, which would be enough to be used together with a treatment to reduce the prostatic volume. However, there were cases (two out of ten), in which the lumen of the stent was compressed, due to the insufficient compressive stiffness of the stents. (Kotsar and Isotalo et al. 2009)

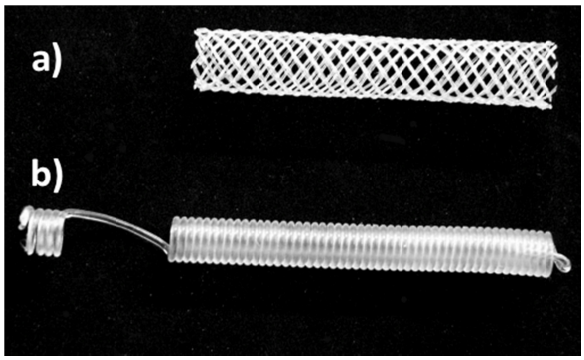

Figure 22 *A biodegradable braided stent (a) compared to a spiral stent (b) (Isotalo et al. 2005)*

Textiles can be used as *scaffolds* in cell studies. Mayer and his colleagues used a non-degradable **woven** (plain weave) PET-scaffold coated with a biodegradable film made of PLGA on the other side. The purpose was to create a polarized scaffold system for hepatocytes. The woven structures were manufactured with different mesh sizes. The composite structure of non-degradable and biodegradable material ensured stable structure as the PLGA degraded. As growing on the scaffold (the film side) the hepatocytes started forming aggregates such as in native hepatic tissue. The mesh size of the woven fabric did not affect the degradation rate of the PLGA film, but the cell aggregates formed faster with bigger mesh size. With bigger mesh size the cells spread through the woven fabric and with smaller mesh size the cells covered also the fibres. (Mayer et al. 2000)

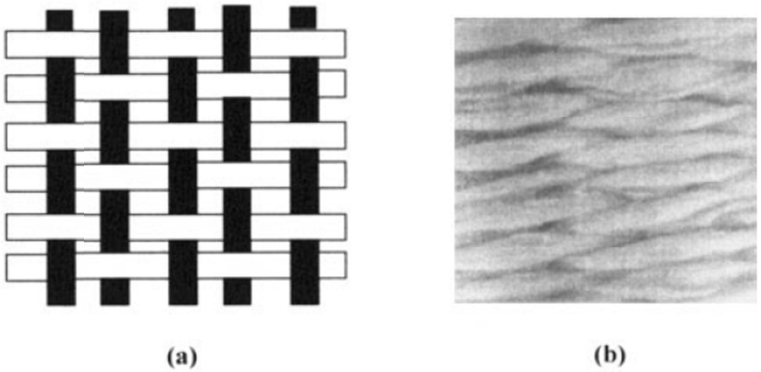

Figure 23 *a) a diagram of plain weave, b) close picture of woven PCL yarn (Khil et al. 2004).*

Khil et al. fabricated a **woven** scaffold of electro-wet spun, porous PCL-fibre using plain weave *(Figure 23)*. The structure was used to cultivate mammary carcinoma cells. It was shown that due to the porous structure the woven scaffold was a good surface for cell spreading. The woven surface supported tissue proliferation and appeared to be suitable for tissue engineering use. (Khil et al. 2004)

6.2.2 Textiles for bone applications

Use of textile structures in bone applications is challenging because of the load-bearing nature of bone. Transplants, and bioactive ceramics combined with different polymers and metals are used, but there is research also in using biodegradable materials. (Adanur 1995, p. 334-344) It is problematic that textiles structures alone cannot fulfill the mechanical properties in bone applications. (Hutmacher, 2000; Sell et al. 2007; Kang et al. 2008) There are several woven, knitted and nonwoven structures, which have been studied for bone repairing application. In addition **braided** structures of steel filaments are used to bone fracture stabilization and as sutures to connect implant to the bone. (Rigby and Anand, 2000, p. 407-424)

Woven structures

Alm et al. manufactured a woven scaffold (*Figure 24*) of bioactive glass fibres, which were coated with $PLGA_{80}$ (as warp, multifilament) and $PLGA_{80}$ fibres (as weft, monofilament) to be used in surgical stabilization of bone graft. The control samples were woven wholly of PLGA-yarns. The bioactive glass was in the structure to stimulate bone growth whereas the PLGA was to give the structure mechanical strength and flexibility. Due to the brittleness of the bioactive glass fibres, the structures woven on PLGA were more easily handled during the surgery. There were no signs of harmful tissue reactions and both of the fabrics were integrated with the bone surfaces and there was new bone formation to be seen. The glass parts were almost completely resorbed. (Alm et al. 2010)

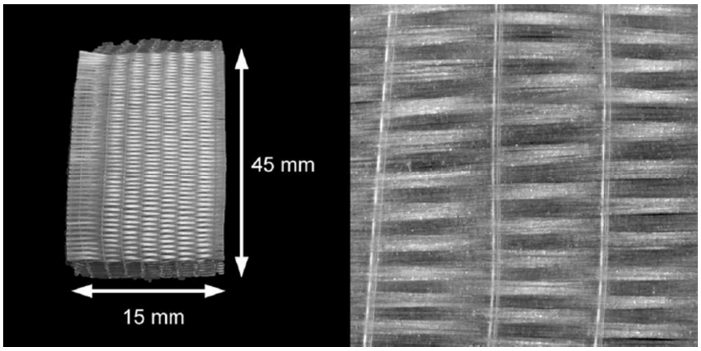

Figure 24 *The woven scaffold made of bioactive glass coated with PLGA and PLGA fibres. (Alm et al. 2010)*

Koh et al. fabricated a woven scaffold (*Figure 25*) out of PLA to strengthen the treatment of torn rotator cuff, since the major problems have been that the sutures cut through the tendon, or the failure of the fixation between the suture and the bone. In addition to failures of the fixation, an important aspect has been the osteoporotic weakness of bone with older people. The purpose of the woven scaffold was to strengthen the suture site, which connected the bone and tendon. This would allow the patients more normal life in the healing period. The scaffold was placed to the connection site of the bone and tendon so that sutures went through it (*Figure 25b*). (Koh et al. 2002) It was discovered that the woven structure resulted in a 25 % stronger structure compared to sutures alone. Failure occurred when the tendon was pulled through the sutures, and in most of the cases the woven scaffold stayed intact. (Koh et al. 2002)

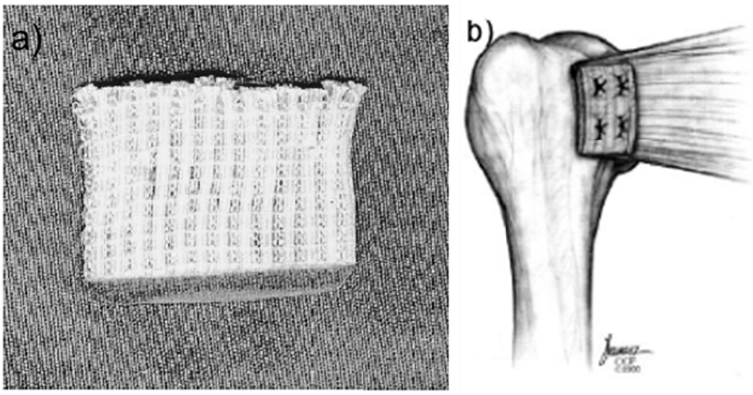

Figure 25 *a) Woven PLA scaffold, b) the rotator cuff suture anchor repair reinforced with the scaffold (Koh et al. 2002).*

Knitted structures

Kellomäki et al. manufactured a composite structure consisting of a film (PCL/PLLA copolymer) and a knitted mesh made of PLA (PLA96) spot-welded together, which resulted in a partly porous membrane. The composite and the knitted mesh alone were tested on a bone craft area. It was noticed that the composite material and the knitted mesh alone were able to protect the bone graft from resorbing and improved osteogenic

activity. The composite structure supported the bone formation better than the mesh alone. (Kellomäki, Niiranen et al. 2000)

Nonwoven structures

Nonwoven fabrics made of PTFE are used as an interface between tissue and the actual implant material for their large surface area and favorable surface for the cell attachment. Nonwoven fabrics made for instance via electrospinning are studied for their excellent properties in cell attachment and proliferation, but there are problems with the mechanical strength and the elimination of used solvent. Furthermore, the electrospinning technique does not enable the control over the porosity, pore size or pore interconnectivity. (Hutmacher, 2000; Sell et al. 2007; Kang et al. 2008)

Gomes et al. fabricated nonwoven fibre meshes of starch blended with ε-polycaprolactone (SPCL) and starch blended with polylactic acid (SPLA) for bone tissue engineering. The fibres were melt-spun and the fibre meshes were achieved by a fibre-bonding process. The scaffolds had adequate porosity and mechanical properties for supporting cell adhesion, proliferation and tissue regeneration. When the fibres were degrading, also the porosity of the structure was increased and thus, more space was released for the ingrowing tissue. The writers point out that the structures have potential to be used in bone tissue engineering. (Gomes et al. 2008)

6.2.3 Textiles for cartilage applications

When replacing cartilage, the cartilage type must be taken into account, because they differ a lot from each other. Hyaline cartilage found in joints is hard and dense and must withstand a lot of friction. On the other hand, fibrocartilage, in intervertebral discs, and elastic cartilage is much more flexible. (Rigby and Anand, 2000, p. 407-424) Cartilage has high modulus, and thus the scaffold used in connective tissue applications must be load bearing and withstand friction typical to e.g. articular cartilage. Connective tissue, especially cartilage, is naturally very avascular and fibroblasts are naturally growing in lacunas and. This must be taken into account in designing a base for cell growth. (Hutmacher, 2000)

The optimal solution for connective tissue damage is an autograft. However, this always results in another healing site and there is limited amount that autograft tissue. A natural choice for cartilage tissue engineering material is collagen (van der Schueren and de Clerck, 2011), due to the native construction of cartilage. However, collagen is not mechanically strong enough and it degrades in two weeks as implanted. Therefore, for example silk fibroine has been researched for its mechanical strength and biocompatibility. (Chen et al. 2008) Low-density polyethylene as nonwoven structures is found to be suitable for facial, ear and throat cartilage repair. For hyaline cartilage applications LDPE lacks in mechanical properties, and thus carbon-fibre reinforced composite structures are used. (Rigby and Anand, 2000, p. 407-424) **Nonwovens** are interesting in connective tissue applications for their high porosity, but their problem in

these applications is low mechanical strength, which could result in breaking of the structure before the tissue has healed (Hutmacher, 2000). Thus, as woven and knitted structures have better mechanical properties, they are researched.

Woven structures

Moutos and his colleagues (2007) manufactured a woven scaffold of biodegradable fibres for cartilage tissue. The scaffold had fibres woven in three directions, and thus the scaffold had different mechanical properties in each direction. The scaffold was seeded with chondrocytes placed in a gel and transplanted to damaged joint. The structure gave the chondrocytes time to synthesize needed proteoglycans and collagen, which are important for the healing tissue. The matrix possessed very similar tensile, compressive and shear moduli as native cartilage tissue. (Moutos, Freed and Guilak, 2007) Moutos et al. (2010) fabricated 3D woven scaffolds of poly-ε-caprolactone (PCL) for cartilage tissue engineering purposes. In the study woven scaffolds were combined with cartilage-derived matrix, woven scaffold alone, and cartilage-derived matrix alone were compared. The composite structures and woven structures did not lose their mechanical properties during the adipose stem cell cultivation. The composite structure promoted chondrogenesis and it had higher compression modulus than the cartilage-derived matrix itself. (Moutos, Estes and Guilak, 2010)

Valonen and her colleagues designed a poly-ε-caprolactone (PCL) scaffold for supporting cartilage tissue differentiation and growth by 3D-weaving technology. The scaffold was based on plain weave, where the warp yarns passed through the different woven planes. The structures were woven of multifilament yarn. Two different structures were fabricated, loosely (warp 8 yarns/cm, weft 20 yarns/cm) and tightly (warp 20-24 yarns/cm, weft 20 yarns/cm) woven structures, to evaluate their properties in chondrocytes cell culture. The loosely woven structure had greater porosity (68 %) than the tightly woven structure (61 %). In addition, the pores were larger in the loosely woven structure. In both, initial scaffolds and seeded scaffolds, the loosely woven structure had lower Young's Modulus. The mechanical properties of both, non-seeded and seeded scaffolds, resembled the mechanical properties of native articular cartilage. The scaffolds cultivated a longer period of time had a greater modulus than the acellular scaffold due to the formation of extracellular matrix. (Valonen et al. 2010) Ousema et al. (2012) used a similarly produced 3D woven scaffold for tissue engineering cartilage tissue. They also noted that it is possible to achieve mechanical properties comparable to native cartilage tissue by these woven scaffolds. The scaffold structure supported cell attachment and tissue formation. (Ousema et al. 2012)

Knitted structures

Vasara, Hyttinen et al. used the same previously mentioned composite of a film and a knitted mesh (Kellomäki, Niiranen et al., 2000) in cartilage damage repair in knee joint,

more specifically in autologous chondrocyte transplantation (ACT). The composite structure was compared with ACT covered with periosteum. The repair using the scaffold was failed due to delamination of the scaffold and no cartilage was generated. There was also loss in the bone matrix and distortion of the trabecular structure of subchondral bone. On the other hand, there were no degenerative changes in the joints, which can indicate that the conditions for cartilage regeneration were favourable. Thus, despite the lamination of the scaffold the inflammation reaction was minor. It was found out that the best results were achieved by using autologous chondrocytes and a periosteum. (Vasara, Hyttinen et al. 2004)

6.2.4 Textiles for restoring of finger joints

Honkanen and Kellomäki manufactured a P(L/D)LA 96/4 **knitted** scaffold (*Figure 26*) to restore the finger joint mobility of rheumatoid arthritis patients. The conventional silicone implants, Swanson prosthesis, have durability and bone resorption problems, prosthesis migration, infections and foreign body reactions. The purpose of the biodegradable implant was to overcome those problems and maintain the space between the bone ends of the finger joint. The scaffold was knitted with multifilament yarn with a tubular single jersey knitting machine. Final form of the mesh-like scaffold was achieved by heating it in a mold. Fibrous tissue ingrowth occurred and the scaffold was mechanically strong a long enough time period. The outcome two years post-operatively was reduced pain and improved joint mobility, meaning that functional joint was achieved *in situ* with the scaffold. At the time point the whole scaffold had not yet been resorbed. (Honkanen and Kellomäki et al. 2003)

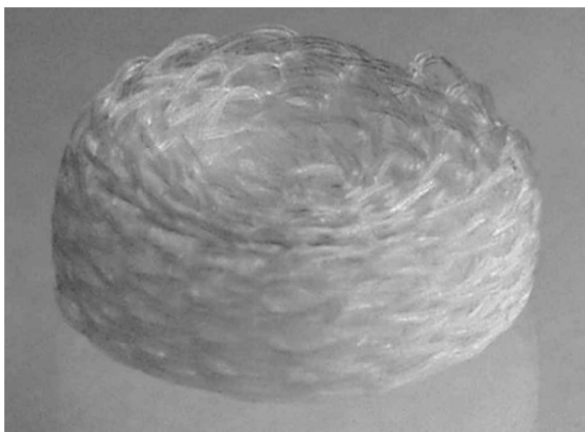

Figure 26 *Resorbable knitted joint scaffold (Honkanen and Kellomäki et al. 2003).*

The group reported later in year 2009, as the whole scaffold had been replaced by fibrous tissue, that the functionality of the hand had improved. There were very little osteolytic changes in the joints, which indicates that the resorption of the implant did not induce osteolysis. The results were comparable with the silicone implants. (Honkanen and Kellomäki et al. 2009)

6.2.5 Textiles for tendon and ligament applications

Karamuk et al. manufactured **woven** scaffolds (*Figure 27b*) of PET monofilaments and the structure seeded with tenocytes was exposed to cyclic mechanical stimulation in 45° direction to warp and weft (*Figure 27a*). The fabric was suitable for the cells to adhere and spread, the surface was 95 % covered with viable cells, as were the openings between the filaments. (Karamuk et al. 2004)

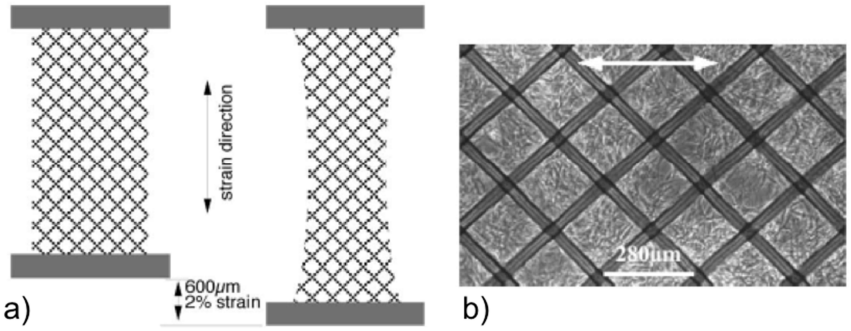

Figure 27 *a) A schematic picture of the woven PET scaffold used for mechanical stimulation of tenocytes. b) Vital/avital composite 6 days after cell seeding (light microscopy). Arrow indicates the stretching direction. (Karamuk et al. 2004)*

In addition to woven structure, **braided** structures can be used in tendon repair, usually fabricated of polytetrafluoroethylene (PTFE), polyester, polyamide, polyethylene or silk. Due to the braiding technique the structures are naturally tubular and elastic, and thus suitable for artificial tendons. Artificial replacements for knee ligaments (especially for anterior cruciate ligament, ACL) are often braided structures made of polyester or a composite of polyester and carbon fibres. They are suitable for their high mechanical properties due to their creep resistance in cyclic loading. (Rigby and Anand, 2000, p. 407-424)

6.2.6 Textiles for vascular applications

Vascular grafts on the market are fabricated of polyester (e.g. Dacron®) or PTFE multifilament yarn via weaving or warp knitting, since both of the materials are biocompatible and hemocompatible. Weft knitting is no longer used because of the risk of unravelling of the structure. (Doser and Planck, 2011) The challenges in vascular applications are aneurysms, intima hyperplacia and possible thrombs and embolia. That concerns also transplants. (Yokota et al. 2008) There are already structures commercially available for blood vessel applications, e.g. to replace obstructed or weakened part of a blood vessel. For instance, Gore-Tex® Stretch Vascular Graft (GoreMedical) or VascuGraft® PTFE (B. Brown). In addition, there are PTFE prostheses coated with e.g. heparin to prevent clotting (GORE®VIABAHN® endoprosthesis with PROPATEN bioactive surface).

Woven structures

Yokota and colleagues fabricated a woven two-component scaffold for small arteries (*Figure 28*), because prosthesis made of expanded polytetrafluoroethylene (ePTFE) can only be used for larger-diameter arteries. The scaffold consisted of a tubular plain weave fabric and collagen spongy structure. The woven fabric was manufactured of fibre that had a PLLA core and a PGA surface. The structure was seeded with fibroblasts and vascular endothelial cells and tested *in vitro*. Cells spread better on the composite structure than on the woven fabric alone. Due to the purpose to use the two-component scaffold cell seeding, it was implanted without cells. *In vivo* the composite structure was covered with uniform monolayer of endothelium, which on the other hand, is not possible with e.g. PTFE. The structure formed *in vivo* was very similar to the natural layer-like structure of arteries. There were no thrombosis, aneurysms nor failure of the sutures. (Yokota et al. 2008)

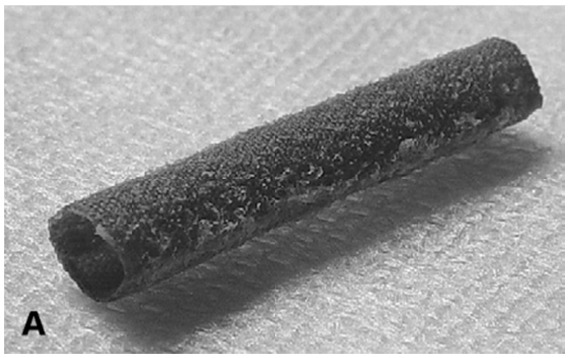

Figure 28 *Woven, tubular structure for vascular prosthesis (Yokota et al. 2008).*

Warp knitted structures

Due to the fact that **warp knitted** structures are highly porous and the pores are often large, there is a risk of blood leakage, even though porosity would be important for the new tissue formation. To prevent haemorrhage and to fill the openings knitted grafts with velour surfaces (inside and outside) have been developed. The openings can also be sealed with patient's blood (preclotting) or by impregnating the graft with collagen or gelatin (Rigby and Anand, 2000, p. 407-424; Doser and Planck, 2011). Impregnating with biodegradable material allows non-porosity in the beginning of the implantation and pores become available to cells after the degradation of the material. (Rigby and Anand, 2000, p. 407-424) A typical type of warp knitted vascular prosthesis is presented in *Figure 29.*

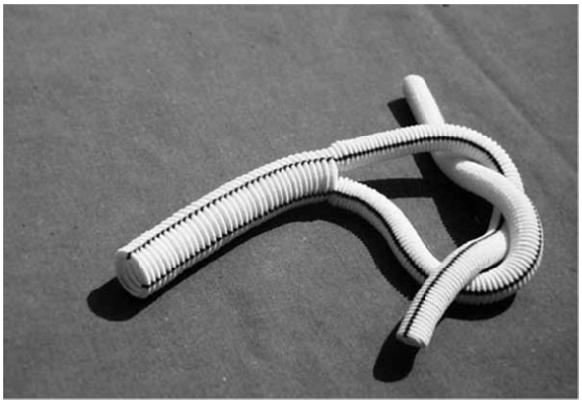

Figure 29 *A typical warp knitted vascular prosthesis out of PET (Doser and Planck, 2011).*

The size of the openings can be reduced also by seeding the inner surface of the graft with endothelial cells. That way it resembles more natural blood vessel and the cells also prevent blood clotting (Doser and Planck, 2011). Compared to warp knitted structures, woven structures are denser and they have lower porosity and elasticity and they are very strong. They can be used in areas where high pressure is directed to the structure. (Rigby and Anand, 2000, p. 407-424; Doser and Planck, 2011)

Koch et al. manufactured a tubular composite structure of a fibrin gel scaffold supported by a warp-knitted mesh (poly(L/D)lactide 96/4 (P(L/D)LA 96/4, on the inner surface) for small caliber vascular applications. The fibrin gel was acting as adhesion material to the cells and the mesh as a supporting structure to give mechanical strength. The scaffolds were seeded with autologous arteria-derived cells and implanted. There was no thrombus or aneurysm formation or calcification during the 6 months of implantation. A confluent monolayer of endothelial cells was achieved in the inner surface of the graft. Compared to more traditional Gore-Tex grafts, which suffered from thrombus formation, the results are promising. (Koch et al. 2010)

Braided structures

Uurto et al. manufactured biodegradable drug-releasing stents of self-reinforced PLDLA by braiding for both vascular and urethral purposes. In animal studies long-time inflammatory changes were not seen after two months. One of the drugs (dexamethasone with high doses) increased the chronic inflammation and foreign body reaction and another (indomethacin) increased fibrosis. It was found out that the material was very biocompatible and the stents seemed to be promising for treating vascular occluding diseases, even though their efficacy still needs to be proven in more accurate studies. (Uurto et al. 2007)

Zamiri et al. fabricated braided, biodegradable vascular stents of PLGA (10:90 and 85:15), polydioxanone (PDO), and PLLA attached to metallic stents to test their biocompatibility *in vivo*. Permanent metallic stents can cause long-term mechanical stress and chronic inflammation to the implantation site. Even PLLA degrades too

slowly (two years) considering that the natural vascular healing after the placing of the stent is completed in one year. The purpose was to achieve more rapidly degrading stents. The stents were implanted in porcine carotid arteries. The inflammation was from minimal to moderate with all the materials after 90 days and there was no foreign body reaction or occlusion of the vessels. The arteries had confluent endothelial layer with all the polymers used. Depending on the material all the stents were degraded in less than a year. (Zamiri et a. 2010)

7 IN VITRO STUDIES FOR OCULAR APPLICATIONS

Retinal pigment epithelial cells can be differentiated by culturing e.g. human embryonic stem cells or induced pluripotent stem cells. Feeder cells, usually of animal-origin, are usually used during the culturing. However, there is a problem using animal-derived products, because they can carry factors such as sialic acid or even pathogens, which can cause immunogenicity. The most used culture media are fetal bovine serum (FBS) and KnockOut™ Serum Replacement (KOSR), which still contains e.g. bovine-derived transferrin. The most used feeder cells are mouse embryonic fibroblasts. It has been suggested that the use of mouse embryonic fibroblasts as feeder cells could induce spontaneous differentiation to RPE cells. Vaajasaari and colleagues differentiated successfully RPE cells from human embryonic stem cells and human induced pluripotent stem cells without the use of animal-derived serum, and feeder cells used were of human origin (human foreskin fibroblasts). The cells cultured with human feeder cells had as good ability to differentiation as those cultured on mouse embryonic fibroblasts. (Vaajasaari et al. 2011)

Ilmarinen et al. cultivated oral mucosal epithelial cells on collagen IV coated culture inserts with 1-μm pores (permeable membranes). The cells were cultivated without feeder cells or serum, which are normally used to achieve stratified tissue. The cell culture was intended for use of ocular surface reconstruction. The non-keratinized oral mucosa epithelium can be used because it resembles a lot the corneal epithelium, it has potential for proliferation and it is easily available. The cells formed stratified tissue, which was wanted. (Ilmarinen et al. 2012)

Subrizi and colleagues cultured human stem cells -derived RPE cells on porous polyimide membranes coated with different biopolymers, such as laminin, heparin sulphate, hyaluronic acid, and collagen types I and IV. The cultured cells had typical properties and functions of retinal pigment epithelium. The cellular attachment and growth was poor on uncoated membranes. Laminin, hyaluronic acid and heparin sulphate coating did not improve the results. On the other hand, laminin and both types of collagen allowed cells to grow and the cells had typical morphology and pigmentation to retinal pigment epithelia. According to the writers, it is not surprising that laminin and collagen are suitable, since they both are naturally present in the retinal pigment epithelial basal lamina, i.e. Bruch’s membrane, which acts as an anchoring surface for the cells. (Subrizi et al. 2012)

Treharne and colleagues designed an electrospun biostable nonwoven scaffold from methyl methacrylate and polyethyleneglycol (PEG) methacrylate copolymer for RPE

scaffold to replace the Bruch's membrane. The scaffolds had a uniform, smooth surface and the fibres were in random directions. The fibre diameter was 1.9 μm and the thickness of the scaffold 50 μm. Treharne et al. pointed out that the thickness must be decreased in the future for the scaffold to fit better to the subretinal space. Some of the scaffolds were surface treated with short-chain peptides to enhance cell adhesion before seeding with human RPE cells. The cells covered the fibres more thoroughly than with untreated scaffolds. In general, the electrospun structure was suitable for the cell growth and possibly potential support in RPE transplantation. (Treharne et al. 2012)

Lu and colleagues designed a parylene-C membrane supported by a mesh and used to culture RPE cells and to replace the Bruch's membrane. Even though parylene-C is usually a very good barrier material, it is semipermeable to macromolecules in submicron scale thickness. Thickness of 0.30 μm enabled the nutrients to pass through. Since the thin membrane did not possess good mechanical strength, the hexamethyldisilaxane coated silicon mesh was included to stabilize the structure. The mesh-supported membrane structure functioned well and monolayer of RPE cells was formed and it resembled the native cells. (Lu et al. 2012) Lu et al. compared the structure to other similar kinds of studies. For example collagen I was difficult to handle and it was hard to manufacture to a larger uniform sheet (Lee et al. 2006 according to Lu et al. 2012). Also using polydimethylsiloxane (PDMS) had its problems: it was hard to obtain a thin enough membrane, even though with proper surface treatment it supported the growth of RPE cells (Krishna et al. 2007 according to Lu et al. 2012). Polyester (Lee et al. 2007 according to Lu et al. 2012) and PMMA (Tao et al. 2007 according to Lu et l. 2012) porous membranes have also been studied, but usually the porous area compared to the whole area was too small and the topography of the membrane differed significantly from the native Bruch's membrane.

Kearns et al. manufactured culturing surfaces for RPE cells of different plasma polymers. The plasma polymers enabled the change the surface properties while the bulk properties remained unchanged. The polymers were acrylic acid (AC), allyl amine (AL) and the control samples were manufactured of octadiene hydrocarbon films and polystyrene films. The surfaces were very different: octadiene hydrocarbon was the most hydrophobic, and on the other hand, acrylic acid was relatively hydrophilic. RPE cell line and primary RPE cells were used. The cells grew confluently and formed a monolayer on all the surfaces except on the octadiene hydrocarbon films. In general, the primary RPE cells had low proliferation. (Kearns et al. 2012)

Shadforth and colleagues fabricated membranes of *Bombyx mori* silk fibroin as a Bruch's membrane substitute by casting from an aqueous solution of poly (ethylene oxide) (PEO). The thickness of the membranes was 3 μm and the pore sizes 4.9 ± 2.3 μm (upper surface) and 2.9 ± 1.5 μm (lower surface). Different extracellular proteins were used in coatings, but the cell attachment was best with vitronectin coating. The structure was suitable in culturing RPE cells and the permeability and thickness resembled the native Bruch's membrane. The morphology of the cells resembled the natural RPE cells especially in long-term cultures. (Shadforth et al. 2012) Kim and

colleagues compared to different culturing surfaces, laminin-coated and plain uncoated surfaces for human retinal pigment epithelial cells. The laminin-coated surface supported the cell adherence, maturation and growth better than the uncoated surface. The stratification of the cells occurred more rarely and typical tight junctions were formed more easily on laminin-coated surfaces. (Kim et al. 2012)

7.1 Polyethylene terephthalate films for ocular cell cultures

In making a film of PET the molecular weight should be suitable to get good-quality film. The polymer chains should be long, but too long chains result in excessively entangled polymer chains, which disturb the film formation. Usually the suitable number of monomer units in polymer is around hundred. For film applications PET has good mechanical strength, it is optically transparent, thermally and dimensionally stabile and resistant to many chemicals. In general, PET films are not very resistant to alkalis, but they resist strong acids well. (Tsunashima et al. 1999, p. 320-352)

When the film is manufactured, the PET pellets are melt in the extruder and made into a thin sheet by pressing it through a slit-shaped die onto the casting drum. This polymer sheet does not have good mechanical properties, because it is not oriented. The sheet needs to be heated again and stretched bi-axially. The stretching causes the polymer chains to orientate, which improves the mechanical properties. The achieved film has a quality of shrinking at high temperatures. Therefore, it needs to be heat set. This heat setting is done under tension and its purpose is to remove stress caused be the stretching and to support further crystallization. Common values for bi-axially stretched PET film are tensile strength of 25 kg/mm^2, tensile elongation of 120 %, elastic modulus of 400 kg/mm^2. PET film, which is partly crystalline, has a relatively high glass transition temperature (T_g), 120 °C, compared to amorphous PET (approx. 70 °C). (Tsunashima et al. 1999, p. 320-352)

In general, gas barrier properties are decreasing as the temperature increases, and water vapour permeability decreases as the film thickness increases (Tsunashima et al. 1999, p. 320-352). The water vapour and oxygen permeability of PET and PP are compared in *Table 3.* Water vapour permeability is greater with PET than PP. On the other hand, PP has significantly greater value in oxygen permeability than PET. The permeability values for different gasses and liquids are presented in *Table 4.*

Table 3 *Comparison of water vapour and oxygen permeability of PET and PP bi-axially stretched films (Tsunashima, Toyoda and Yoshii. 1999. p. 320-352).*

	Water vapour permeability, 40 °C, 90 % RH, $\left(\frac{g \cdot 0.1mm}{day \cdot m^2}\right)$	**Oxygen permeability,** 25°C, 1 atm, $\left(\frac{cc \cdot 0.1mm}{day \cdot m^2}\right)$
PET	5.5	19
PP	1.5	240

Table 4 *Gas and liquid permeability values for PET film (modified from Tsunashima, Toyoda and Yoshii. 1999. p. 320-352)*

Gas	**Gas permeability,** 25 °C, 50 % RH $\left(\frac{cc \cdot \mu m}{10^4 cm^2 \cdot day \cdot atm}\right)$	**Liquid**	**Liquid permeability**, 25 °C $\left(\frac{g \cdot \mu m}{10^4 cm^2 \cdot day}\right)$
O_2	28	**H_2O**	3.0
CO_2	120	**C_2H_5OH**	≤ 2.0
SO_2	6.0	**C_7H_{16}**	≤ 2.0
		$CH_3COOC_2H_5$	1.7

PET films with micron scale pores are used in culturing RPE cells among many others. The pore size can be chosen depending on the cells. Several companies are manufacturing PET membrane culture insets. (Becton, Dickinson and Company. 2012. Biosciences Cell Culture – Cell Culture Inserts – Features – Multiwell Insert Systems; Greiner Bio-One, ThinCerts™ Cell Culture Inserts; Millipore Corporation. Millicell 24-well Cell Culture Plate; Millipore Corporation. 2009. Millicell® Hanging Cell Culture Inserts - Single and Preloaded Inserts.) The principle and different possible culturing methods are presented in *Figure 30.* In general the whole structure consists of an insert that can be hung inside normal laboratory well plates. The surrounding housing polystyrene and the thin, porous PET membrane is located as the bottom of the cup. The cells can be cultivated as submersed in the medium (*Figure 30a*), or in contact with air at the air-medium interface (*Figure 30b, 30c*). (Greiner Bio One Catalogue Benelux 2010/2011 at http://epub02.publitas.com/625/1/#/zoompage/53/ p. 52)

The company Greiner Bio-One is manufacturing cell culture inserts consisting of a polystyrene housing and PET membrane. The pores are different sizes, 0.4 µm, 1.0 µm, 3.0 µm and 8.0 µm, of which pores sizes less than 3.0 microns can be used to cultivate RPE cells that can have diameter of a few microns minimum. The well-defined pore sizes and densities ensure optimal exchange of nutrients and metabolites and do not

limit the gas change. The cellular adherence to the membrane surface is ensured with physical surface treatment. (Greiner Bio-One, ThinCerts™ Cell Culture Inserts)

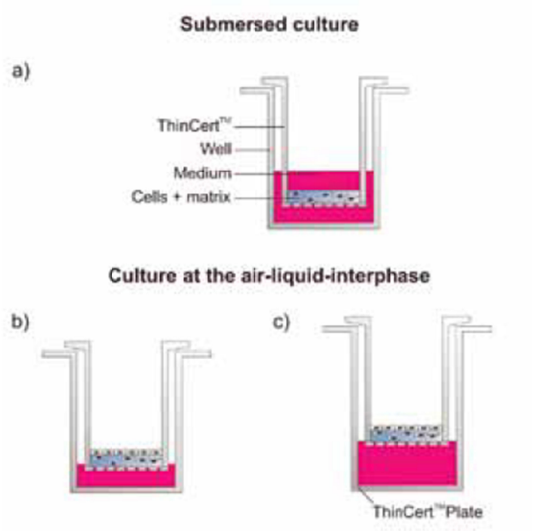

Figure 30 *Different culture types, which can be used with culture inserts with hanging geometry a) Culture submersed in medium, b, c) culture at the air-liquid-interphase (Catalogue Benelux 2010/2011 by Bio Greiner One at http://epub02.publitas.com/625/1/#/zoompage/53/ p. 52).*

Becton, Dickinson and Company as well make these kinds of cell culture inserts with 24 or 94 wells and various pore sizes. The surface is coated with fibrillar collagen (pore size of 1 µm) or fibronectin (pore size of 3 µm) to improve cell adherence. (Becton, Dickinson and Company. 2012. Biosciences Cell Culture – Cell Culture Inserts – Features – Multiwell Insert Systems.) Millipore is manufacturing similar type culture inserts of PET membrane with pore sizes 0.4 µm (1×10^8 pores/cm^2), 1.0 µm (2×10^6 pores/cm^2), 3.0 µm (2×10^6 pores/cm^2), 5.0 µm (6×10^5 pores/cm^2), and 8.0 µm (2×10^5 pores/cm^2). Their purpose is to support cell attachment, growth and differentiation. The culture insert is designed to inhibit air bubble formation and to ensure the nutrients for the cells. (Millipore Corporation. Millicell 24-well Cell Culture Plate; Millipore Corporation. 2009. Millicell® Hanging Cell Culture Inserts - Single and Preloaded Inserts)

RESEARCH PART

8 MATERIALS AND METHODS

8.1 Materials

The samples were woven of PET multifilament yarn, which was 78 dtex in fineness and 20 turns/meter in twist (Finn-Nauha Oy, Haapamäki, Finland). Each yarn was constructed of 24 separate filaments (manufactured by Sinterama, Biella, Italy). The warp yarns were laid on four identical section beams instead of just one warp beam. Each section beam had 25 warp yarns. The same multifilament yarn was also used as the filling yarn. To get high warp and weft densities, paraffin oil was used in making some of the samples and ethanol to rinse out the paraffin oil. Cotton yarn (approximately 35 tex in fineness, manufacturing information not available) was used for modelling before the actual samples. Because the cotton yarn, that was used, is not as fine as PET or PLA yarns, it is considered just as a rough model for its cheaper cost.

8.2 Methods

8.2.1 Weaving loom and winding machine

The samples were woven by using a Saurer narrow weaving loom (*Figure 31*) (Aktiengesellschaft Adolph Saurer, Arbon, Switzerland, model number or name not available) with all together hundred warp yarns from four separate section beams. The machine was cam-controlled and used a mechanical shuttle for the weft insertion. The warp let-off was done by mechanical weights for each of the section beams and fabric drawing.

Figure 31 *Saurer cam-controlled narrow weaving machine.*

In the weaving loom there were several possibilities to adjust the fabric properties and to achieve optimal yarn density. The weft density was adjusted in the front side of the machine by increasing or decreasing the fabric up-take. In addition, increasing or decreasing the weights in the warp let-off had an effect on the warp tension, and thus to weft density. The weft yarn was wound with Hacoba-winding machine (Hacoba Textilmaschinen GmbH & Co, Wuppertal-Barmen, Germany, model BSAX/1, machine number 030).

8.2.2 Microscopical imaging

Stereomicroscopes, Zeiss SV8 (Zeiss, Germany) and UNION US601 (Union Optical CO., Ltd. Tokyo, Japan), were used to get an overall appearance of the structure, and to inspect the surface of the fabric. Magnifications of 0.8 and 1.2 were used for cotton samples and magnification of 6.3 (UNION US601) or 6.4 (Zeiss SV8) for the PET samples. Two stereomicroscopes were used due to the unavailability of the Zeiss SV8. An Olympus BH2-UMA microscope (Union Optical CO., Ltd. Tokyo, Japan) and Leica DM 2500-M (Leica Microsystems, Wetzlar, Germany, with Leica Application Suite program) with magnification of 10 (f=180) were used to get a more accurate image of the pores between yarns crossing in the interlacing points and between the filaments. This particular imaging was only used for the PET samples. All the samples were inspected on both sides, taking 2-4 parallel photographs of the structure.

From the best weave patterns, plain weave and plain weave derivative, the highest warp densities (ten and twelve yarns/reed dent) were imaged with polarized light on a microrobotics platform (on the Department of Automation Science and Engineering), mentioned in the Master's Thesis by Saketi (2010). The platform uses two high optical resolution digital cameras with a 1.5 times magnifying lens, an effective zoom and micro- and nanorobotics to achieve high quality images. The images were processed by using appropriate threshold values by using Gimp, Image Manipulation Program (Gimp 2.8.3, © 1995 – 2012). This was done to separate all the through-going light from the background shades. Polarized light was used because the round, smooth and clear polyester fibres reflect unpolarized light making the imaging very hard.

8.2.3 Optimizing the parameters with cotton yarn

In *Table 5* are presented the weave patterns used for the modelling. These structures were the base in deciding the densest weave patterns to be woven out of PET filament yarn. Different weft densities were tested to see the differences in the fabric's surface and porosity by altering the fabric take-up rate. The specimens are unnamed because some of the weave patterns did not have names, and many of those were not used further to make PET samples.

Table 5 *Weave patterns out of cotton yarn, number of tested weft densities and suitability to be woven with PET filament yarn.*

Number of harnesses	Specimen number	Weave pattern	Number of different weft densities	Further made of PET
4	Specimen 1	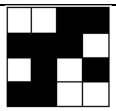	2	
4	Specimen 2	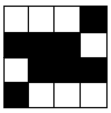	1	
4	Specimen 3, plain weave	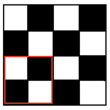	1	X
4	Specimen 4, weft rib	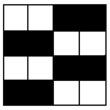	3	X
4	Specimen 5, twill-like weave	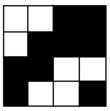	3	X
4	Specimen 6	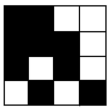	3	
4	Specimen 7	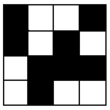	3	
4	Specimen 8	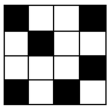	4	
4	Specimen 9	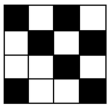	3	
5	Specimens 10 and 11, satin	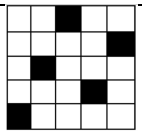	1, 2	X
6	Specimen 12	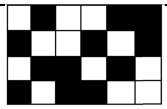	2	
6	Specimen 13	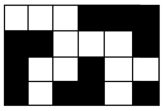	1	

Specimens 2, 3 and 13 were woven only with one weft density. Specimens 1 and 12 were woven with two different weft densities and specimens 5 –7 and 9 with three different weft densities. Only specimen 8 was woven with four weft densities. Two types of satin (specimens 10 and 11) were woven, one with 4 yarns/reed dent and other

with 5 yarns/reed dent. The satin with 4 yarns/reed dent was woven also with two weft densities.

8.2.4 Weaving with polyethylene terephthalate yarn

Different weave patterns of the cotton samples were chosen, and woven also out of PET filament yarn. To compare the different weave patterns, control samples of plain weave were woven with three different warp densities (4, 6 and 8 warp yarns/reed dent). The other weave patterns were woven with two different warp densities, with 6 and 8 yarns/reed dent. The chosen weave patterns are summarized in *Table 6.*

Table 6 *Woven samples out of PET filament yarn.*

Number of harnesses	Pattern name	Weave pattern
4	Plain weave	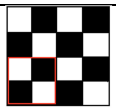
4	Weft rib	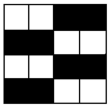
4	Twill derivative	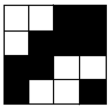
5	Satin	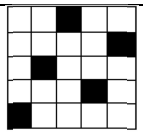
6	Plain weave/twill combination	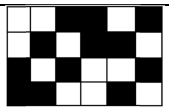
6	Plain weave/twill combination 2	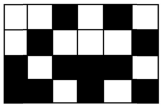
6	Plain weave derivative	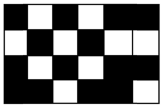
6	Twill derivative	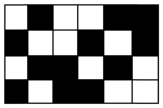
6	Twill derivative 2	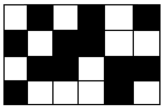

To get denser structures, plain weave and plain weave derivative, were woven with warp densities of 10 and 12 yarns/reed dent. The weaving was done with the help of paraffin oil, which was washed away by rinsing three times with ethanol (ETAX Ba,

99.9 V-%). Paraffin oil was chosen for its non-toxicity and easy removal without organic solvents.

8.2.5 Fabric properties

The fabric's **mass per unit area** was determined according to standard SFS 3192 Tekstiilit. Tasomaisten tekstiilituotteiden neliömassan ja juoksumetrimassan määrittäminen. Textiles: Determination of mass per unit area and per unit length of textile fabrics. Because the fabric was so narrow, several small samples were cut total area of them being at least 100 cm^2, if possible 250 cm^2. Due to the difficulties in fabricating uniform samples, the minimum area was chosen and the mass per unit area was calculated on one locations for each sample. They are weighed with analytic scales, Mettler PC220 (Mettler Toledo International Inc, Greifensee, Switzerland). The mass per unit area is reported in g/m^2 (three significant digits) in Appendix 1.

The **thickness** of the samples was determined by using a micrometer gauge (Mitutoyo Micrometer (No. 293-521-30 5031529, Mitutoyo Scandinavia AB Finnish branch, Vantaa, Finland). The thickness was measured in five different locations. The samples were not conditioned before the testing and they were kept in room temperature and humidity. The thickness is the arithmetic mean of the results. The results and their standard deviations are presented in Appendix 2.

The **yarn numbers per unit length** were determined according to standard SFS-EN 1049-2 Tekstiilit. Kudotut kankaat. Rakenne. Analyysimenetelmät. Osa 2: Lankatiheyden määrittäminen. Textiles. Woven fabrics. Construction. Methods of analysis. Part 2: Determination of number of threads per unit length. Method A, Dissection of fabric, was selected. The cut samples were unraveled to single yarns and count. For a fabric of 10 – 25 threads per centimetre the minimum measuring distance is 5 cm on weft direction according to the standard. With narrow fabrics all the yarns are count in the warp direction. The samples were not conditioned before the counting. In weft direction the threads were count from five different locations, the counting length was 5 cm. The results and the standard deviations of the weft densities are reported in yarns/cm, in Appendix 2.

8.2.6 Permeability and wetting

The **geometrical cover factor** (CF) was calculated according to the equations 3 – 5. The yarn count results were used in calculating the cover factors and the cover factor for warp and weft direction are presented in Appendix 3. **Void volume**, which describes the density and permeability properties of the samples, was calculated according to equation 12 using the mean values of thickness and mass. These results are also reported in Appendix 3.

Contact angle measurements were done to the densest samples, i.e. plain weave and plain weave derivative with warp densities of 10 and 12 yarns/reed dent. To be certain that the previous handling with paraffin oil does not affect the contact angle

results, the samples were washed in ethanol using V011 m-Range ultrasonic wash M12 (FinnSocic Oy, Lahti, Finland). De-ionized water (DI-water) and Dulbecco's Modified Eagle Medium (DMEM) culture media were used with the contact angle measurement program Attension Theta Software (version 4.1.0, 1997-2009, Biolin Scientific Oy, Stockholm, Sweden). DMEM was chosen for the purpose of using the fabric in cell culturing. Plain weave with warp density of 8 yarns/reed dent was used as a control. Ten parallel measurements were done to the weave samples using droplets around 6 µm in volume. The volume of the droplet was estimated by eye in the case of DI-water and with a microliter pipette with cell medium. The droplet was carefully lowered to the surface and the images were taken after 1 second the droplet had been put to the surface. The program calculated automatically the left and right contact angles. Mean values and standard deviations of the contact angles were count and are presented in Appendix 4. It was also approximated whether the droplet was absorbing through the structure.

8.2.7 Tensile testing

The defining of the **tensile strength** of the PET samples was done according to European Standard EN ISO 13934-1:1999 "Textiles – Tensile properties of fabrics – Part 1: Determination of maximum force and elongation at maximum force using the strip method (ISO 13934-1:1999)". The Instron 4411 mechanical testing machine was used (Instron Ltd., High Wycombe, Great Britain). At least five parallel samples in the warp direction were tested. Due to the maximum width of the fabric being significantly less than 50 mm, the whole fabric was used in the testing in the warp direction and weft direction was not used at all. In addition the fringing of the fabric's longitudinal edges cannot be done due to the width of the fabric. Instead, only the wefts were cut loose on the edges so that they do not affect the results. The length of the specimens was decided so that the ratio width : length was 1 : 5. Gauge length was the same as the specimen length. The jaws were corrugated (25 mm in width) and rate of extension 20 mm/min, with maximum load of 5 kN. Due to the intension of using the structures in cell studies, the tests were only done wet by using room temperature distilled water. For wet testing the samples were immersed in the water overnight in room temperature. The sample was mounted on the test machine straight from the water (carefully drying) without pretension. The test results with asymmetric or more than 2 mm slippage were excluded. According to the standard also samples that broke within 5 mm of the jaws were to be excluded, but breakage near the jaws was typical to the samples, and thus all the results were taken into account. The test parameters for both, fabric and yarn, are given in *Table 7.*

Strength, maximum load and strain at maximum load values were count by the Intron IX program directly (Intron Series IX, Automated Materials tester, Version 8.31, High Wycombe, Great Britain). Young's modulus was determined by using Microsoft Excel from the load-displacement graphs by calculating the slope of the second linear part of the curves. The moduli were count to the woven PET samples separately using the average of all the values. The area where the slope was count is marked in the

graphs with a rectangular shape. That part of the curve resembles the straightening of the warp crimp. Therefore, the particular slope was decided. Thus, by comparing the moduli the differences between the weave patterns and their influence on the mechanical behaviour can be seen. All the tensile testing results are presented in Appendix 5.

Table 7 *Test parameters for tensile testing of PET fabric and yarn.*

	Fabric	**Yarn**
Parallel samples	5 – 6	20
Specimen length (mm)	1 : 5 (ratio width : length)	250 / 50
Gauge length	Specimen length	Specimen length
Rate of extension (mm/min)	20	250 / 20
Maximum load	5 kN	500 N

To get control values, tensile testing was done to **the PET filament yarn** according to the standard SFS-EN ISO 2062 Tekstiilit. Kehiöllä olevat langat. Yksittäisen langan murtokuormituksen ja murtovenymän määrittäminen. Textiles. Yarns from packages. Determination of single-end breaking force and elongation at break. The Instron machine was used to test two sets of samples: dry according to the standard and wet to make the comparison between the yarn and narrow fabric easier. Power cell of 500 N was used. The dry samples were tested without preconditioning, with the gauge length of 250 mm and rate of displacement 250 mm/min and the wet samples with the gauge length of 50 mm and the rate of displacement 20 mm/min. Flat, rubber-faced jaws were used and the samples were mounted on the machine without pretension. 20 parallel samples were made of both yarn sets, all of them of the same cone of yarn. The wet samples were kept in distilled water more than three hours before testing.

9 RESULTS AND DISCUSSION

9.1 Microscopic evaluation of cotton fabric

For **specimen 1** the surface was very rough and had clear and strong rises parallel to weft. There was random unevenness in the warp direction, which caused openings to the structure. With the magnification of 1.2 the structure seemed relatively even and dense. With greater weft density (i.e. smaller take-up rate as weaving) the structure was denser in weft direction, but unevenness parallel to the warp yarns was greater. Due to the unevenness of the warp yarns, there were clear openings to be seen in the structures, with both weft densities. **Specimen 2** had the weave pattern, which is very dense in the middle but less dense in the sides. Due to this alternating pattern there were denser and sparser regions in the fabric. The openings through the fabric were clear, repeating, parallel to the warp. The plain weave, i.e. **specimen 3**, was identical on both sides, because of the small repeating unit of weave pattern. It did not have long yarn floatings, and the structure was significantly denser as the samples 1 – 2. With the same magnification of 1.2 there were no openings to be seen.

Specimen 4, weft rib, was woven with three different weft densities. All the specimens were very even on both sides and there were no openings to be seen. Sample with the largest weft density was the densest. The surface of **specimen 5** (a twill-like weave) resembled a normal twill surface on both sides. The sample with greatest weft density was denser than the samples with two smaller weft densities. The right side of the fabric was even, and the reverse side had cavities. However, they did not pass through the fabric. **Specimen 6** was very sparse even to bare eye and there were openings with all weft densities. **Specimen 7** was sparse, it had regular, repeating openings in weft direction with two of the lower weft densities. With the highest weft density there were openings but were not regular. **Specimen 8** was very sparse and had large openings in the three smallest weft densities. The densest structure was more even on the right side. However, the reverse side had regular unevenness in the warp direction. **Specimen 9** (with all the weft densities) was more even than specimen 8, but the structure still had regularly repeating openings even with the greatest weft density.

Both of the satin, **specimens 10 and 11**, had a dense and consistent surface on both sides of the fabric. There were typical long yarn floatings on the reverse side. The satin woven with warp density of 4 yarns/reed dent was denser than with 5 yarns/reed dent (smaller weft density). This was probably due to the greater fabric up-take. Satin with 5 yarns/reed dent and greater weft density was clearly denser than with smaller weft density. In addition, it was denser than the satin with 4 yarns/reed dent. In **specimen 12 (**so-called plain weave derivative) the structure had floatings of two yarns at the longest,

and partially the weave pattern resembled plain weave. With smaller weft density the structure seemed dense and uniform. No visible through-going openings were seen with magnification of 1.2. There were cavities in the areas without yarn floatings, since the yarns were more crimped in those areas. The cavities, however, did not pass through the fabric. With greater weft density there was visible unevenness in the warp direction. **Specimen 13** had yarn floating of maximum three yarns. The purpose of the yarn floatings was to get the yarns closer to each other to achieve smaller openings. However, the structure had numerous openings and it was very uneven.

To summarize, these findings were used to evaluate, which of these weave patterns could be woven out of PET yarn. The best weave patterns had numerous interlacing points and the interlacing points were regularly distributed, i.e. there are no long yarn floatings.

9.2 Evaluation of polyethylene terephthalate yarn in weaving

9.2.1 Weaving parameters vs. density

With **plain weave**, 4 yarns/reed dent, the result was a sparse structure. With 6 yarns/reed dent the structure became visibly denser and the machine was able to function with greater weft densities. On the other hand, with 8 yarns/reed dent there was significantly more friction between the yarns of the same reed dents. Therefore, the warp yarns broke easily. Samples could be woven with high weft density sufficiently enough to get a proper sample but most of the time the weft density had to be decreased to prevent the yarns from breaking. Thus, plain weave with 8 yarns/reed dent was woven with two different weft densities.

In **weft rib** with 6 yarns/reed dent the dense weave pattern resulted in the need for greater fabric up-take. Therefore, the sample had a very low weft density. Weights were added to the warp let-off but the warp tension still remained too low to weave with greater weft densities. With 8 yarns/reed dent the weft density was almost double compared to plain weave with 8 yarns/reed dent (lower weft density). With **twill derivative** the weft density could be increased even greater than with other weave patterns. Due to the few interlacing points of the weave pattern in **satin,** weft density could not be increased very high. The friction between the yarns during lifting and lowering just one of the yarns in the warp bundle caused yarn breakage more often than with other weave patterns. Therefore, the take-up speed needed to be higher.

With a **combination of plain weave and twill (**referred as plain weave/twill combination) with 6 yarns/reed dent the weft density could not be increased as high as with many other weave patterns. Due to the friction between the yarns they broke easily. With 8 yarns/reed dent the weft density was further decreased. Only three of the six cams were timed differently in weaving **plain weave/twill combination 2**. With this weave pattern was clearly seen how different type of weaves can be woven by using the

same cams in weaving. The weft density could be doubled for both 6 and 8 warp yarns/reed dent compared to the first plain weave/twill combination. The weaving was significantly easier.

Plain weave derivative as a weave pattern allowed very high weft densities with both warp densities. Especially the sample with 6 yarns/reed dent was easy to weave because of the lack of friction between the yarns. With six harnesses two different types of **twill derivatives** were woven. **Twill derivative** was very hard to weave and no proper samples were achieved. Also the edges of the fabric were fringed. On the other hand, **twill derivative 2** was woven with 6 and 8 yarns/reed dent quite easily.

Out of the previous weave patterns two were woven with higher warp densities. Paraffin oil was used as a lubricant between the warp yarns reducing the friction and yarn breakage. As **plain weave** was woven with 10 yarns/reed dent the weft density could be increased significantly higher than without lubricant with8 yarns/reed dent (lower warp density). With 12 yarns/reed dent the friction was very significant between the warp yarns, and the weft density was only a little higher than with 8 yarns/reed dent. Due to yarn breakage the samples were very hard to manufacture. **Plain weave derivative** was fairly easily woven with both warp densities. The warp yarns were divided to large sections and empty space was left between the yarn bundles. Therefore, the more there were yarns in one reed dent the more there was inconsistency in the longitudinal direction of the fabric.

Since fabric with high weft and warp density was desired, the fabric up-take was decreased as low as possible to get maximum weft density. The main problem with increasing weft density was that as the take-up speed was reduced the warp yarns loosened. Therefore yarns rubbed against each other, wore out and eventually broke when the shuttle passed the open shed. The problem could be overcome by adding more weight to the warp let-off to retain the warp tension. Warp density was changed by changing the number of the yarns drawn into one reed dent. The more yarns in one reed dent the greater the warp density. The problem with high warp density was the friction between the yarns, which caused the yarns to wear and stick together. Due to the low take-up speed and friction the yarns broke easily. The weft density was optimized for every sample individually depending on the weave pattern’s warp yarn consumption, i.e. the crimp. Some pattern crimped the yarns less, which resulted in lower weft density. Due to combining high warp and weft density, some compromises were to be done to achieve the best result. In most of the cases greater warp density demanded lower weft density and vice versa.

9.3 Fabric properties

The higher the warp density the greater were both thickness and mass per unit area of the samples. The mass per unit area and thickness grew as the warp and weft density got higher, which is reasonable, since more yarns were packed closer together. The samples with the same warp densities had relatively similar mass per unit area values, except for

weft rib with 8 yarns/reed dent, which was very hard to weave, and hat thus had lower weft density than the others. Due to the friction between the yarns in higher warp densities, the weft density tended to be slightly lower the higher the warp density was raised.

To summarize the thicknesses (*Figure 32*) of the samples with warp densities of 6 – 12 yarns/reed dent are 0.18 – 0.25 mm, depending on the warp density. The samples were very uniform, since the standard deviations were only 0.001 – 0.008 mm. The standard deviations of the samples are presented in Appendix 2. The mass per unit area (*Figure 33*) varied from approximately 7.8 to 14.0 g/m^2. The weft densities (*Figure 34*) were 17 – 38 yarns/cm for samples with 6 yarns/reed dent, 15 – 38 yarns/cm with 8 yarns/reed dent, 20 – 22 yarns/cm for 10 yarns/reed dent and 15 – 25 yarns/cm for 12 yarns/reed dent. Thus, the minimum weft densities did not vary significantly, but in the maximum values could be seen that the weft density must be lowered slightly as the warp density was raised. The lack of differences between the minimum values was probably caused by the inconstancy of the warp yarns. The weft density was very uniform between all the yarn count results in the same sample, since the standard deviations only 0.1 – 0.8 yarns/cm. The standard deviations of the weft densities are presented in Appendix 2.

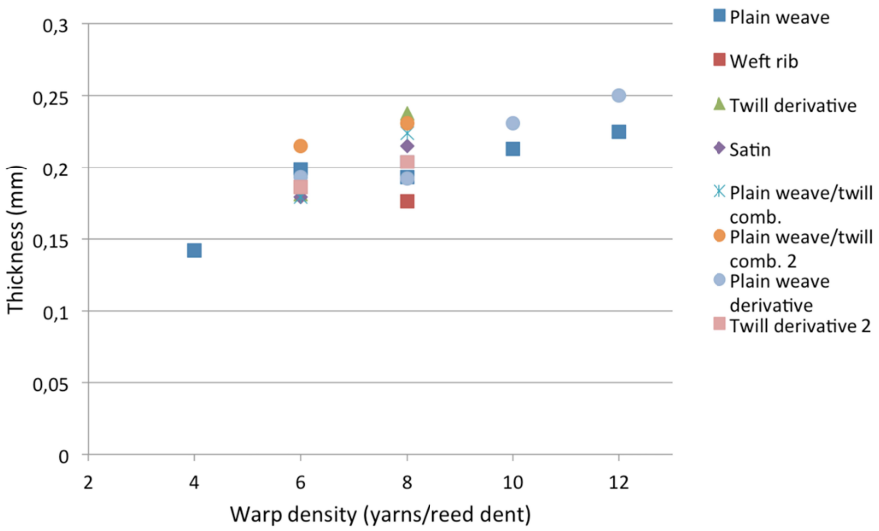

Figure 32 *Mean values of thickness of the woven PET samples (n = 5). The accurate values are presented in Appendix 2 with standard deviations.*

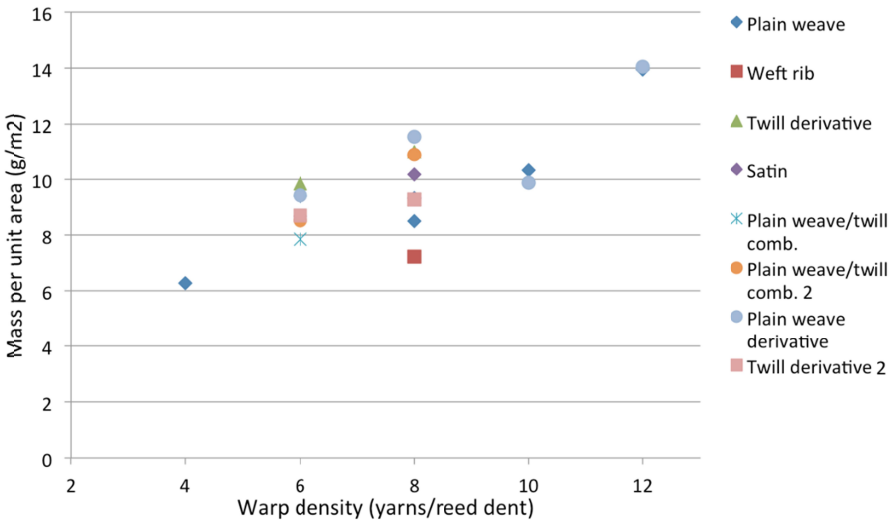

Figure 33 *Mass per unit area of all the woven PET samples (n = 1).*

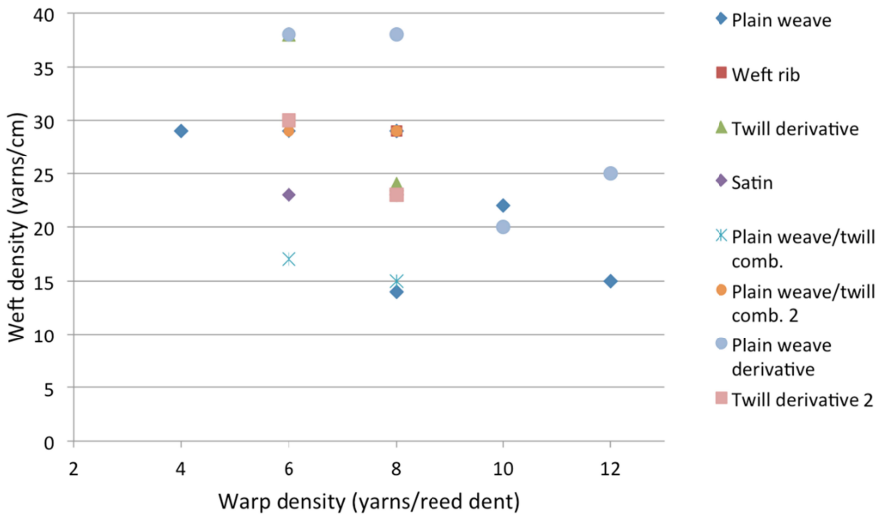

Figure 34 *Mean values of weft density of the woven PET samples (n = 5). The accurate values are presented in Appendix 2 with standard deviations.*

To compare the samples woven with 10 and 12 yarns/reed dent: the thicknesses were very close to each other and mass per unit area was a bit higher for samples with 12 yarns due to the tighter yarn packing. With plain weave the weft density must be lowered to weave with higher warp density but with plain weave derivative the weft density was even higher with 12 yarns than with 10 yarns/reed dent.

9.4 Contact angle measurements and wetting

The cover factors (*Figure 35*) and total void percentages (*Figure 36*) of all the samples were calculated, all the number values are in Appendix 3. The filling factor was not calculated due to the presumption that the weave patterns should be more symmetrical. The equation assumes the weave patterns having the same number of interlacing points

in each of the columns. That is not the case in the samples. It can be concluded that in all of the samples the warp cover was higher than the weft cover, which is reasonable, because the warp yarns were drawn very tightly into the reed dents, and thus the weft density could not have been made higher. The cover factors confirm the result that the other values also indicate; the samples with higher warp densities were also the densest and have the least openings and greatest cover factors. The samples with warp density of 12 yarns/reed dent had actually cover factors very close to 100 %.

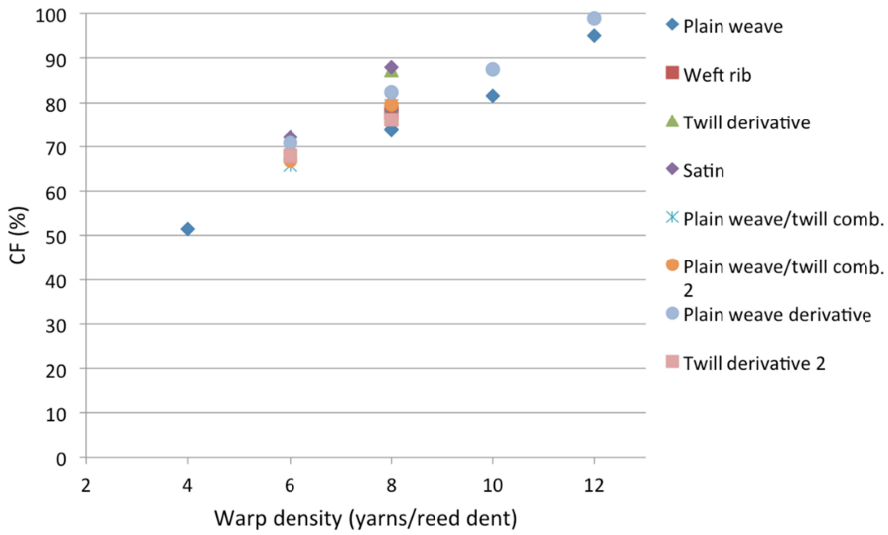

Figure 35 *Total cover factors of the woven PET samples (n = 5 – 6).*

Due to the usage of this particular PET multifilament yarn, the total void percentage values did not differ significantly between weave patterns or warp and weft densities. The largest difference can be seen between the warp density of plain weave with 12 yarns/reed dent and the rest. Any more detailed analysis cannot be done of these values, since they are only calculated theoretical values, and thus only directional.

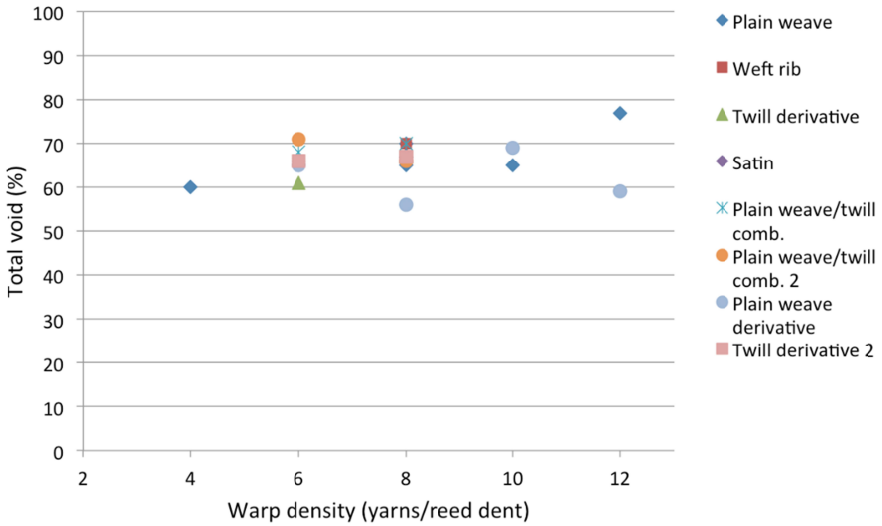

Figure 36 *Total void percentages of the woven PET samples (n =5 – 6).*

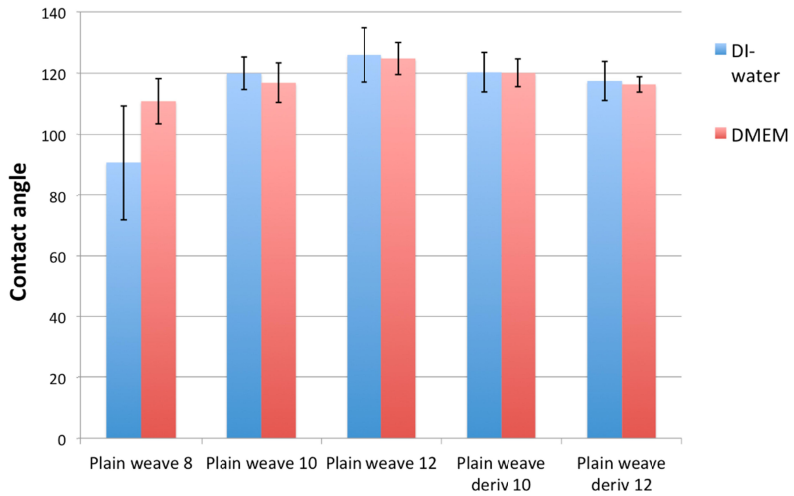

Figure 37 *Average contact angles and standard deviations measured with DI-water and DMEM for plain weaves 8, 10 and 12 yarns/reed dent, and plain weave derivatives 10 and 12 yarns/reed dent (n = 10).*

The cover factors and total void percentages are only theoretical values. Therefore, contact angle measurements (*Figure 37*) were done to get more accurate view of the wettability and permeability of the structures. The contact angles did not differ significantly between the results measured with DI-water and DMEM culture medium. Only the sample of plain weave with 8 yarns/reed dent had significantly higher contact angles measured with DMEM than DI-water. All the samples with warp yarn density of 10 and 12 yarns/reed dent had contact angles around 120°. All the droplets penetrated the plain weave with 8 yarns/reed dent in less than ten seconds, which is understandable when the warp density is considered. The numerous through-going openings let the liquid penetrate easily. The droplets kept their round shape during time around two minutes measured on all the denser samples. The droplets were approximately 1.5 mm in diameter, which made it quite likely that there were openings under it. This estimation is based on microscopical imaging. Due to the small size of the openings the liquid was not allowed to pass straight through them. Thus the liquid must diffuse into the structure to pass. To conclude, the samples with 10 and 12 yarns/reed dent were significantly denser and more slowly wetting than the control sample.

9.5 Microscopic evaluation

The samples' uniformity was evaluated from the microscope taken with magnification 6.3 and 6.4 (*Figure 38*). The uniformity was in four different categories. Some of the best samples were very consistent and regular (*Figure 38A*) and some had minor inconsistency still not showing openings in the structure (*Figure 38B*). The samples with more inconsistency (*Figure 38C – D*) had clearly visible openings in the structure. The warp yarns were divided into sparser and denser sections, especially with extremely high warp densities.

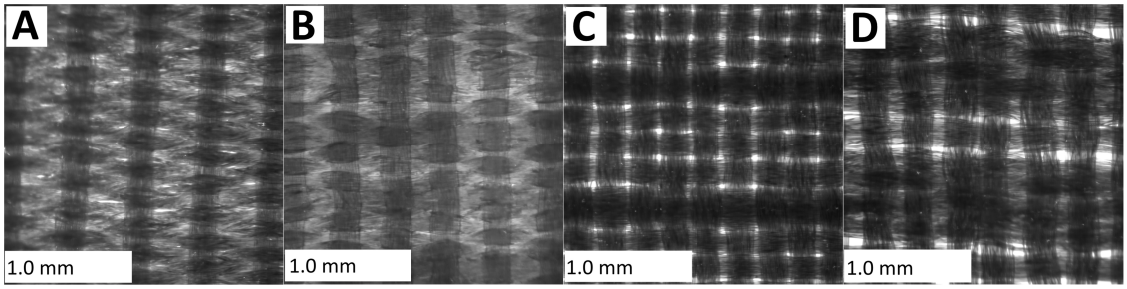

Figure 38 *Magnification of 6.3 tells of the consistency of the fabric surface. Plain weave: A) 10 yarns/reed dent. Plain weave derivative: B) 12 yarns/reed dent, reverse side, C) 6 yarns/reed dent, reverse side, D) 10 yarns/reed dent, reverse side. (Warp → Weft ↑)*

Plain weave with 4 yarns/reed dent (*Figure 39A*) had visible openings regularly in the interlacing points. There was free space to be seen between the filaments of same yarns. The openings were seen already with the magnification of 6.4 and even more clearly with the magnification of 10. The openings were approximately 0.3 – 0.4 mm in size. In the plain weave with 6 yarns/reed dent (*Figure 39B*) no openings were seen even in the interlacing points with the magnification of 6.4. With the magnification of 10 there were some irregular openings between the filaments but still no openings in interlacing points. Most of the narrow openings in all samples were in the warp direction.

With eight yarns/reed (*Figure 39C*) with the lower weft density there were smaller openings between individual filaments, width 10-15 μm, to be seen with the magnification of 10. The long narrow openings were caused by the low weft density. Due to the high number of yarns in same reed dent, plain weave (8 yarns/reed dent) with higher weft density (*Figure 39D*) had clear sections of denser and sparser fabric in the warp direction. There were small openings between the fibres, mostly located in the sparser sections of the fabric. The openings were clearly more located in the sides of the yarn. With the magnification of 10 the slit-like openings between filaments were only half of the width of a filament, approximately 10 μm.

Plain weave woven with the help of paraffin oil had two warp densities, 10 (*Figure 39E*) and 12 yarns/reed dent (*Figure 39F*). With magnification of 6.3 they both had clear sparse and dense sections in warp direction, due to the great number of yarns in one reed dent. With both warp densities there were minor slit-like openings between fibres (in the warp direction). Their width was approximately 15 – 20 μm, in the same order of magnitude as the fibre diameter. They were located more to the sparser areas. The sample with 12 yarns/reed dent had less openings. With the magnification of 10 with 10 yarns/reed dent there were few slit-like openings, size 20 μm x 0.1 mm, and otherwise smaller openings a few micrometres in size. With 12 yarns/reed dent there were no through-going openings to be seen. The distances between the filaments were approximately 10 μm, but there was always another fibre to be seen underneath. Both of the samples looked very dense and uniform.

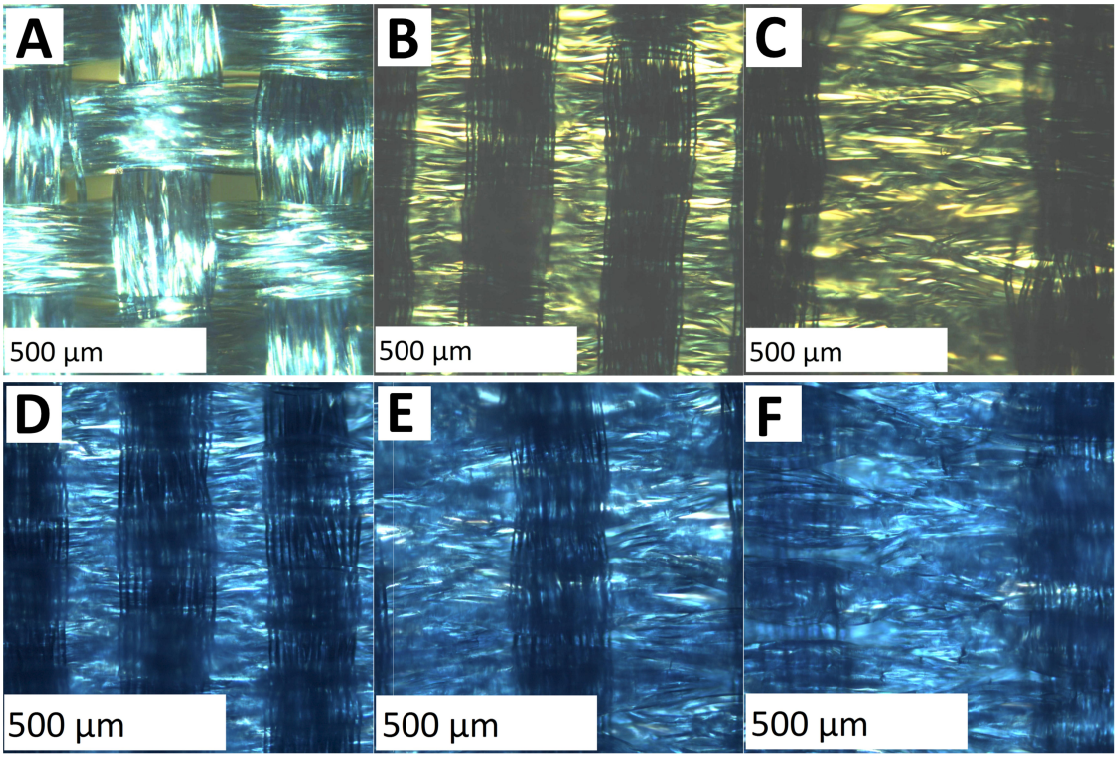

Figure 39 *Plain weave, magnification of 10. A) 4 yarns/reed dent, B) 6 yarns/reed dent, C) 8 yarns/reed dent, lower weft density, D) 8 yarns/reed dent, higher weft density, E) 10 yarns/reed dent, F) 12 yarns/reed dent. (Warp → Weft ↑)*

Weft rib (*Figure 40*) was dense and had no visible openings with the magnification of 6.4. On the other hand, with the larger magnification, there were clear and visible openings in the interlacing points. Their size was approximately 20 – 30 µm and the minor openings approximately 20 µm in width. The sample was sparse and not suitable when evaluating its use in cell culturing.

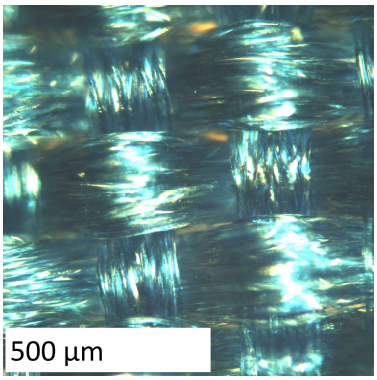

Figure 40 *Weft rib, magnification of 10, 8 yarns/reed dent. (Warp → Weft ↑)*

With the magnification of 6.4 there were darker areas in certain interlacing points in **twill-derivative** (*Figure 41*) with both warp densities. The larger magnification revealed that there were larger square-shaped openings in those interlacing points with 6 yarns/reed dent (*Figure 41A*). The sample with 8 yarns/reed dent (*Figure 41B*) was

denser and there were no openings in interlacing points. Instead, there were smaller openings between individual filaments, 15 µm in width, around the fibre diameter.

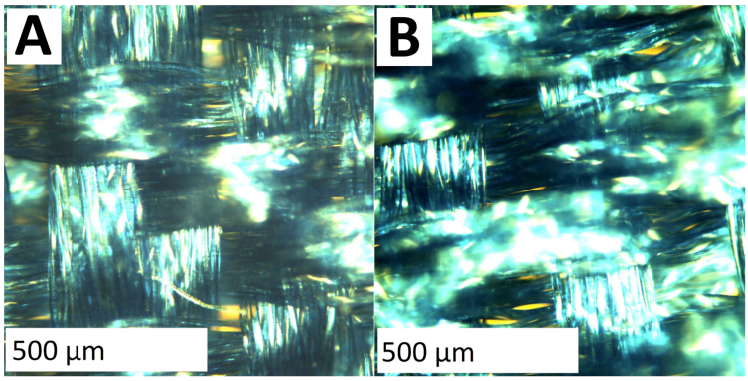

Figure 41 *Twill derivative, magnification of 10. A) 6 yarns/reed dent, B) 8 yarns/reed dent. (Warp → Weft ↑)*

Satin was woven with 6 and 8 yarns/reed dent and both of the structures were quite sparse. The microscope images on the right and reverse ride resembled each other, and thus only right side images are presented. The side with the long yarn floatings (reverse side) was with both warp densities a little more regular, yet sparse. With 6 yarns/reed dent (*Figure 42A*) the largest openings were even 30 – 40 µm x 120 µm. On the reverse side the larger openings were not as visible as on the right side, but there were still approximately 20 µm openings between the filaments, mostly in the warp direction. With 8 yarns/reed dent (*Figure 42B*) there were regular openings between filaments, size approximately 20 µm in width. In addition, there were a few random larger openings, 30 – 40 µm in size. The openings were caused by long yarn floatings, which are loose parts of yarn.

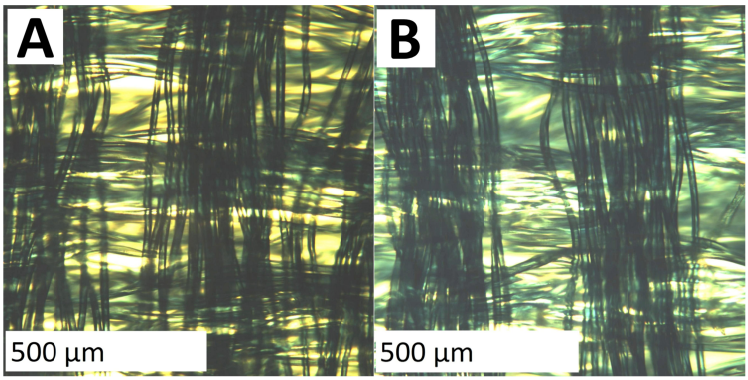

Figure 42 *Satin, magnification of 10. A) 6 yarns/reed dent, right side, B) 8 yarns/reed dent, right side. (Warp → Weft ↑)*

There were two versions of **combination of plain weave and twill**, plain weave/twill combination and plain weave/twill combination 2. With both warp densities the **plain weave/twill combination** (*Figure 43)* had numerous long, slit-shape openings between the filaments in the warp direction. They were approximately 20 – 30 µm in width and 0.1 mm in length. No larger openings in interlacing points were seen.

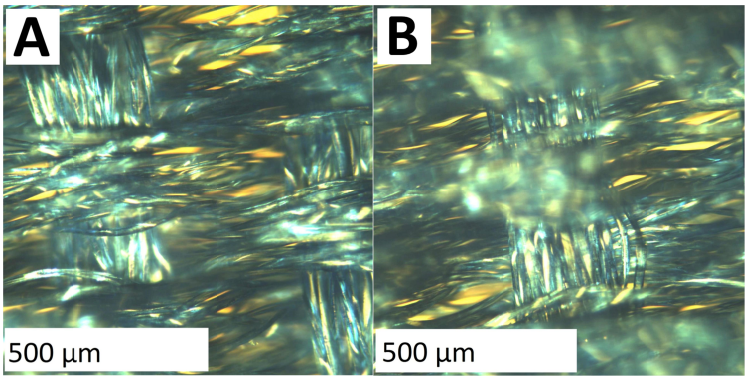

Figure 43 *Plain weave/twill combination, magnification of 10. A) 6 yarns/reed dent, B) 8 yarns/reed dent. (Warp → Weft ↑)*

Plain weave twill combination 2 with 6 yarns/reed dent (*Figure 44A*) had greater openings in the interlacing points (0.1 mm x 0.2 mm) and in addition numerous openings between filaments, 15 – 20 µm in width. The sample with weft density of 8 yarns/reed dent (*Figure 44B*) had filaments very sparsely in the interlacing points The long, narrow openings between individual filaments were approximately 20 µm in width. Both of the samples were sparse and very porous.

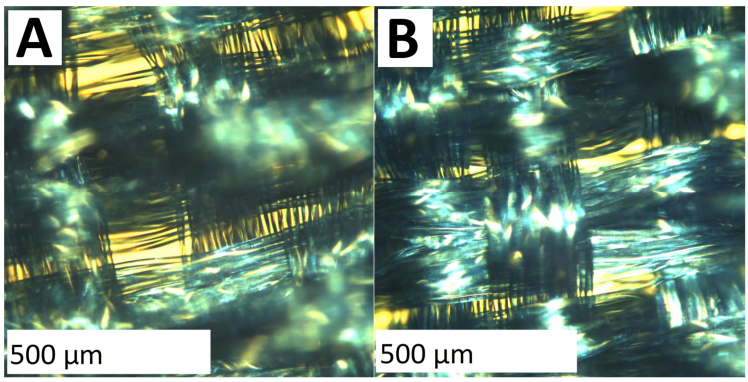

Figure 44 *Plain weave/twill combination 2, magnification of 10. A) 6 yarns/reed dent, B) 8 yarns/reed dent. (Warp → Weft ↑)*

With the magnification of 6.3 **plain weave derivative** had sections of sparse and dense areas in the warp direction. With 6 yarns/reed dent (*Figure 45A*) the dense sections consisted of just two warp yarns. Those sections were not as clearly seen with 8 yarns/reed dent (*Figure 45B*) due to the denser structure. With 6 yarns/reed dent there were visible square-shaped openings in the interlacing points. With 8 yarns/reed dent there were long slit-like openings between individual filaments, located in the sparse areas. They were approximately 20 µm x 0.1 mm in size. No openings were seen in the dense parts. With the magnification of 10 the square-shaped openings in 6 yarns/reed dent were 40 µm x 60 µm and the slit-like openings 20 µm x 0.1 mm in size. The sample with 8 yarns/reed dent was really consistent, and the largest openings were around 10 µm in width, others being only a couple of micrometres. The larger openings were very few in number and they were located randomly.

In **plain weave derivative** with 10 yarns/reed dent (*Figure 45C*) the openings were not as long as with lower warp densities. The microscope images on the right and reverse ride resembled each other, and thus only reverse side images are presented here. With the magnification of 10 a few minor slit-like openings between the filaments were seen. Their size was less than 10 µm in width. Most of the openings were smaller, a couple of micrometres and most of them were not going through. The denser sample, 12 yarns/reed dent (*Figure 45D*), was very even and only had a few random bigger openings in size of the fibre diameter and otherwise there were no through-going openings to be seen. The sparser and denser areas could be seen on both of the samples, but the sparser sections did not have any more openings than the denser sections. The surface was very consistent and even on both sides.

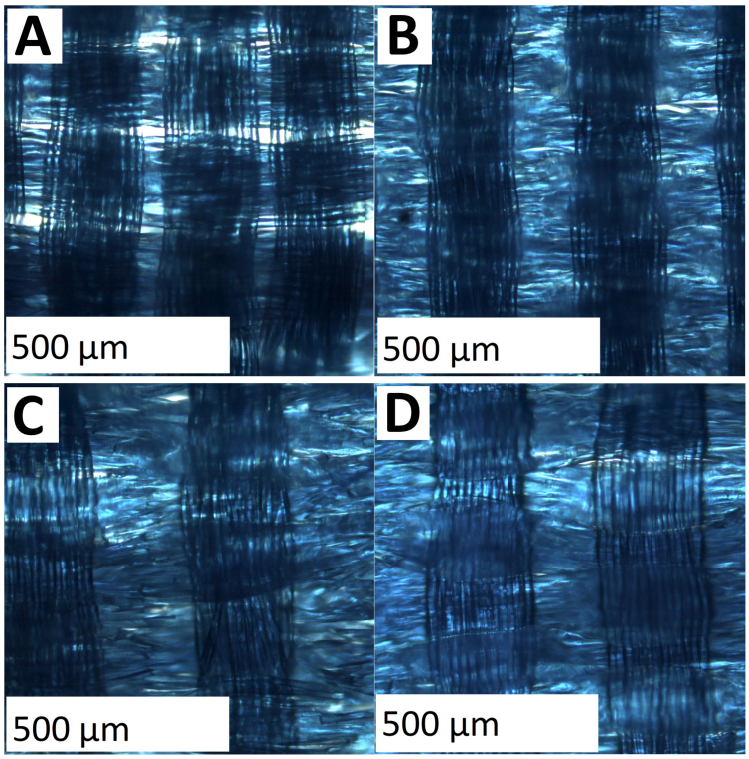

Figure 45 *Plain weave derivative, magnification of 10. A) 6 yarns/reed dent, reverse side, B) 8 yarns/reed dent, reverse side, C) 10 yarns/reed dent, reverse side, D) 12 yarns/reed dent, reverse side. (Warp → Weft ↑)*

Twill derivative 2 with 6 yarns/reed dent (*Figure 46A*) had clear sparse and dense sections in the warp direction. The sparse areas had square-shaped openings in interlacing points, 0.1 x 0.1 mm in size. In the denser sections there were only minor slit-like openings between fibres, 30 µm x 0.2 mm in size. The sample with the greater warp density, 8 yarns/reed dent (*Figure 46B*), also had sections of denser and sparser fabric. However, the difference between those areas was not as clear as with the 6 yarns/reed dent. The slit-like openings were 15 µm x 0.1 mm in size, and mostly located in the sparse areas.

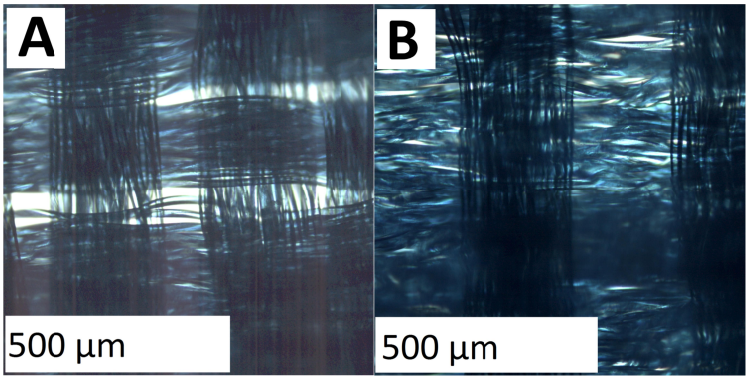

Figure 46 *Twill derivative 2, magnification of 10. E) 6 yarns/reed dent, F) 8 yarns/reed dent. (Warp → Weft ↑)*

To summarize, weave patterns with regularly distributed interlacing points were the densest and had the most uniform surface. In general, the warp density of 6 yarns/reed dent was relatively sparse. Warp density of 8 yarns/reed dent was significantly denser, but still several samples had visible openings in the structure. The raising of the warp density was a solution to the through-going openings, since the structures became significantly denser with warp densities of 10 and 12 yarns/reed dent.

9.5.1 Microrobotics platform imaging and threshold value manipulation

Plain weave samples with warp densities ten and twelve yarns/reed dent were imaged with microrobotics platform (*Figure 47A, 47C*) and the images were processed with threshold values. It was confirmed that the samples really had rare openings only a few micrometres in size. Part of the openings formed clusters around random interlacing points. Only the light, which goes directly through the structure, shows in the threshold-processed images (*Figure 47B, 47D*). That rules out the openings, which had fibres underneath, which were shown in regular light microscope images.

In **plain weave derivative** (*Figure 47E – H*) the openings were a few micrometres in width but somewhat longer than in plain weave. The openings were not as randomly located as with plain weave. They were more located near the interlacing points, and there were always several of them in different sizes in the same area.

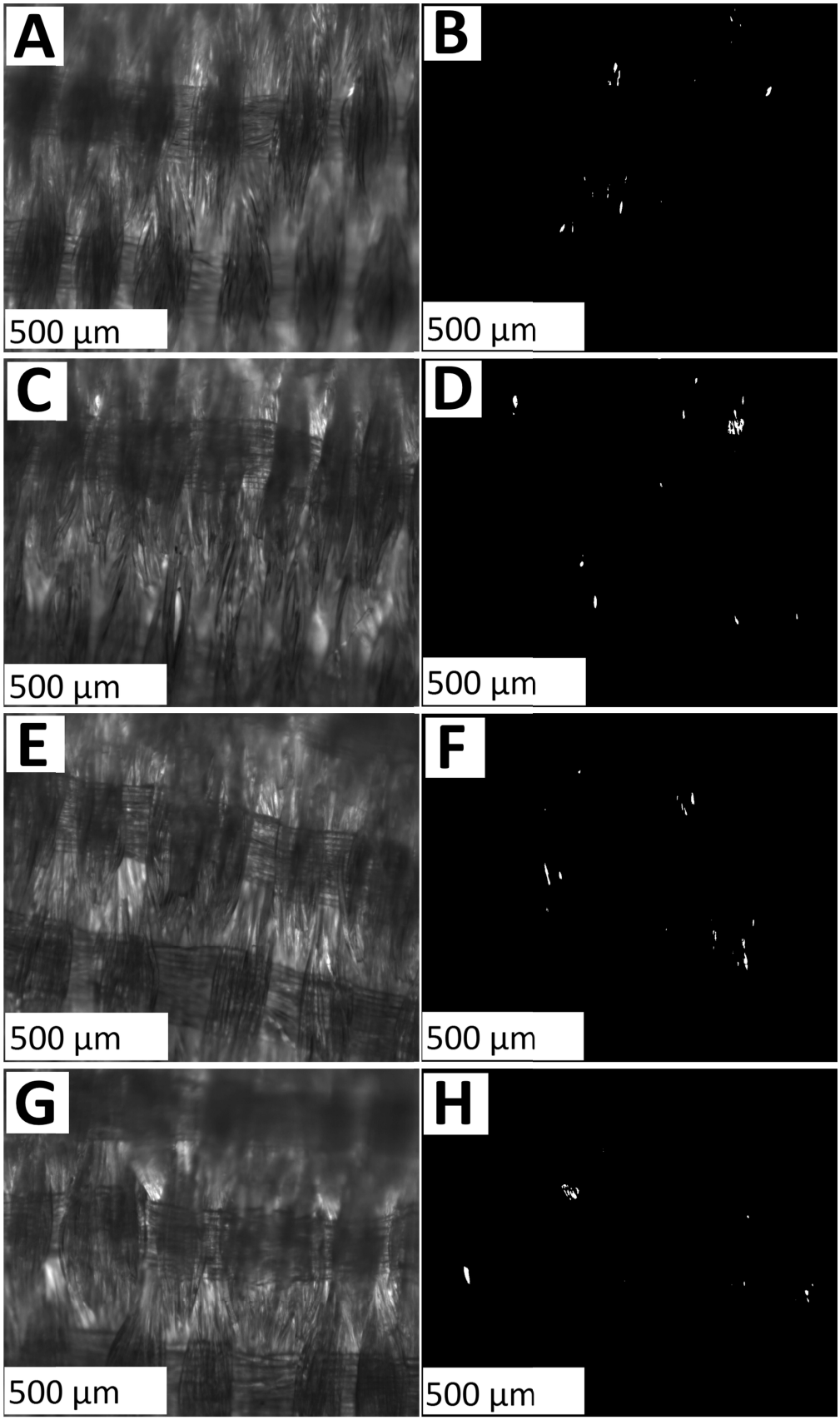

Figure 47 *Polarized images. Plain weave. A) 10 yarns/reed dent, B) threshold values, 10 yarns/reed dent. C) 12 yarns/reed dent, D) threshold values, 12 yarns/reed dent. Plain weave derivative. E) 10 yarns/reed dent, F) threshold values, 10 yarns/reed dent. G) 12 yarns/reed dent, H) threshold values, 12 yarns/reed dent. (Warp ↑ Weft →)*

To summarize, both of the chosen weave patterns resulted in very dense structures with extremely high warp densities, 10 and 12 yarns/reed dent. Through-going openings were clustering near random interlacing points and they were few in number. All of the openings were slit-like in shape and in the warp direction.

9.6 Tensile properties

The PET multifilament yarn was drawn wet with the same crosshead speed than with woven PET samples and with the gauge length of 50 mm. The mean strength was 4.04 ± 0.16 GPa and mean maximum load 3.5 ± 0.1 N. The mean strain was 31.7 ± 2.7 %. Considering the problems with the yarn breakage and increasing hairiness during the weaving it is very likely that the stresses and the wear caused by the weaving process had an effect on the tensile properties of the woven fabrics.

Maximum load, strength and strain were calculated from the tensile testing results of all PET samples. Young's modulus was determined from the slope of the second linear part of the load-displacement curve (*Figure 48*).

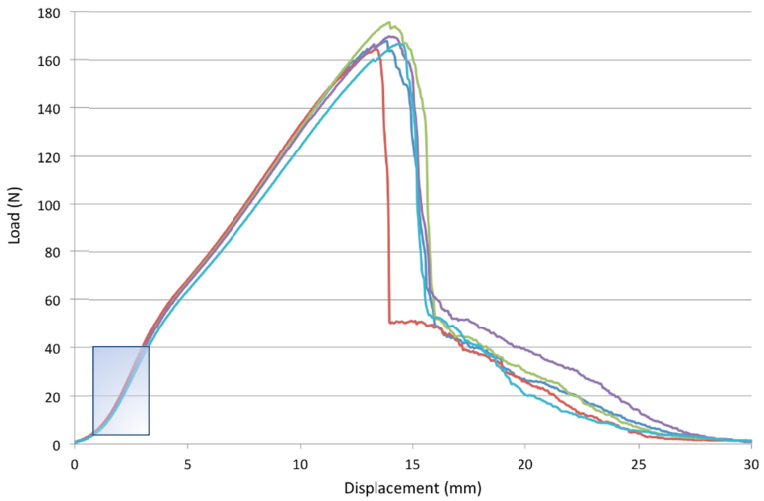

Figure 48 *A load-displacement curve. The typical behaviour of a woven PET sample in tensile testing. The rectangular indicates the area where the Young's modulus was calculated. (Plain weave derivative, 12 yarns/reed dent)*

The strength (*Figure 49*) was higher with higher warp densities of the same sample. The only differing sample of the others was weft rib, with stress at maximum load of ~ 110 MPa, while the others were 50 – 95 MPa. For the samples with 6 yarns/reed dent the strength was ~ 70 MPa, except for plain weave derivative, which was ~80 MPa, and plain weave with 4 yarns/reed dent ~ 60 MPa. For samples with 8 yarns/reed dent the strength was 70 – 80 MPa, except for plain weave with the higher weft density, which has the strength very close to 90 MPa. The samples with extremely high warp densities had the strength of 80 – 90 MPa.

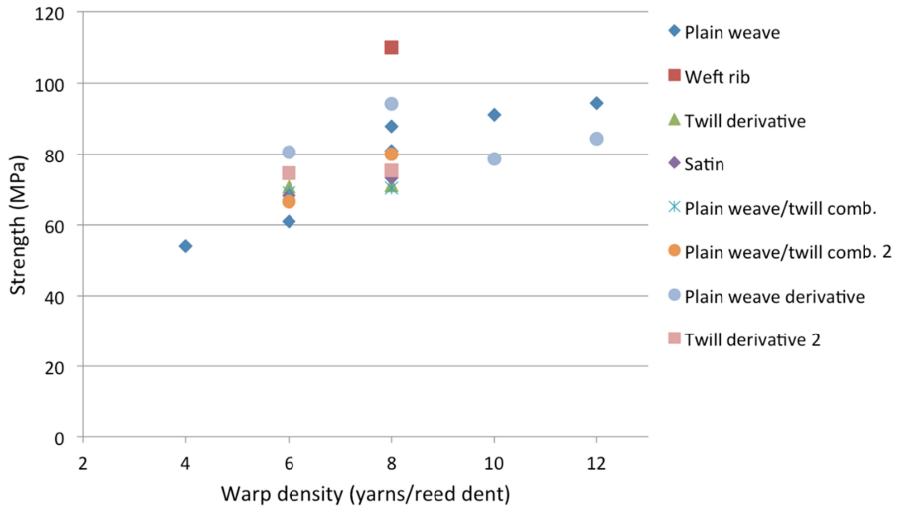

Figure 49 *Mean values of tensile strength of all the woven PET samples (n = 5 – 6). The accurate values are presented in Appendix 5 with standard deviations.*

The strain values (*Figure 50*) did not differ significantly from each other, since they were all around 25 %. All the curves followed the same pattern. The first part of the curve reflected the straightening of the sample, since they were mounted on the testing machine without pretension. The second part with different slope resembled the straightening of the yarns in the structure, i.e. the decreasing of the crimp of the warp yarns. The third part resembled the actual strain, which is targeted to the yarns and as the curve drops, the yarns break.

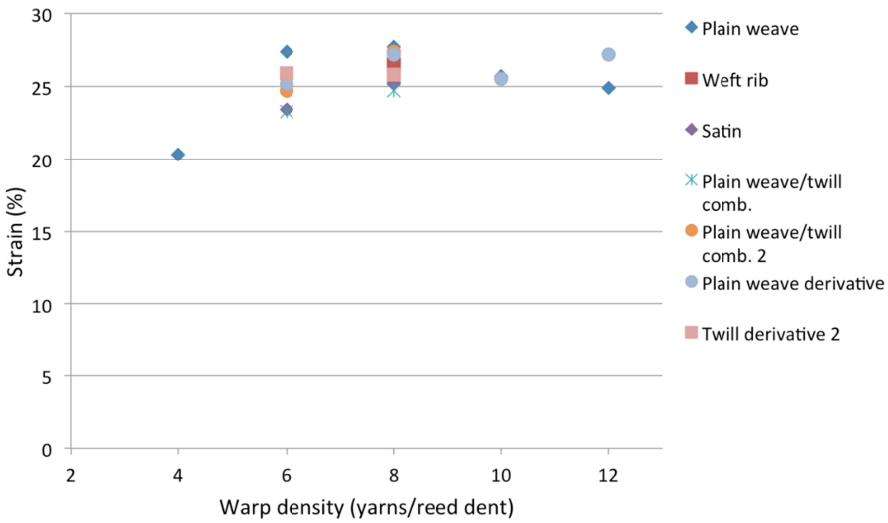

Figure 50 *Mean values of strain of the woven PET samples (n = 5 – 6). The accurate values are presented in Appendix 5 with standard deviations.*

Young's modulus (*Figure 51*) of each of the PET samples was determined from the slope of the second linear part of the graphs. The specific values are in Appendix 6. The modulus is rising as the warp density raised. However, the increase of the Young's modulus decreases with the extremely high warp densities and the moduli of the 10 and

12 yarns/reed dent samples are very close to each other. There are no great differences between the weave patterns with the same warp densities. The moduli are around 17 – 21 MPa for samples with 6 yarns/reed dent, 17 – 23 MPa for 8 yarns/reed dent, 23 – 26 MPa for 10 yarns/reed dent and 22 – 26 MPa for 12 yarns/reed dent.

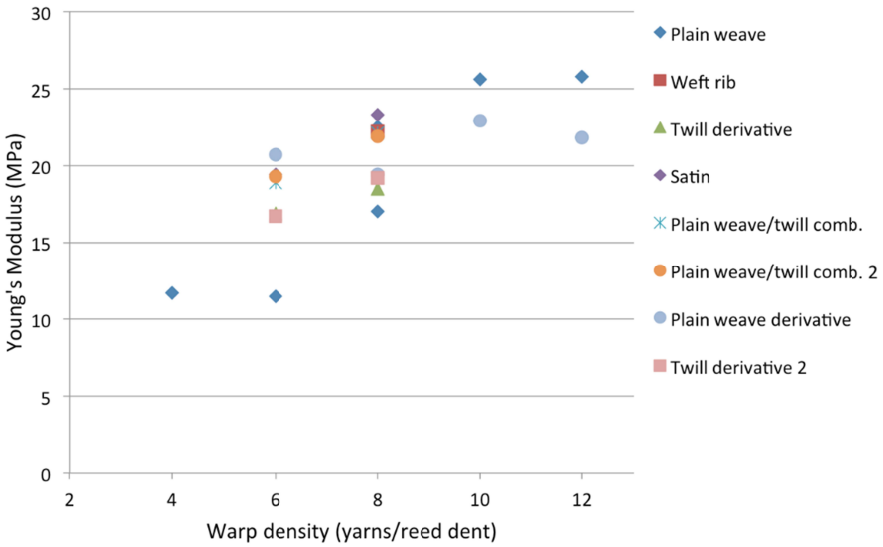

Figure 51 *Young's Moduli of the woven PET samples (n = 5 – 6).*

10 CONCLUSION

Nine different weave patterns were used to weave extremely dense fabric. The best weave patterns were those of which had numerous regularly distributed interlacing points, i.e. no long yarn floatings. Since fabric with large weft and warp density was desired, the fabric up-take was decreased as low as possible to get maximum weft density. This resulted in several problems such as warp breakage caused by wear and reduced yarn tension. The weft density was optimized for each sample individually depending on the warp yarn consumption of the weave pattern, i.e. the crimp. Combining these two variables, warp and weft density, compromises were to be done to achieve the best result, since greater warp density demanded lower weft density.

Based on microscope imaging and the estimated porosity of each weave pattern, two of the best, plain weave and plain weave derivative, were woven with extremely high warp densities with the help of paraffin oil as a lubricant. The lubricant reduced friction between the warp yarns and thus prevented yarn breakage. Therefore, even weft density could be kept relatively high. The higher the warp density, the greater were both thickness and mass per unit area of the samples. The mass per unit area and thickness increased as the warp and weft density were raised, since yarns were packed closer together. All the samples with the same warp densities had relatively similar mass per unit area. The minimum weft densities did not vary significantly between different samples, but in the maximum values could be seen that the weft density must be lowered slightly as the warp density raised. The lack of differences between the minimum values was probably due to the inconsistency of the warp yarns. To compare the samples with extremely high warp densities: the thicknesses were very close to each other and mass per unit area was slightly higher for samples with 12 yarns/reed dent due to the tighter yarn packing. With plain weave the weft density must be lowered to weave with higher warp density. On the other hand, with plain weave derivative the weft density was even higher with the higher warp density. It was clearly visible that the greater was the warp density, the more there was inconsistency in the longitudinal direction of the fabric. This was due to the fact that the warp yarns were divided to large sections and empty space was left between them.

The porosity and permeability were modelled by calculating theoretical void volume percentages and cover factors, which both describe the empty space or area left between the yarns. Total void percentages did not differ significantly between the weave patterns or warp and weft densities. To conclude, in all of the samples the warp cover was higher than the weft cover, which is reasonable, since the warp yarns were drawn very tightly into the reed dents. Thus, the weft density could not have been increased. The cover

factors confirmed the result the other outcomes also indicate; the samples with higher warp densities were the densest and had the least openings and greatest cover factors.

For more accurate information about the permeability of the two best weave patterns, contact angle measurements were done using DI-water and DMEM. The contact angles between warp densities or the two weave patterns did not differ significantly between the results measured with DI-water and DMEM culture medium. Only plain weave with 8 yarns/reed dent, which was used as a control, had significantly smaller contact angles ans the liquid penetrated the surface in less than 10 seconds. The numerous through-going openings let the liquid pass easily. The droplets kept their round shape during time of two minutes on the denser samples. The droplets were 1.5 mm in diameter, which made it quite likely that there were a few openings under it. The openings were so small that they would not allow the liquid pass straight through them, and thus the liquid must diffuse into the structure to pass. The imaging with microscope and microrobotics platform confirmed that the two best samples really had rare openings only a few micrometres in size. The openings formed small clusters near interlacing points. There were no significant differences between the weave patterns or the warp densities. All of the openings were slit-like in shape and in the warp direction.

Strength was higher with higher warp densities of the same sample. The only differing sample was weft rib, which had higher strength value than the others. The strain values of the samples did not differ significantly from each other, they were all approximately 25 %. All the load-displacement curves followed the same pattern. The first part of the curve reflected the straightening of the sample, since they were mounted on the testing machine without pretension. The second slope resembled the straightening of the yarns in the structure, i.e. the decreasing of the crimp. The third part resembles the actual strain, which is targeted to the yarns and as the curve dropped, the yarns broke. Young's moduli were calculated of the second linear part of the curves to compare the influence of the weave pattern on the mechanical behaviour. Young's modulus was rising as the warp density was higher, but with the extremely high warp densities the values were very close to each other.

The openings were too large considering the RPE cells, which demand pores only a few micrometres in size to form a confluent cell monolayer. To decrease the three-dimensionality and the pore size a heat-pressure treatment can be applied to the fabrics in the future. The heat treatment would flatten the structure permanently simultaneously reducing the pore size and decreasing the distance between individual fibres, which would help in forming a monolayer. It would be important to fabricate similar structures out of a material, which would enable the implanting. Studying the water permeability of the samples would be important, since it would tell more about the porosity and reveal the through-going pores, which are not visible with light microscope. The affect of the biodegradation on the tensile values would be tested. The compatibility of the structure and material for the cells would be seen in cell tests. Combining the woven structures with e.g. hydrogels would be interesting, and to study whether the combining would have a positive impact on the cellular proliferation on the surface.

REFERENCES

Adanur S. 2000. Handbook of Weaving. CRC Press. p. 9-17; 19-34; 109–128; 361-373.

Adanur S. 1995. Wellington Sears Handbook of Industrial Textiles. Technomic Publishing Co, Inc. p. 334-344.

Adolf F-P. 1999. Ch. 2 The Structure of Textiles: an Introduction to Basics. In: Robertson J. (edit.) Forensic Examination of Fibres, Second Edition. CRC Press. p. 33-54.

Alm J. J., Frantzén J. P. A., Moritz N., Lankinen P., Tukiainen M., Kellomäki M., Aro H. T. 2010. In vivo testing of a biodegradable woven fabric made of bioactive glass fibers and $PLGA_{80}$ – A pilot study in the rabbit. Wiley Periodicals, Inc. Journal of Biomedical Materials. Research Part B: Applied Biomaterials 93B. p. 573–580.

Becton, Dickinson and Company. 2012. Biosciences Cell Culture – Cell Culture Inserts – Features – Multiwell Insert Systems. [WWW]. [Cited on 15.11.2012]. Available at: http://www.bdbiosciences.com/eu/cellculture/inserts/features/79ardiovas.jsp

Behera B. K., Militky J., Mishra R. and Kremenakova D. 2012. Modeling of Woven Fabrics Geometry and Properties, Woven Fabrics. Prof. Han-Yong Jeon (Ed.). ISBN: 978-953-51-0607-4. InTech. [WWW]. [Cited on 29.7.2013]. Available at: http://www.intechopen.com/books/woven-fabrics/modeling-of-woven-fabrics-geometry-and-properties.

Bigg, D. M. 2005. Polylactide copolymers: Effect of copolymer ratio and end capping on their properties. Advances in Polymer Technology 24 (2) p. 69-82.

Boland E. D., Coleman B. D., Barnes C. P., Simpson D. G., Wnek G. E., Bowlin G. L. 2005. Electrospinning polydioxanone for biomedical applications. Acta Biomaterialia 1. p. 115–123.

Chen X., Qi Y-Y, Wang L-L, Yin Z., Yin G-L, Zou X-H, Ouyang H-W. 2008. Ligament regeneration using a knitted silk scaffold combined with collagen matrix. Biomaterials 29. p. 3683–3692.

Doser M. and Planck H. 2011. Textiles for implants and regenerative medicine. In: Bartels, V. T. Handbook of Medical Textiles. Woodhead Publishing. [WWW]. [Cited on 3.12.2012]. Available at: http://www.knovel.com/web/portal/browse/display?_EXT_KNOVEL_DISPLAY_bookid=4321&VerticalID=0. p. 132-152.

East A. J. 2009. The Structure of Polyester Fibers. In: Eichhorn S. J., Hearle J.W.S., Jaffe M., Kikutani T. (Edit.) Handbook of Textile Fibre Structure, Volume 1 – Fundamentals and Manufactured Polymer Fibres. Woodhead Publishing. [WWW]. [Cited on 30.11.2012]. Available at: http://www.knovel.com/web/portal/browse/display?_EXT_KNOVEL_DISPLAY_bookid=4365&VerticalID=0. p. 206-231.

Ethier C. R., Simmons C. A. 2007. Introductory Biomechanics – From Cells to Organisms. Cambridge University Press. [WWW]. [Cited on 10.1.2013]. Available at: http://www.knovel.com/web/portal/browse/display?_EXT_KNOVEL_DISPLAY_bookid=2341&VerticalID=0. p. 250-251.

Gomes M. E., Azevedo H. S., Moreira A. R., Ellä V., Kellomäki M. and Reis R. L. 2008. Starch–poly(ε-caprolactone) and starch–poly(lactic acid) fibre-mesh scaffolds for bone tissue engineering applications: structure, mechanical properties and degradation behavior. Journal of Tissue Engineering and Regenerative Medicine 2. p. 243-252.

Greiner Bio One, Catalogue Benelux 2010/2011. [WWW]. [Cited on 26.3.2013]. Available at: http://epub02.publitas.com/625/1/#/zoompage/53/ p. 52.

Greiner Bio One, ThinCerts™ Cell Culture Inserts. [WWW]. [Cited on 15.11.2012]. Available at: http://www.greinerbioone.com/nl/80ardiov/articles/catalogue/article-groups/418_8_bl/.

Hatch K. L. 2006. Textile Science. Tailored Text Custom Publishing. p. 14-43; 212-224; 276-285; 287-299; 317-370.

Hegde R. R., Dahiya A., Kamath M. G., Kotra R. and Gao X. 2004. Polyester fibers. [WWW]. [Cited on 29.11.2012]. Available at: http://web.utk.edu/~mse/Textiles/Polyester%20fiber.htm.

Honkanen P. B., Kellomäki M., Konttinen Y. T., Mäkelä S. Lehto M. U. K. 2009. A Midterm Follow-Up Study for Bioreconstructive Polylactide Scaffold Implants in Metacarpophalangeal Joint Arthroplasty in Rheumatoid Arthritis Patients. Journal of Hand Surgery (European Volume) 34E(2). p. 179–185. (Online version available at: http://jhs.sagepub.com/content/34/2/179)

Honkanen P.B., Kellomäki M., Lehtimäki M. Y., Törmälä P., Mäkelä S., Lehto M. U. K. 2003. Bioreconstructive Joint Scaffold Implant Arthroplasty in Metacarpophalangeal Joints: Short-Term Results of a New Treatment Concept in Rheumatoid Arthritis Patients. Tissue Engineering 9(5). p. 957-965.

Hunley M. T. and Long T. E. 2008. Electrospinning functional nanoscale fibers: a perspective for the future. Polymer International 57. p. 385–389.

Hutmacher D. W. 2000. Scaffolds in tissue engineering bone and cartilage. Biomaterials 21. p. 2529-2543.

Hutmacher, D., Hürzeler M. B., et al. 1996. A Review of Material Properties of Biodegradable and Bioresorbable Polymers and Devices for GTR and GBR Applications. The International Journal of Oral & Maxillofacial Implants 11. p. 667-678.

Ilmarinen T., Laine J., Juuti-Uusitalo K., Numminen J., Seppänen-Suuronen R., Uusitalo H. and Skottman H. 2012. Towards a defined, serum- and feeder-free culture of stratified human oral mucosal epithelium for ocular surface reconstruction. Acta Ophthalmologica (September 11th), doi: 10.1111/j.1755-3768.2012.02523.x.

Isotalo T., Nuutinen J-P., Vaajanen A., Martikainen P. M., Laurila M., Törmälä P., Talja M. and Tammela T. L. J. 2005. Biocompatibility and implantation properties of 2 differently braided, biodegradable, self-reinforced polylactic acid urethral stents: an experimental study in the rabbit. The Journal of Urology Vol. 174. p. 2401–2404. DOI: 10.1097/01.ju.0000180412.53702.4a.

Juuti-Uusitalo K., Vaajasaari H., Ryhänen T., Narkilahti S., Suuronen R., Mannermaa E., Kaarniranta K., Skottman H. 2012. Efflux Protein Expression in Human Stem Cell-Derived Retinal Pigment Epithelial Cells. PloS ONE 7(1): e30089. doi:10.1371/journal.pone.0030089

Järvinen K. Development of filter media treatments for liquid filtration. Dissertation. Lappeenranta University of Technology. Lappeenranta. 2005. Publication 227. 92 p.

Kang Y-M et al., 2008. Evaluations of osteogenic and osteoconductive properties of a non-woven silica gel fabric made by the electrospinning method. Acta Biomater. doi:10.1016/j.actbio.2008.07.004

Karamuk E., Mayer J., Raeber G. 2004. Tissue engineered composite of a woven fabric scaffold with tendon cells, response on mechanical simulation in vitro. Composites Science and Technology 64. p. 885–891.

Kearns V., Mistry A., Mason S., Krishna Y., Sheridan C., Short R., Williams R. L. 2012. Plasma polymer coatings to aid retinal pigment epithelial growth for transplantation in the treatment of age related macular degeneration. Journal of Materials Science: Materilas in Medicine 23. p. 2013–2021. DOI 10.1007/s10856-012-4675-6.

Kellomäki M., Niiranen H., Puumanen K., Ashammakhi N., Waris T., Törmälä P. 2000. Bioabsorbable scaffolds for guided bone regeneration and generation. Biomaterials 21. p. 2495-2505.

Khil M-S, Bhattarai S. R., Kim H-Y, Kim S-Z, Lee K-H 2005. Novel Fabricated Matrix Via Electrospinning for Tissue Engineering. Wiley Periodicals, Inc. Journal of Biomedical Material Research Part B: Applied Biomaterials 72B: 117–124. [WWW]. [Cited on 4.11.2012]. Available at: Wiley InterScience 27.8. 2004, DOI: 10.1002/jbm.b.30122.

Kim M-H, Sonoi R., Yamada K., Inamori M., Kino-oka M. 2012. Note: Analysis of locality of early-stage maturation in confluent state of human retinal pigment epithelial cells. Journal of Bioscience and Bioengineering 113 (6). p. 778–781.

Kipp H. W. 1989. Narrow Fabric Weaving. Verlag Sauerländer. p. 9-16; 20-134; 145-157; 371-400.

Koch S., Flanagan T. C., Sachweh J. S., Tanios F., Schnoering H., Deichmann T., Ellä V., Kellomäki M., Gronloh N., Gries T., Tolba R., Schmitz-Rode T., Jockenhoevel S. 2010. Fibrin-polylactide-based tissue-engineered vascular graft in the arterial circulation. Biomaterials 31. p. 4731-4739.

Koh J. L., Szomor Z., Murrell G. A. C. 2002. Supplementation of Rotator Cuff Repair with a Bioresorbable Scaffold. The American Journal of Sports Medicine. Vol. 30, No. 3.

Kotsar A., Isotalo T., Juuti H., Mikkonen J., Leppiniemi J., Hänninen V., Kellomäki M., Talja M. and Tammela T. L.J. 2009. Biodegradable braided poly(lactic-co-glycolic acid) urethral stent combined with dutasteride in the treatment of acute urinary retention due to benign prostatic enlargement: a pilot study. BJU International, 103. p. 626–629. doi: 10.1111/j.1464-410X.2008.08111.x. [WWW]. [Cited on 13.10.2013]. Available at: http://onlinelibrary.wiley.com/doi/10.1111/j.1464-410X.2008.08111.x/full.

Li S. 1999. Hydrolytic degradation characteristics of aliphatic polyesters derived from lactic and glycolic acids. Journal of Biomedical Materials Research. 48 (3) p. 342-353.

Lim, L. T., Auras R., et al. 2008. Processing technologies for poly(lactic acid). Progress in Polymer Science. 33 (8): p. 820-852.

Liu C., Xia Z. and Czernuszka J. T. 2007. Review Paper: Design and Development of Three-Dimensional Scaffolds for Tissue Engineering. Research and Design 85 (7). p. 1051-1064.

Liu H., Fan H., Wang Y., Toh S. L., Goh J. C. H. 2008. The interaction between a combined knitted silk scaffold and microporous silk sponge with human mesenchymal stem cells for ligament tissue engineering. Biomaterials 29. p. 662–674.

Lu B., Zhu D., Hinton D., Humayun M. S., Tai Y-C. 2012. Mesh-supported submicron parylene-C membranes for culturing retinal pigment epithelial cells. Biomedical Microdevices 14. p. 659–667.

Macular Degeneration Research. Macular Degeneration: The Essential Facts. [WWW]. [Cited on 14.1.2013 on American Health Assistance Foundation, 2000 – 2012]. Available at: http://www.ahaf.org/docs/pdf-publications/md_essentialfacts.pdf.

Ma Peter X. 2004. Scaffolds for tissue fabrication. Materials Today 3. p. 30–40.

Mayer J., Karamuk E., Akaike T., Wintermantel E. 2000. Matrices for tissue engineering-scaffold structure for a bioartificial liver support system. Journal of Controlled Release 64. p. 81–90.

Millipore Corporation. Millicell 24-well Cell Culture Plate. [WWW]. [Cited on 15.11.2012]. Available at: http://www.millipore.com/catalogue/module/c10077.

Millipore Corporation. 2009. Millicell® Hanging Cell Culture Inserts – Single and Preloaded Inserts. [WWW]. [Cited on 15.11.2012]. Available at: http://www.millipore.com/userguides.nsf/a73664f9f981af8c852569b9005b4eee/1fe7f84d88d07bc78525745800558d19/$FILE/P90740.pdf.

Mochizuki M. 2009. Synthesis, properties and structure of polylactic acid fibres. In: S. J., Hearle J. W. S., Jaffe M., Kikutani, T. (edit.) Handbook of Textile Fibre Structure, Volume 1 – Fundamentals and Manufactured Polymer Fibres. Woodhead Publishing. [WWW]. [Cited on 9.11.2012]. Available at: http://www.knovel.com/web/portal/browse/display?_EXT_KNOVEL_DISPLAY_bookid=4365&VerticalID=0. p. 257-275.

Moutos F. T., Freed L. E., Guilak F. 2007. A biomimetic three-dimensional woven composite scaffold for functional tissue engineering of cartilage. Nature Materials (6): 162-67.

Moutos F. T., Estes B. T., Guilak F. 2010. Multifunctional Hybrid Three-dimensionally Woven Scaffolds for Cartilage Tissue Engineering. Macromolecular Bioscience (10). p. 1355-1364.

Mäkinen M. 1998. Kudotut kankaat. Opintomoniste. Tampereen teknillinen yliopisto. 145 p.

Nair, L. S. and Laurencin C. T. 2007. Biodegradable polymers as biomaterials. Progress in Polymer Science 32 (8–9). p. 762-798.

Normal Macula. [WWW]. [Cited on 14.1.2013 on American Health Assistance Foundation, 2000 – 2012]. Available at: http://www.ahaf.org/macular/about/understanding/normal-macula.html.

Onnela N., Savolainen V., Juuti-Uusitalo K., Vaajasaari H., Skottman H., Hyttinen J. 2012. Electric impedance of human embryonic stem cell-derived retinal pigment epithelium. Medical & Biological Engineering & Computing 50. p. 107–116.

Ousema P. H., Moutos F. T., Estes B. T., Caplan A. I., Lennon D. P., Guilak F., Weinberg J. B. 2012. The inhibition by interleukin 1 of MSC chondrogenesis and the development of biomechanical properties in biomimetic 3D woven PCL scaffolds. Biomaterials 33. p. 8967-8974.

Rigby A. J. and Anand S. C. 2000. Ch.15 Medical textiles. In: Horrocks, A.R., Anand, S.C. (edit.) Handbook of Technical Textiles. Woodhead Publishing. [WWW]. [Cited on 8.11.2012]. Available at: http://www.knovel.com/web/portal/browse/display?_EXT_KNOVEL_DISPLAY_bookid=926&VerticalID=0. p. 407-424.

Saketi Pooya. 2010. Microrobotics platform for manipulation and flexibility measurement of individual paper fibers, Master of Science Thesis. 94 p.

Scriven S. D., Trejdosievicz S. K., Thomas D. F. M., Southgate J. 2001. Urothelial cell transplantation using biodegradable synthetic scaffolds. Journal of Materials Sciences: Materials in Medicine 12. p. 991-996.

Sell S., Barnes C., Smith M., McClure M., Madurantakam P., Grant J., McManus M., Bowlin G. 2007. Extracellular matrix regenerated: tissue engineering via electrospun biomimetic nanofibers. Polymer International 56. p. 1349–1360.

Shadforth A. M. A., George K. A., Kwan A. S., Chirila T. V., Harkin D. G. 2012. The cultivation of human retinal pigment epithelial cells on Bombyx mori silk fibroin. Biomaterials 33. p. 4110-4117.

Smith Philip A. 2000. Ch 6 Technical fabric structures – 3. Nonwoven fabrics. In: Horrocks, A.R., Anand, S.C. (edit.) Handbook of Technical Textiles. Woodhead Publishing. p. 130-151.

Subrizi A., Hiidenmaa H., Ilmarinen T., Nymark S., Dubruel P., Uusitalo H., Yliperttula M., Urtti A., Skottman H. 2012. Generation of hESC-derived retinal pigment epithelium on biopolymer coated polyimide membranes. Biomaterials 33. p. 8047-8054.

Södergård, A. and Stolt M. 2002. Properties of lactic acid based polymers and their correlation with composition. Progress in Polymer Science 27 (6). p. 1123-1163.

Treharne A. J., Thomson H. A. J., Grossel M. C., Lotery A. J. 2012. Developing methacrylate-based copolymers as an artificial Bruch's membrane substitute. Journal of Biomedical Materials Research – Part A 100 (9). p. 2358-2364.

Tsuji H. 2007. Poly(lactide) Stereocomplexes: Formation, Structure, Properties, Degradation, and Applications. Macromolecular Bioscience 7 (12). p. 1299-1299.

Tsunashima K., Toyoda K., and Yoshii T. 1999. Ch. 6.3 Stretching Conditions, Orientation, and Physical Properties of Biaxially Oriented Film. In: Kanai T., Campbell G. A. Film Processing. Hanser Publishers. [WWW]. [Cited on 9.11.2012] Available at: http://www.knovel.com/web/portal/browse/display?_EXT_KNOVEL_DISPLAY_bookid=982&VerticalID=0. p. 320-352.

Uurto I., Kotsar A., Isotalo T., Mikkonen J., Martikainen P. M., Kellomäki M., Törmälä P., Tammela T. L. J., Talja M., Salenius J-P. 2007. Tissue biocompatibility of new biodegradable drug-eluting stent materials. Journal of Materials Science: Materials in Medicine Vol. 18. p. 1543–1547. DOI 10.1007/s10856-007-3060-3.

Vaajasaari H., Ilmarinen T., Juuti-Uusitalo K., Rajala K., Onnela N., Narkilahti S., Suuronen R., Hyttinen J., Uusitalo H., Skottman H. 2011. Toward the defined and xeno-free differentiation of functional human pluripotent stem cell–derived retinal pigment epithelial cells. Molecular Vision 17. p. 558-575.

Valonen P. K., Moutos F. T., Kusanagi A., Moretti M. G., Diekman B. O., Welter J. F., Caplan A. I., Guilak F., Freed L. E. 2010. In vitro generation of mechanically functional cartilage grafts based on adult human stem cells and 3D-woven poly(3-caprolactone) scaffolds. Biomaterials 31. p. 2193-2200.

van der Schueren L. and de Clerck K. 2011. Nanofibrous textiles in medical applications. In: Bartels, V. T. Handbook of Medical Textiles. Woodhead Publishing. [WWW]. [Cited on 3.12.2012]. Available at: http://www.knovel.com/web/portal /browse/display?_EXT_KNOVEL_DISPLAY_bookid=4321&VerticalID=0. p. 547-566.

van Alst M., Eenink M. J. D., et al. 2009. ABC's of bioabsorption: application of lactide based polymers in fully resorbable cardiovascular stents. Euro Intervention 5: F23-F27.

Vasara A. I., Hyttinen M. M., Lammi M. J., Lammi P. E., Långsjö T. K., Lindahl A., Peterson L., Kellomäki M., Konttinen Y. T., Helminen H. J., Kiviranta I. 2004. Subchondral Bone Reaction Associated with Chondral Defect and Attempted Cartilage Repair in Goats. Calcified Tissue International 74. p. 107–114. DOI: 10.1007/s00223-002-2153-8.

Wulfhorst B., Gries T., Weit D. 2006. Textile technology, Hanser Puplishers. [WWW]. [Cited on 22.11.2012]. Available at: http://www.knovel.com/web/portal/browse/ display?_EXT_KNOVEL_DISPLAY_bookid=4235&VerticalID=0. p. 13-73; 74-123; 124-151; 152-166; 188-204.

Yokota T., Ichikawa H., Matsumiya G., Kuratani T., Sakaguchi T., Iwai S., Shirakawa Y., Torikai K., Saito A., Uchimura E., Kawaguchi N., Matsuura N., Sawa Y. 2008. In situ tissue regeneration using a novel tissue-engineered, small-caliber vascular graft without cell seeding. The Journal of Thoracic and Cardiovascular Surgery. p. 1-8, (doi:10.1016/j.jtcvs.2008.02.058)

Zamiri P., Kuang Y., Sharma U., Ng T.F., Busold R.H., Rago A.P., Core L.A., Palasis M. 2010. The biocompatibility of rapidly degrading polymeric stents in porcine carotid arteries. Biomaterials Vol. 31. p. 7847-7855.

APPENDIX 1: MASS PER UNIT AREA

Table 8 *Mass per unit area of woven PET samples (n = 1).*

Sample	Warp density (yarns/reed dent)	Mass	Mass per unit area (g/m^2)
Plain weave	**4**	1.568 g / 250 cm^2	6.272
	6	1.881 g / 200 cm^2	9.405
	8(1)	1.703 g / 200 cm^2	8.515
	8(2)	1.399 g / 150 cm^2	9.327
	10**	2.067 g / 200 cm^2	10.335
	12**	1.395 g / 100 cm^2	13.950
Weft rib	**8**	1.085 g / 150 cm^2	7.233
Twill derivative	**6**	2.466 g / 250 cm^2	9.864
	8	1.650 g / 150 cm^2	11.000
5-harness satin	**6**	2.168 g / 250 cm^2	8.672
	8	2.034 g / 200 cm^2	10.170
Plain weave/twill comb.	**6**	1.961 g / 250 cm^2	7.843
	8	2.318 g / 250 cm^2	9.271
Plain weave/twill comb. 2	**6**	2.135 g / 250 cm^2	8.540
	8	2.180 g / 200 cm^2	10.900
Plain weave derivative	**6**	1.885 g / 200 cm^2	9.425
	8	2.887 g / 250 cm^2	11.548
	10**	2.471 g / 250 cm^2	9.884
	12**	2.110 g / 150 cm^2	14.067
Twill derivative (6 harness)	*****	*****	*****
Twill derivative 2	**6**	2.178 g / 250 cm^2	8.712
	8	2.318 g / 250 cm^2	9.272

(1) Lower weft density.

(2) Higher weft density.

*It was not possible to make a proper sample.

** Samples were woven with lubricant.

APPENDIX 2: WARP AND WEFT DENSITIES AND THICKNESS MEASUREMENTS

Table 9 *Warp density (n = 1), average weft density (n = 5) and average thickness (n = 5) and their standard deviations of woven PET samples.*

Weave pattern	Warp density (yarns/reed dent)	Warp density (yarns/cm)	Weft density (yarns/cm)	Thickness (mm)
Plain weave	**4**	42	29 ± 0.27	0.142 ± 0.007
	6	67	29 ± 0.41	0.199 ± 0.006
	8(1)	83	13 ± 0.15	0.204 ± 0.007
	8(2)	77	29 ± 0.78	0.193 ± 0.003
	10**	91	22 ± 0.74	0.213 ± 0.003
	12**	111	15 ± 0.39	0.225 ± 0.005
Weft rib	**8**	83	29 ± 0.62	0.176 ± 0.001
Twill derivative	**6**	66	38 ± 0.67	0.181 ± 0.004
	8	99	24 ± 0.50	0.238 ± 0.006
5-harness satin	**6**	77	23 ± 0.34	0.179 ± 0.005
	8	100	23 ± 0.28	0.215 ± 0.008
Plain weave/twill comb.	**6**	71	17 ± 0.23	0.179 ± 0.011
	8	90	15 ± 0.15	0.224 ± 0.009
Plain weave/twill comb. 2	**6**	66	29 ± 0.08	0.215 ± 0.005
	8	86	29 ± 0.32	0.231 ± 0.003
Plain weave derivative	**6**	67	38 ± 2.17	0.193 ± 0.002
	8	87	38 ± 1.91	0.192 ± 0.003
	10**	100	20 ± 0.25	0.231 ± 0.004
	12**	116	25 ± 0.65	0.250 ± 0.007
Twill derivative (6 harness)	*****	*	*	*
Twill derivative 2	**6**	67	30 ± 0.52	0.186 ± 0.004
	8	83	23 ± 0.27	0.204 ± 0.005

(1) Lower weft density.

(2) Higher weft density.

***** It was not possible to make a proper sample.

** Samples were woven with lubricant.

APPENDIX 3: COVER FACTORS AND TOTAL VOID PERCENTAGES

Table 10 *Total void percentages and calculated cover factors (in percentages) for warp and weft direction and the total cover factor for woven PET samples.*

Sample	Warp density (yarns / reed dent)	C_w	C_f	CF	Total void (%)
Plain weave	**4**	35.7	24.6	51.5	60
	6	56.9	24.6	67.5	66
	8(1)	70.5	11.0	73.7	70
	8(2)	65.4	24.6	73.9	65
	10**	77.3	18.7	81.5	65
	12**	94.3	12.7	95.0	77
Weft rib	**8**	70.5	24.6	77.7	70
Twill derivative	**6**	56.0	32.3	70.2	61
	8	84.1	20.4	87.3	67
5-harness satin	**6**	65.4	19.5	72.1	65
	8	84.9	19.5	87.9	67
Plain weave/twill comb.	**6**	60.3	14.4	65.9	68
	8	76.4	12.7	79.4	70
Plain weave/twill comb. 2	**6**	56.0	24.6	66.9	71
	8	73.0	24.6	79.7	66
Plain weave derivative	**6**	56.9	32.3	70.8	65
	8	73.9	32.3	82.3	56
	10**	84.9	17.0	87.5	69
	12**	98.5	21.2	98.8	59
Twill derivative (6 harness)	*****	*****	*****	*	*****
Twill derivative 2	**6**	56.9	25.5	67.9	66
	8	70.5	19.5	76.2	67

(1) Lower weft density.

(2) Higher weft density.

***** It was not possible to make a proper sample.

** Samples were woven with lubricant.

APPENDIX 4: CONTACT ANGLES

Table 11 *Mean values and standard deviations of contact angle measured with DI-water for plain weave and plain weave derivative, warp densities, 10 and 12 yarns/reed dent. Control sample plain weave 8(2) yarns/reed dent. (n = 10)*

	DI-water		DMEM	
	Mean value (°)	**St. dev**	**Mean value (°)**	**St. dev**
Plain weave 8 yarns/reed dent (2)	90.58	18.81	110.91	7.38
Plain weave 10 yarns/reed dent	120.02	5.30	116.92	6.49
Plain weave 12 yarns/reed dent	126.01	8.85	124.84	5.24
Plain weave derivative 10 yarns/reed dent	120.34	6.41	120.14	4.53
Plain weave derivative 12 yarns/reed dent	117.50	6.35	116.41	2.53

APPENDIX 5: TENSILE TESTING

Table 12 *Maximum load, stress at maximum load and strain values and their standard deviations, and Young's Modulus of woven PET samples and PET yarn tested wet.*

	Yarns/reed dent	Max. load (N)	Stress at Max. load (MPa)	Strain at Max. load (%)	Young's Modulus (MPa)
Plain weave	**4**	152.5 ± 11.4	53.9 ± 4.0	20.3 ± 1.6	11.7 (n=6)
	6	169.6 ± 11.7	60.9 ± 4.2	27.4 ± 1.3	11.5 (n=6)
	8[(1)]	164.6 ± 6.6	80.8 ± 3.2	25.3 ± 1.8	22.5 (n=6)
	8[(2)]	186.5 ± 4.9	87.9 ± 2.3	27.7 ± 1.3	17.0 (n=5)
	10**	174.4 ± 4.7	91.0 ± 2.4	25.7 ± 1.2	25.6 (n=5)
	12**	169.8 ± 10.2	94.3 ± 5.7	24.9 ± 1.3	25.8 (n=5)
Weft rib	**8**	193.8 ± 10.9	109.9 ± 6.2	26.5 ± 1.7	22.2 (n=5)
Twill derivative	**6**	179.9 ± 9.9	70.8 ± 3.9	25.5 ± 1.6	16.9 (n=5)
	8	152.1 ± 5.1	71.1 ± 2.4	27.7 ± 1.5	18.5 (n=5)
5-harness satin	**6**	159.2 ± 5.5	68.3 ± 2.3	23.4 ± 0.8	19.4 (n=6)
	8	153.4 ± 9.4	73.3 ± 3.7	25.2 ± 0.8	23.3 (n=5)
Plain weave/twill comb.	**6**	160.6 ± 11.9	69.0 ± 5.1	23.3 ± 2.5	18.9 (n=6)
	8	157.6 ± 7.9	70.3 ± 3.5	24.7 ± 1.6	22.1 (n=5)
Plain weave/twill comb. 2	**6**	185.8 ± 4.1	66.5 ± 1.5	24.7 ± 0.6	19.3 (n=5)
	8	184.9 ± 7.9	80.0 ± 3.4	27.4 ± 1.3	21.9 (n=5)
Plain weave derivative	**6**	202.0 ± 9.3	80.5 ± 3.7	25.2 ± 1.2	20.7 (n=5)
	8	199.0 ± 5.3	94.2 ± 2.5	27.2 ± 1.5	19.4 (n=5)
	10**	163.4 ± 4.9	78.6 ± 2.4	25.5 ± 1.7	22.9 (n=5)
	12**	168.8 ± 6.7	84.4 ± 3.3	27.2 ± 0.9	21.8 (n=5)
Twill derivative (6 harness)	*****	*****	*****	*****	*****
Twill derivative 2	**6**	180.4 ± 5.8	74.6 ± 2.4	25.9 ± 1.9	16.7 (n=5)
	8	168.9 ± 4.3	75.3 ± 1.9	25.8 ± 0.6	19.2 (n=5)

(1) Lower weft density.

(2) Higher weft density.

***** It was not possible to make a proper sample.

** Samples were woven with lubricant.